Visible-Light Photocatalysis Using $CsPbX_3$ Perovskite Nanocrystals for Organic Transformations

Pravat Nayek, Buddhadeb Pal and Prasenjit Mal*

School of Chemical Sciences, National Institute of Science Education and Research (NISER) Bhubaneswar, An OCC of Homi Bhabha National Institute, PO Bhimpur-Padanpur, Via Jatni, District Khurda, Odisha 752050, India.

*Corresponding author: Prasenjit Mal, E-mail: pmal@niser.ac.in

TOC GRAPHIC

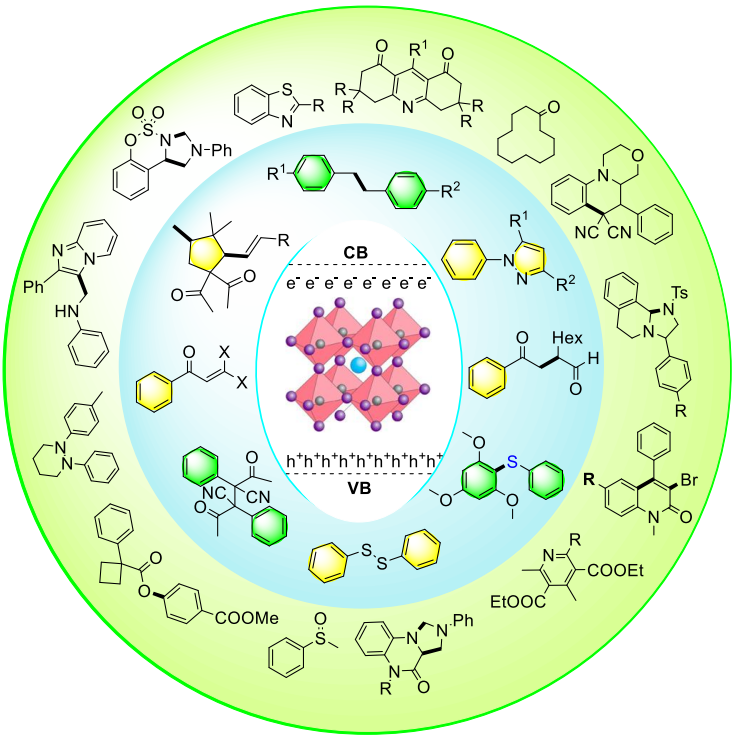

ABSTRACT

The increasing interest in efficient organic synthesis by applying solar radiation has propelled a surge in the demand for introducing new types of photocatalysts in synthetic toolboxes. During the last few decades, tremendous efforts have been invested in developing low-cost, non-toxic, stable, and potent photocatalysts. In this perspective, Cesium Lead Halide perovskite ($CsPbX_3$) nanocrystal has emerged as a brand new photocatalyst, creating a

renaissance in pioneering organic photochemistry with its enchanting optoelectronic features. Due to their unique band structure, tunable bandgap, and near unity quantum yield, these highly fluorescent nanocrystals are exceptional candidates to catalyze numerous fundamental organic transformations by absorbing energy from ultraviolet to visible regions. Also, anion metathesis, long average excited state lifetime, tunable morphology, and photo-generated charge carriers, make them capable of a broader range of organic substrate activation in bench-stable conditions. These nanocrystals are well known for their superb power conversion efficiency (PCE) of solar radiation which reached up to 26.3% in the last few years, and its potential has already surpassed everyone's expectations in multiple fields like photovoltaics, photoelectronics, lasers, scintillators, etc. But, its use in photo organic chemistry just started and we believe this typical promising material is going to fetch a new era in the field of organic photocatalysis. This comprehensive review systematically summarizes the development made over $CsPbX_3$ perovskite catalysis in the last few years by assembling pieces of literature on perovskite-based organic reactions. And also, explores the intricacies of the underlying mechanistic cycles and discusses limitations with future scope of exploration.

KEYWORDS: $CsPbX_3$ Perovskite Nanocrystals; Visible-Light Photocatalysis; Organic Transformations; Tunable Bandgap; Photogenerated Charge Carriers

INTRODUCTION

A. Photocatalysis – The beginning

Life was initiated on this planet when Mother Nature started storing solar energy in the form of glucose by using chlorophyll as the catalyst through a process called 'Photosynthesis'. And, by mimicking natural photosynthesis[1], when a chemical compound catalyzes an organic

reaction by absorbing light as a form of energy is termed as 'Photocatalysis'[2-4]. In the early 19th century, idea of the photocatalysis was invented and people started to photolyze organic compounds by using sunlight or mercury lamps[5]. At the end of the 20th century, significant advances were achieved in this field with the use of versatile compounds as photocatalysts including ketones[6], nitriles[7], organic dyes[8], metal salts, etc. Eventually, photocatalysis emerged as a separate discipline in synthetic organic chemistry to serve the natural tendency of storing solar radiation in chemical bonds. After that, the discovery of transition metal complexes' ability to absorb light and catalyze photo organic reactions marked a major turning point, when the concept of a photocatalyst was modified with a completely new idea[9-12]. And, this discovery resulted in the search for a much superior photocatalyst in different fields of science including semi-conductor, inorganic salts, MOFs, COFs, etc. The search for a photocatalyst never ended after that, and demand increased for a much more efficient photocatalyst day by day. In this contest, Cesium Lead Halide perovskite ($CsPbX_3$) nanocrystal emerged as a brand new photocatalyst[13-14], creating a renaissance in pioneering organic photochemistry with its enchanting features[15-17].

B. Perovskite Era

Any material with a formula ABX_3 is termed Perovskite where 'A' and 'B' are typically cations with a large size difference and 'X' is an anion like halide or oxide. Perovskites like calcium titanate ($CaTiO_3$) existed in nature since ancient times, but their potential was unknown and disclosed only after the arrival of its Lead (Pb) version[18]. Among all, Cesium lead halide perovskites ($CsPbX_3$) are well known for their superb power conversion efficiency (PCE) of solar radiation which reached up to 26.3%[19-21] in the last few years. So, employing lead halide perovskite (LHP) NCs to accomplish photocatalytic organic transformation practically means capturing the sun directly in chemical bonds[22]. The morphology of these materials can be

controlled using various reaction parameters like reaction duration, temperature, additives, precursor source, etc. and every differently shaped nanoparticle leads to a different excited state lifetime, fluorescence maxima, and a different extent of reactivity[23-27]. Also, low cost, unique band structure, near unity quantum yield, tunable-shape[28], strong sunlight absorption[29], long average excited state lifetime, high reaction turnover number[30], anion metathesis[31], and large separation of photogenerated charge carriers[32-33] make them dominant over any other conventional photocatalysts with a broader range of organic substrate activation.

C. Cesium Lead Halide Perovskite – A blessing or curse

The halide atom in Cesium lead halide perovskite can be tuned like chloride, bromide, or iodide leading to the generation of $CsPbCl_3$, $CsPbBr_3$, or $CsPbI_3$ perovskite nanocrystals[34]. Among them, Cesium lead chloride perovskite NCs have the highest band gap (~ 3.0 eV) between the valance band (VB) and the conduction band (CB) which shifted its absorption in higher energy ultra-violet (UV) region (Figure 1). Also, these nanocrystals are much more robust toward stability than the other two opponents, can stay alive for several months in low temperatures without agglomeration, and perform their catalytic activity as a dispersed phase in a non-polar solvent. Whereas, Cesium lead iodide ($CsPbI_3$) perovskite nanocrystals absorb in the red end of the visible light spectra illustrated by their lowest band gap energy among all (~ 1.8 eV) between two electronic bands. Also, it is the least stable among all three types, surviving only a few minutes to a few hours at room temperature, arresting its broader use in organic photochemistry. Cesium lead bromide perovskite NCs ($CsPbBr_3$) are the most suitable ones for practical sustainable use, their stability is in between the other two, and also the energy gap between the two electronic bands (~ 2.34 eV) permits them to absorb energy from the visible spectrum.

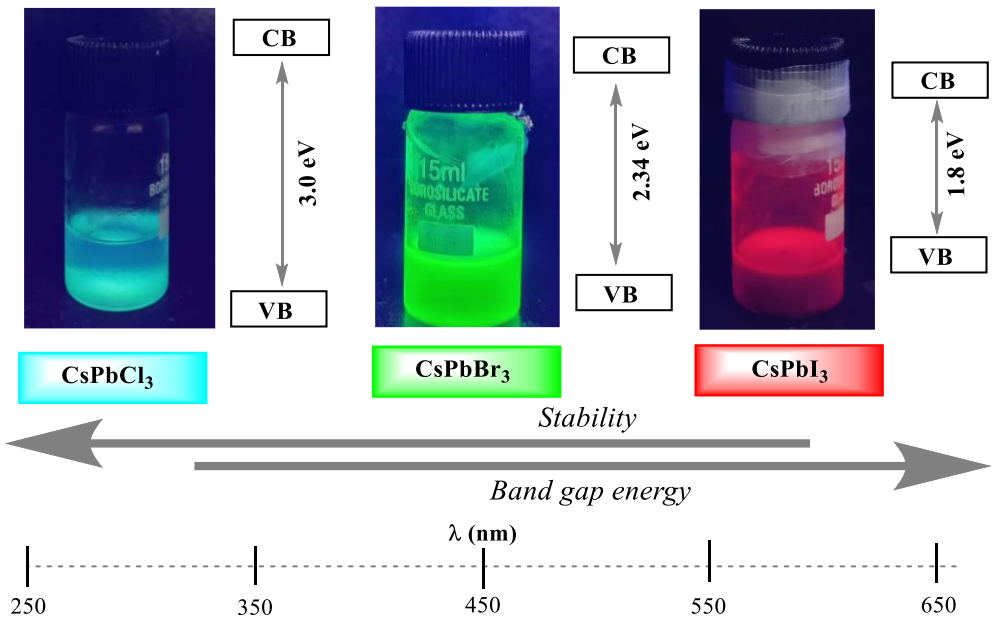

Figure 1. Cesium lead halide perovskites under UV irradiation.

D. The challenges in its way

The potential of LHP NCs has already been proven in multiple sustainable fields like photovoltaics, photoelectronics, lasers, scintillators[35], etc. However, its activity in organic photochemistry is still scarce due to its instability in moisture, oxygen, heat, and polar solvents. In a highly polar solvent like DMSO, DMF, or H_2O with a large dielectric constant, the three-dimensional ionic framework of perovskite gets ruptured indicating diminishment in the intense fluorescence, and lead (Pb) is leached out from the system as simple lead salts like PbX_2, PbO, etc. In the presence of heat, or oxygen, the nanocrystals of $CsPbX_3$ get assembled which eventually leads to agglomeration with destruction in its activity towards photocatalysis. Also, lack of intellectuality about its tunable band gap, ion-exchange nature, morphology-based activity, and a bunch of hidden features, concise its practical use in organic photochemistry[36].

E. Why do we need this article?

The C-H, C-C, C-N, C-O, C-P, C-S, S-S, etc. bond formations that are of fundamental significance in organic synthesis, efficiently achievable by using $CsPbX_3$ catalysis with visible light irradiation in certain conditional environments. Various reaction parameters and the reactants are designed in a way to enhance the stability of the $CsPbX_3$ photocatalyst during the reaction in the dispersed phase. For that reason, reactants with high capping capability like mercaptans, zwitter ions, carboxylates, etc. always remained the best choice for perovskite catalysis where the reactant is utilized to gear up the stability of the catalyst by surface-capping. On the other hand, anion-metathesis with halogenated compounds leads to the utilization of various organohalogen solvents like DCM, DBM, etc. for perovskite-based photo-solvolysis reactions and this strategy is used to activate previously inaccessible synthetic goals with very high reaction yield. So, very high expertise and experience are required in this field to design any new fruitful synthetic protocol. Perovskite-based organic photocatalysis is a completely new field, just began only a few years ago and there is no adequate information about it which restricts its use in photo organic synthesis. On the way to its potential use, a series of challenges have been overcome already, while some still remain. This comprehensive review article strives to provide the history of the advancement of visible-light-induced organic photocatalysis by utilizing $CsPbX_3$ NCs as photocatalysts, demonstrating their capability to accomplish multiple challenging organic syntheses. And, we strongly believe this article will enable beginners in this field to design new synthetic routes with a significant stride toward a sustainable environment.

Here, in this article, we have illustrated the development made over perovskite catalysis in the last few years since its beginning in 2017 (Figure 2). And, we have succinctly described every reaction by maintaining the corresponding year and their simplified reaction procedure through

oxidative, reductive, or energy transfer mechanistic cycle. As photocatalysis is concerned with a chemical reaction that is initiated by light while cyclic voltammetry (CV) plays a very crucial role in determining the redox potentials of the photocatalyst and the reactants. So, we have also included one data table (Figure 3) which contains redox potentials for all the reactants that were employed in any of the perovskite-based reactions for future reference and easy comparison of the designed organic substrates with the existing one.

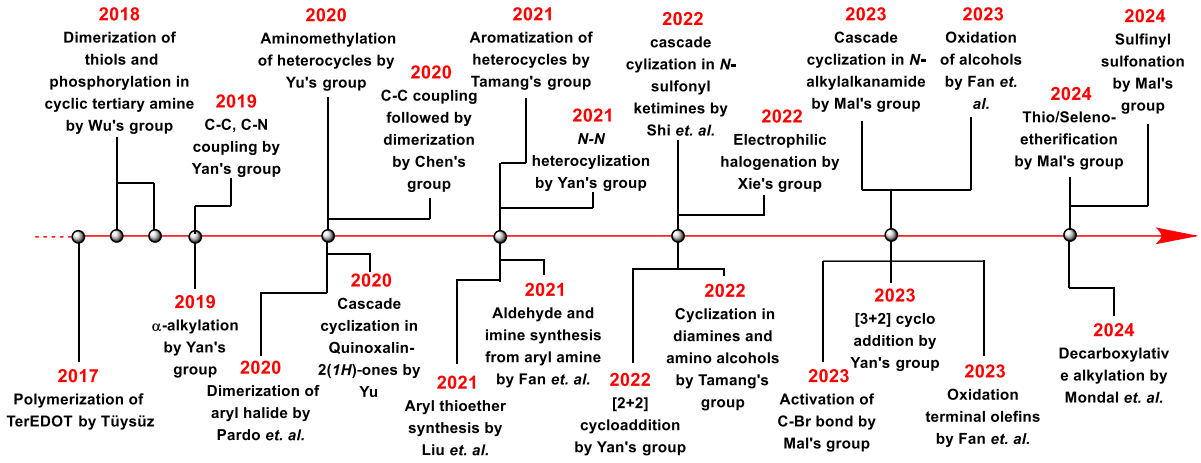

Figure 2. Development made over $CsPbX_3$ catalysis in the last few years.

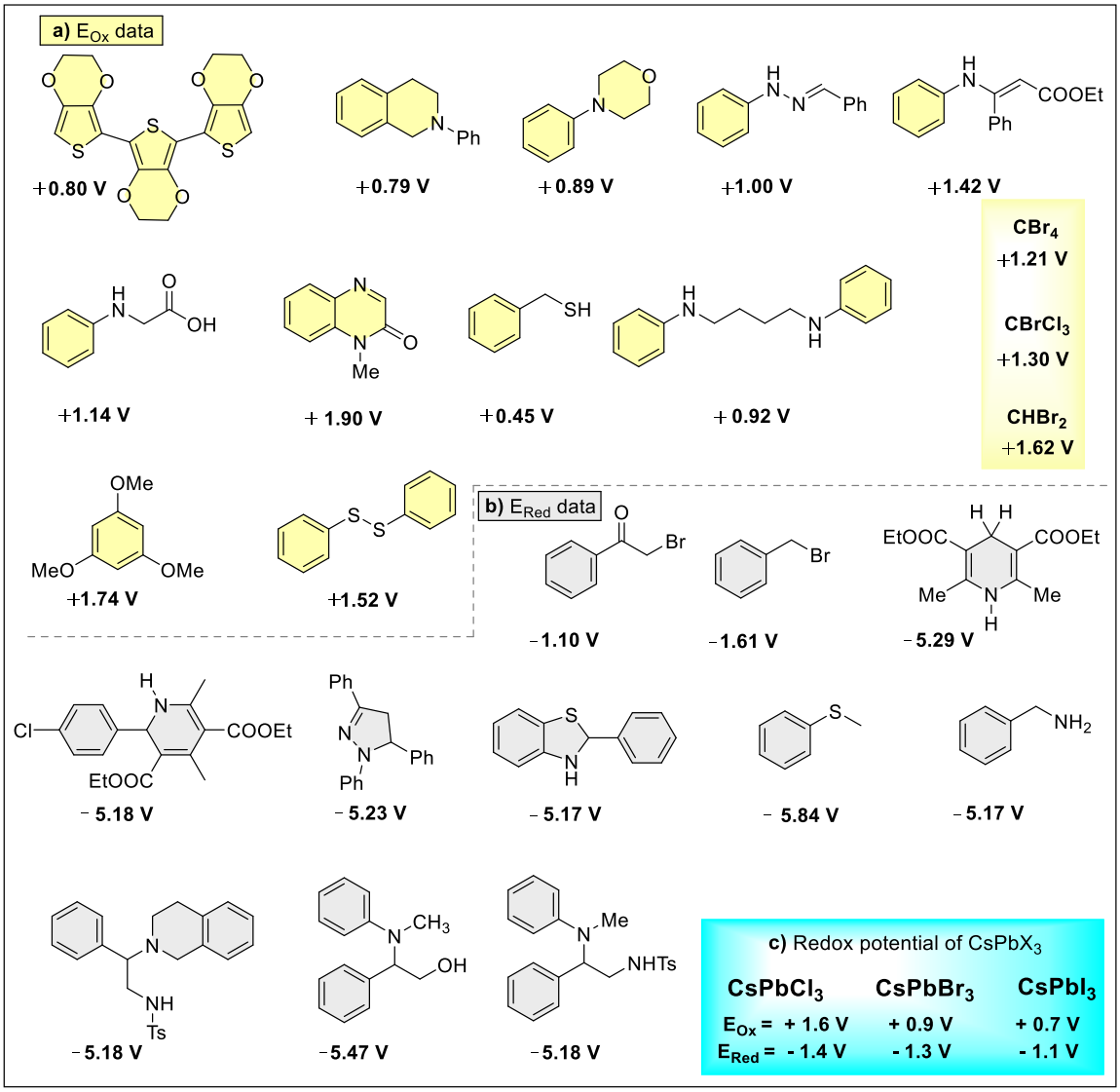

Figure 3. (a) Oxidation and (b) Reduction potentials for various organic substrates employed in different reaction schemes (c) Redox potentials of cesium lead halide perovskite ($CsPbX_3$).

For simplicity of the mechanisms in all the cases, a radical cation or a radical anion of the photocatalyst ($CsPbX_3$) has been considered which is originally generated by transferring an excited electron from the conduction band (CB) to an acceptor or shifting a photogenerated hole (formed by electronic excitation) from the valance band (VB) to the substrate respectively (Figure 4a). When a photocatalyst serves the role of an excited state reductant, it reduces any substrate molecule to its radical anion and itself oxidizes to a radical cation (Figure 4b) whereas

the vice-versa scenario observed for photocatalyst with an excited state oxidant nature (Figure 4c).

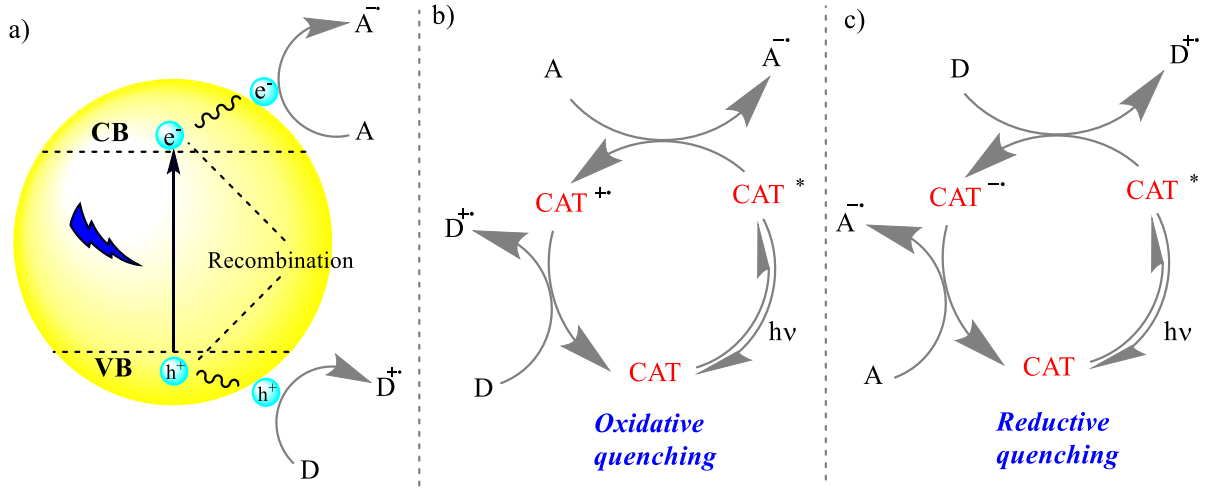

Figure 4. a) Electron and hole transfer in mechanistic cycle b) oxidative quenching cycle c) reductive quenching cycle.

1.1 $CsPbI_3$ Perovskite QDs catalyzed polymerization of TerEDOT

The utilization of lead halide perovskite quantum dots in the organic field started nearly in 2017 for a polymerization reaction to furnish a conducting polymer material by the Tüysüz group[37] (Scheme 1). Cesium lead iodide perovskite quantum dots ($CsPbI_3$ QDs) was used to promote the polymerization of 2,2′,5′,2″-ter-3,4-ethylenedioxythiophene (TerEDOT) under solar stimulator irradiation to form poly(3,4- ethylenedioxythiophene) (PEDOT). And, the newly generated conducting polymer stabilizes the morphology of the $CsPbI_3$ QDs by encapsulating them in a dispersed phase inside dry octane solvent. This photocatalytic polymerization process depends on the concentration of the catalyst where molecular oxygen and 1,4-benzoquinone served as the terminal oxidant during the polymerization process. The morphology of these perovskite nanocrystals can easily modified using various reaction parameters like reaction time, reaction temperature, impurity, precursor, etc. Also, in some cases, the morphology of the

nanocrystal gets converted into a different form in the course of the reaction. In this case, when molecular oxygen served the role of terminal oxidant, the morphology of the $CsPbI_3$ QDs changed from cubic to orthorhombic in situ reaction while usage of 1,4-benzoquinone preserves the cubic phase of $CsPbI_3$ QDs after the reaction. Mechanistic investigation depicted that $CsPbI_3$ QDs irradiated with solar stimulation (LCS-100) behaved as an excited state oxidant. By transferring a photogenerated hole from the valence band (VB), excited perovskite nanocrystals oxidize TerEDOT monomers to form a cationic intermediate (**1.1**) which initiates a chain reaction and finally polymerize to form the PEDOT polymer. Molecular oxygen or *para*-benzoquinone both can play the role of terminal oxidant but *para*-benzoquinone is preferred over molecular oxygen as it keeps the morphology of $CsPbI_3$ QDs intact during the catalytic cycle. PbI_2 was used as the source of both Lead (Pb) and Iodide (I) during the preparation of perovskite QDs, and dry octane was used in the last step to make the dark red ink solution.

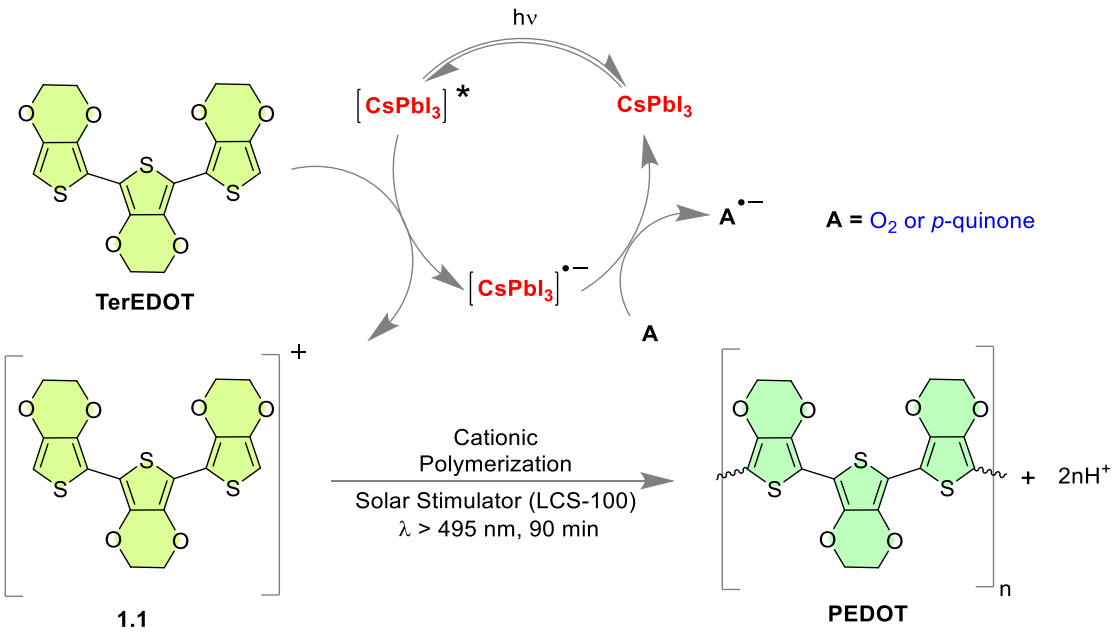

Scheme 1. Photocatalyzed polymerization of TerEDOT by Tüysüz's group.

1.2 Dimerization of mercaptans to form symmetric and unsymmetric disulfides

After this polymerization report, people worldwide started searching for perovskite's activity in different photocatalytic organic reactions. In the next year, Wu's group disclosed the dimerization of thiols or mercaptanes (**2a, 2b**) to form symmetric and unsymmetric di-sulfides (**2c**) with the utilization of $CsPbBr_3$ catalysis in white LED irradiation in DCM solvent (Scheme 2).[38] The reaction was typically completed within 12 hours with an average reaction yield of around 80%. This synthetic protocol successfully delivered symmetric disulfides from aromatic thiols with electron donor and acceptor substitution on the ring (**2aa-2ad**), cyclic aliphatic thiol (**2ae**), benzylic thiol (**2af**), and also one unsymmetrical disulfide (**2ag**) with a 68% reaction yield. Also, simple aliphatic thiol (**2ah**), and a heteronuclear substitution (**2ai**) responded with an excellent yield. Upon exposure to white LEDs, $CsPbBr_3$ nanocrystals become excited and undergo an electronic transition from the valence band (VB) to the conduction band (CB). Afterward, the excited electron in the conduction band reduces molecular oxygen to a superoxide radical anion. And, the photogenerated hole in the valance band (VB) oxidizes thiol molecules to an 'S'-centered thiyl radical. Eventually, the thiyl radical dimerizes to furnish di-sulfides by forming stable S-S bonds. Dichloromethane (DCM) here found to be the best solvent, which is due to the anion metathesis of chlorine atoms from the solvent with bromide vacancy in the perovskite nanocrystal leading to the formation of a much stable mixed halide perovskite NCs ($CsPbCl_xBr_y$) with different ratios of halide ions. Also, this particular protocol can be executed with $CsPbCl_3$ perovskite nanocrystals with higher energy UV irradiation ($\lambda <$ 400 nm). Also, another mechanistic possibility of hydrogen formation is claimed in this work by capping the thiol groups as surface passivating ligands on the outer layer of perovskite nanocrystals.

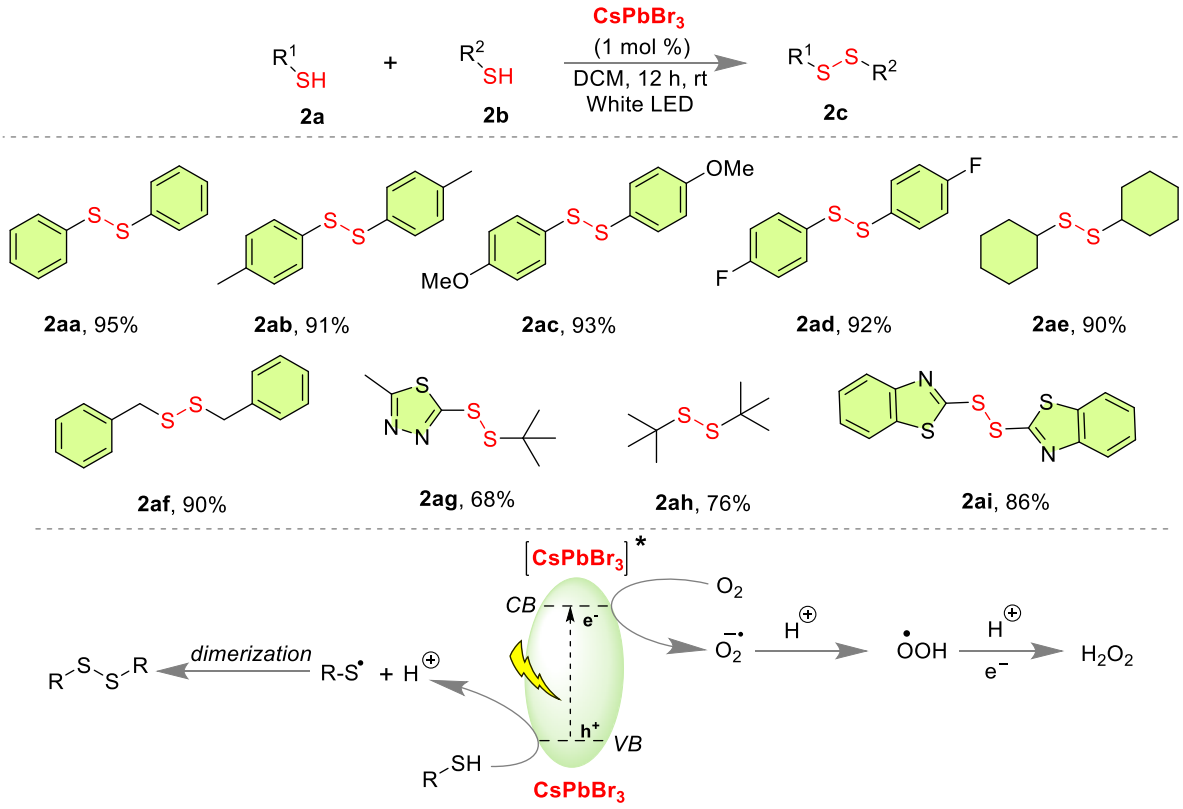

Scheme 2. $CsPbBr_3$ perovskite NCs catalyzed dimerization of thiols by Wu's group.

1.3 Photocatalytic phosphonylation in cyclic tertiary amines using perovskite NCs

Like carbon-carbon, carbon-chalcogen bond formation is also one of the prime interests in organic chemistry[39-40]. Usually, carbon-oxygen bond generation is much easier compared to carbon-phosphorous due to the lack of overlap of the atomic orbitals for bigger-size phosphorous atoms. So, furnishing C-P bonds in an efficient way at bench-stable conditions is of great importance[41-42]. Wu's group reported another C-H functionalization on aromatic cyclic tertiary amine (**3a**) to form numerous phosphonylated compounds with just 1 mol % of $CsPbBr_3$ perovskite catalyst loading in visible light irradiation (Scheme 3)[38]. Lead halide perovskite nanocrystals are very prone to degradation in high-polar solvents like DMF, DMSO, and H_2O. At the same time, this becomes another major advantage of the utilization of $CsPbBr_3$ perovskites, easily washable from the reaction system in the form of lead salts by simple work-

up with water unlike most of the transition metal salts. So utilization of non-polar solvents like toluene, hexane, octane, dimethyl carbonate (DMC), etc. is always preferable. In this dehydrogenative cross-coupling strategy, molecular oxygen plays the role of terminal oxidant, whereas cyclic *tert*-amine itself oxidizes to an *N*-centred radical cation (**3.1**) by accepting one photo-generated hole from the valance band of the perovskite NCs. After that, the oxygen radical anion helps to form a radical species (**3.2**) which is highly stable due to its benzylic nature, and being adjacent to a heteroatom. This stable radical again reduces molecular oxygen to generate an *N*-centered cationic species (**3.3**) which reacts with phosphite ether (**3b**) to furnish the phosphorylated product (**3c**). This synthetic protocol tolerated well for a library of substrates with an average reaction yield of 65-70 % in almost all cases regardless of the number and type of substitution. Initially, the phosphite ether part was fixed, and the yields of the reaction were investigated by changing substitutions on the aromatic part of the cyclic tertiary amine (**3aa-3ac**). In all the cases, the synthetic strategy delivered a good reaction yield within just 4 h. The protocol was also successful in the modification of the phosphite ether part (**3ad**). Then, substitution on the nitrogen part of cyclic tertiary amine was varied from simple bromo-substituted aromatic ring (**3ae**) to polyaromatic ring (**3af**), and the strategy was found to perform smoothly with a good reaction yield. To make the $CsPbX_3$ NCs, a 'two-precursor method' has been utilized developed by Protesescu *et. al*[18], where lead salt (PbX_2) was used as the precursor for both lead (Pb) and halide (X) ions.

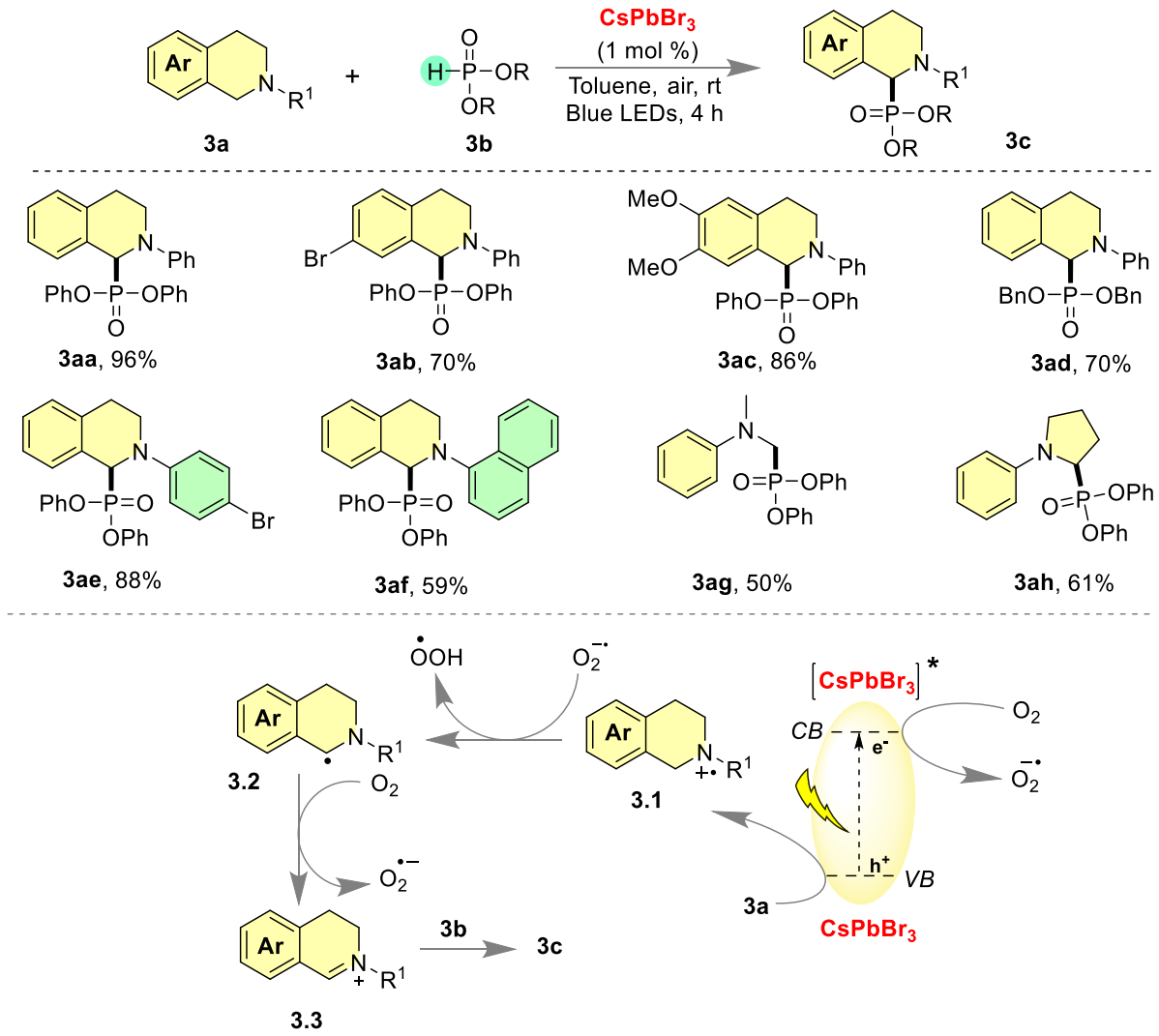

Scheme 3. Photocatalytic dehydrogenative phosphonylation on tertiary amine by Wu's group.

1.4 The $CsPbBr_3$ NCs catalyzed C-C and C-H bond formation

Up to 2018, perovskite material couldn't manage to enter the core of basic organic chemistry and hasn't found its potential to furnish very fundamental bonds like C-C, C-H, etc., in synthetic chemistry. In 2019, Yan's group first disclosed a $CsPbBr_3$ perovskite NCs catalyzed photochemical C-C and C-H bond formation in visible light illumination (Scheme 4)[30]. The synthetic protocol delivered a variety of products controlling different reaction parameters and the turnover number (TON) for this specific conversion was found to be near 50000 under 455 nm Blue LED irradiation. Three different products (**4c-4e**) were observed by installing different

optimized reaction conditions and nitrogen-based bases like DIPEA, NEt_3, or enamine offered the role of terminal oxidant to bring back the excited perovskite nanocrystals in their ground state. Cesium metal in $CsPbX_3$ may be replaced with an organic cationic species of a similar size like methyl ammonium (MA), or formamidinium (FA), leading to the formation of $MAPbBr_3$, or $FAPbBr_3$ respectively. $MAPbBr_3$ i.e. methyl ammonium lead bromide perovskite[25] also capable of catalyzing this conversion with declined reaction yield but due to the poor stability of those perovskites in organic solvents, they are very prone to degradation to normal lead salts like $PbBr_2$, hence not utilizable as compared to which $CsPbBr_3$ can be reused up to four times indicating a TON over 52000. The α-alkylation product with aliphatic aldehyde (**4ca-4cc**) formed with a very high reaction yield for all aromatic phenacyl bromide derivatives and also performed very well in combination with aliphatic acyl bromide (**4cd**). The C-H coupled product (**4ea-4ec**) is furnished with a very high reaction yield of over 85-90% in almost all cases. The mechanism for α-alkylation (**4e**) product formation is slightly different compared to the C-C coupling. Upon blue LED irradiation, $CsPbBr_3$ NCs get excited, reducing acyl bromide to a radical intermediate (**4.1**) by eliminating a bromide ion. On the other side, the Schiff-base reaction between amine and aldehyde forms enamine which plays the role of terminal reductant and transforms into radical cation (**4.2**) on an electron donation to excited state perovskite radical cation. Then, (**4.1**) and (**4.2**) species react to form a cationic species (**4.3**) which eventually hydrolyzed to form the anticipated α-alkylated C-C coupled product (**4c**). In the catalytic cycle, when DIPEA is replaced with (5S)--2,2,3-trimethyl 5-benzyl-4-imidazolidinone, an expensive cocatalyst commonly used in photo redox catalysis[43], the freshly formed acyl radical being stabilized somehow and lead to the production of dimerized product (**4d**). When a nitrogen-centered base is present in the reaction system, this acyl radical abstracts one proton from the adjacent position to nitrogen in the base to form the reduced ketone or C-H coupled product (**4e**). So, the outline of this work delivers a very crucial

fact about perovskite catalysis that a nitrogen-containing base and α-halo substrates in the halogenated solvent are a nice combination for designing a perovskite-based synthetic protocol.

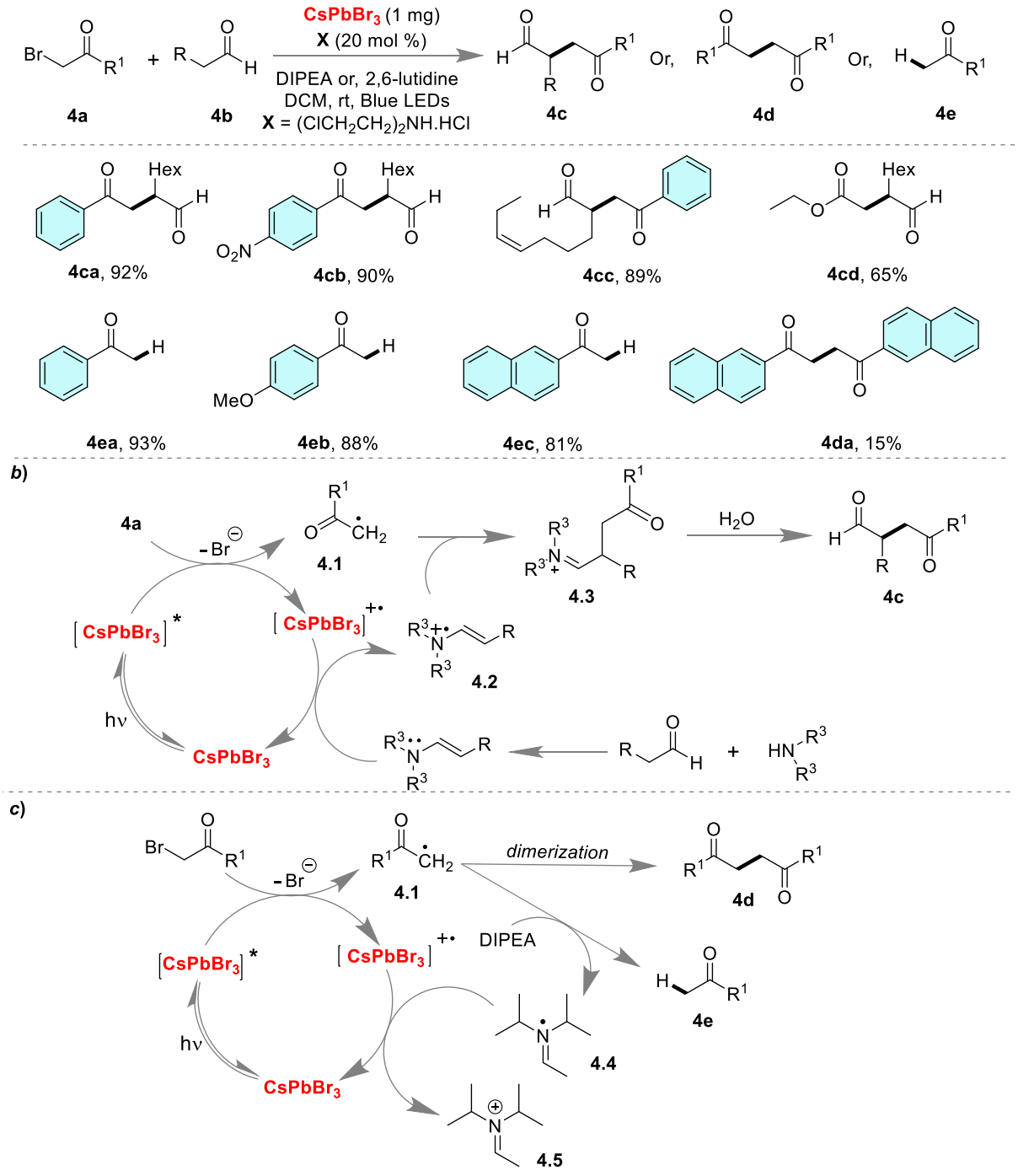

Scheme 4. Photochemical α-alkylation and C-H bond formation by Yan's group.

1.5 Michael-type C-C coupling reaction in visible light irradiation

Following this work, Yan's group extended their strategy to another blue LED-assisted Michael-type conjugated C-C coupling reaction adjacent to the nitrogen center on cyclic tertiary amines using *α*,*β*-unsaturated ketone as the precursor and trifluoro acetic acid (TFA) as the protonating source (Scheme 5)[44]. With the blue LED irradiation, an electronic excitation from the valance band (VB) to the conduction band (CB), leads to the generation of a hole in the valance band, and the excited electron in the conduction band reduces cyclic *tert*-amine (**5a**) to a radical-anion (**5.1**). This radical anion further eliminates one proton (H^+) to make a stable benzylic-radical intermediate (**5.2**), which reacts with *α*,*β*-unsaturated ketone to generate another stable radical intermediate (**5.3**). Finally, this radical species serves the role of terminal reductant for excited perovskite nanocrystals to come back into the ground state, accepting one photogenerated hole from the valance band of nanocrystals. When methyl vinyl ketone (MVK) was utilized as the source of *α*,*β*-unsaturated ketone, an isolated reaction yield of 85% was observed with just 1 mg of catalyst loading in dichloromethane solvent with 455 nm blue LED irradiation.

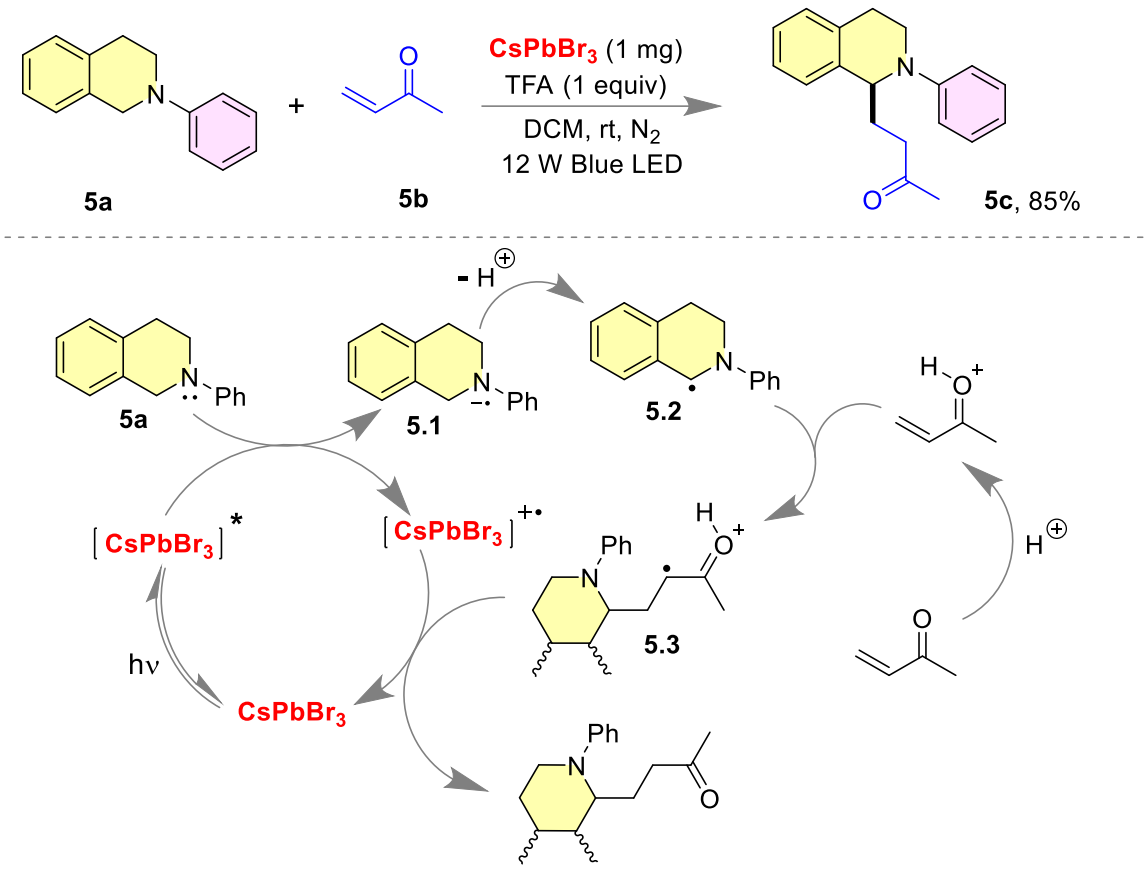

Scheme 5. Conjugated C-C coupling in *α,β*-unsaturated ketones by Yan's group

1.6 LHP Perovskite NCs catalyzed cascade cyclization of cyclic tertiary amine

After the conjugated C-C coupling in *α,β*-unsaturated ketones, they extended the protocol to a 1,1-dicyano styrene system like benzylidene malononitrile (**6b**), where the initially formed radical is stable enough to make a six-membered cascade cyclization in the parent aromatic ring (Scheme 6)[44]. In that way, they successfully created a very stable radical intermediate (**6.3**) The mechanistic investigation depicts that excited state perovskite NCs oxidize tertiary amine (**6a**) to a radical cation intermediate (**6.1**) by donating one photogenerated hole from its valance band. Then the cation loses one proton (H^+) to make a stable radical species (**6.2**), which attacks 1,1-dicyano fragments to generate a highly stable radical intermediate (**6.3**) which has enough potential to attack the existing aromatic system to furnish another (**6.4**) radical intermediate.

Eventually, the loss of a proton to generate stable H_2O_2 furnishes the final cyclized product (**6c**) where the molecular oxygen serves the role of terminal oxidant and trifluoroacetic acid (TFA) was employed as an additive. Perovskites are sensitive to both inorganic cations and anions, very prone towards ion exchange with any suitable external source, and the photoluminescence (PL) emission enhancement is often observed with organic carboxylic acids like benzoic acid, propionic acid, or TFA. This may be because of the strong hydrogen bonding of acid groups with the halides present in the corners of perovskite's three-dimensional framework[45] or because of the interaction of carboxylate and lead (Pb) ion as reported by Tan *et al*[46]. Also, there is a high binding probability of carboxylate anions on the halide vacancy of the perovskite skeleton[47]. This PL enhancement is workable up to a certain optimum concentration e.g. 6.5-13 mM of TFA, after that optimal concentration is reached, excess acidic proton initiates the deactivation process and eventually ruptures the perovskite framework by leaching halide ions from the system.

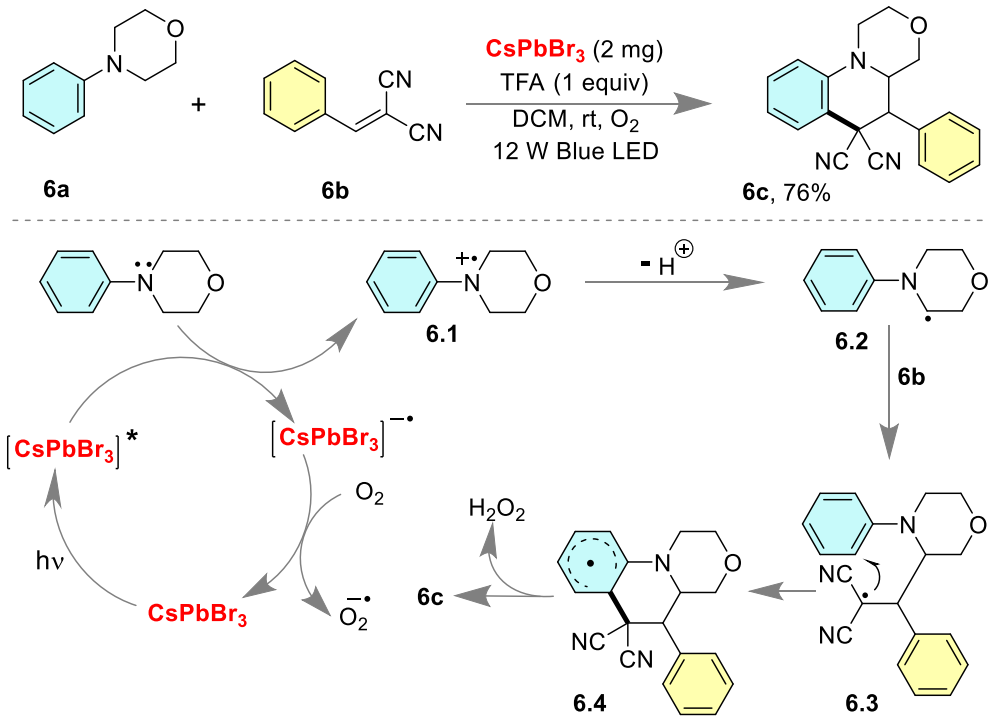

Scheme 6. Cascade cyclization on cyclic tertiary amine by Yan's group.

1.7 Perovskite-catalyzed pyrazole synthesis from acyl halide and hydrazone

Pyrazoles are a very important structural motif to synthesize numerous drugs and bio-active medicinal compounds[48]. Yan's group elongated their work over $CsPbBr_3$ catalysis and extended their strategy toward the synthesis of such an important heterocyclic nucleus. In the same literature, they reported another $CsPbBr_3$ catalyzed visible light-mediated five-membered cyclization leads to the formation of various pyrazole derivatives from the reaction between acyl bromides and hydrazone derivatives in ethyl acetate solvent (Scheme 7)[44]. This strategy outlined a very nice combination where a polar solvent and an inorganic base like cesium carbonate (Cs_2CO_3) in stoichiometric amounts are utilized to deliver optimum reaction yield in an aerial atmosphere. This high-yielding protocol was successful in furnishing a library of substrates with various substitutions on the aromatic ring in hydrazone derivative (**7aa-7ad**) employing Cs_2CO_3 as a proton-scavenger. And, the mechanistic investigation depicted a similar kind of trend as of previous mechanistic cycles proposed by this research group. First, an acyl radical (**7.1**) formed on an electron acceptance from the conduction band of the blue LED irradiated-$CsPbBr_3$ NCs, which reacts with another radical intermediate (**7.3**) to form an acyl hydrazone derivative (**7.4**). Then, this acyl hydrazone species (**7.4**) isomerizes to its enol form via 'keto-enol tautomerization' and subsequently goes through a five-membered cyclization to furnish the anticipated pyrazole derivative. The catalytic cycle is completed with the donation of a photogenerated hole to the hydrazone substrate (**7b**), leading to the formation of radical species (**7.2**) which further eliminate one proton (H^+) to furnish (**7.3**) radical intermediate. Here, the reactant acyl bromide itself plays a very crucial role behind the stabilization of perovskite nanocrystals by acting as a surface-capping or surface-passivating agent as illustrated by Prieto and coworkers in 2020[49].

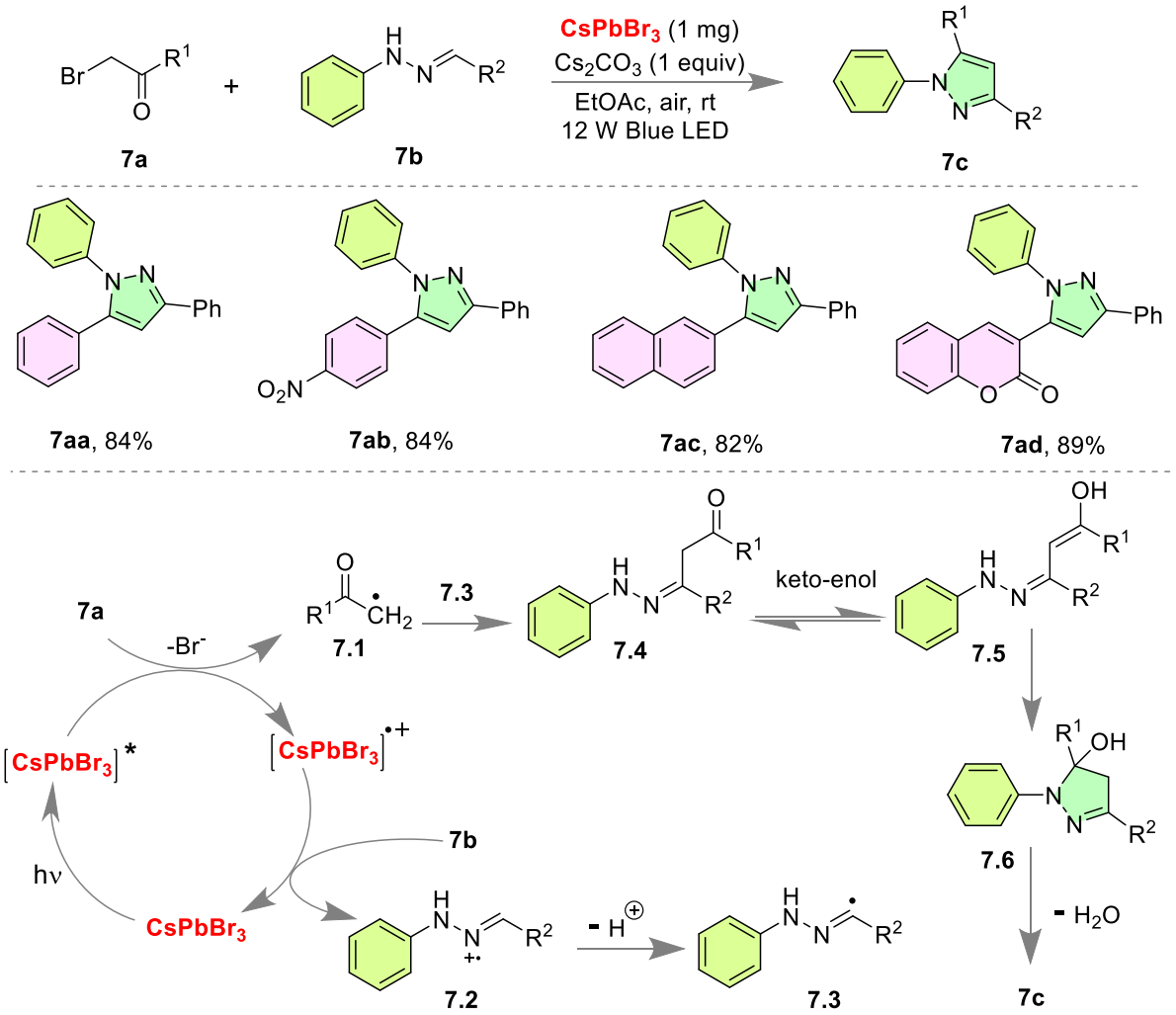

Scheme 7. Photocatalyzed pyrazole synthesis by Yan's group.

1.8 Photochemical pyrrole synthesis utilizing an enamine and acyl halide

Like pyrazole, pyrroles are also considered to be the heart of several important bioactive compounds[50-52]. In the same work, Yan's group reported another strategy to synthesize several pyrrole derivatives by replacing hydrazone derivatives with a suitable enamine source. This synthetic protocol was executed in dichloromethane (DCM) solvent with 12 W blue LED irradiation in an aerial atmosphere using an organic base like triethyl amine (TEA) as a proton abstractor. Numerous pyrrole derivatives were successfully synthesized in this protocol with an average reaction yield of 60 to 70%. The mechanism proposed is slightly different from that

of previous pyrazole synthesis, first $CsPbBr_3$ NC absorbs visible light and one electron gets excited from its valence band to the conduction band. Upon release of that electron from the conduction band to the acyl bromide (**8a**), an acyl radical formed (**8.1**) which gets coupled with an enamine (**8b**) to form another radical intermediate (**8.2**). This radical intermediate offered the role of the terminal reductant, accepting one photogenerated hole from the valance band of the excited $CsPbBr_3$ nanocrystal and transforming itself to an imine (**8.3**). This imine substrate rearranges itself to furnish the anticipated pyrrole derivative (**8c**).

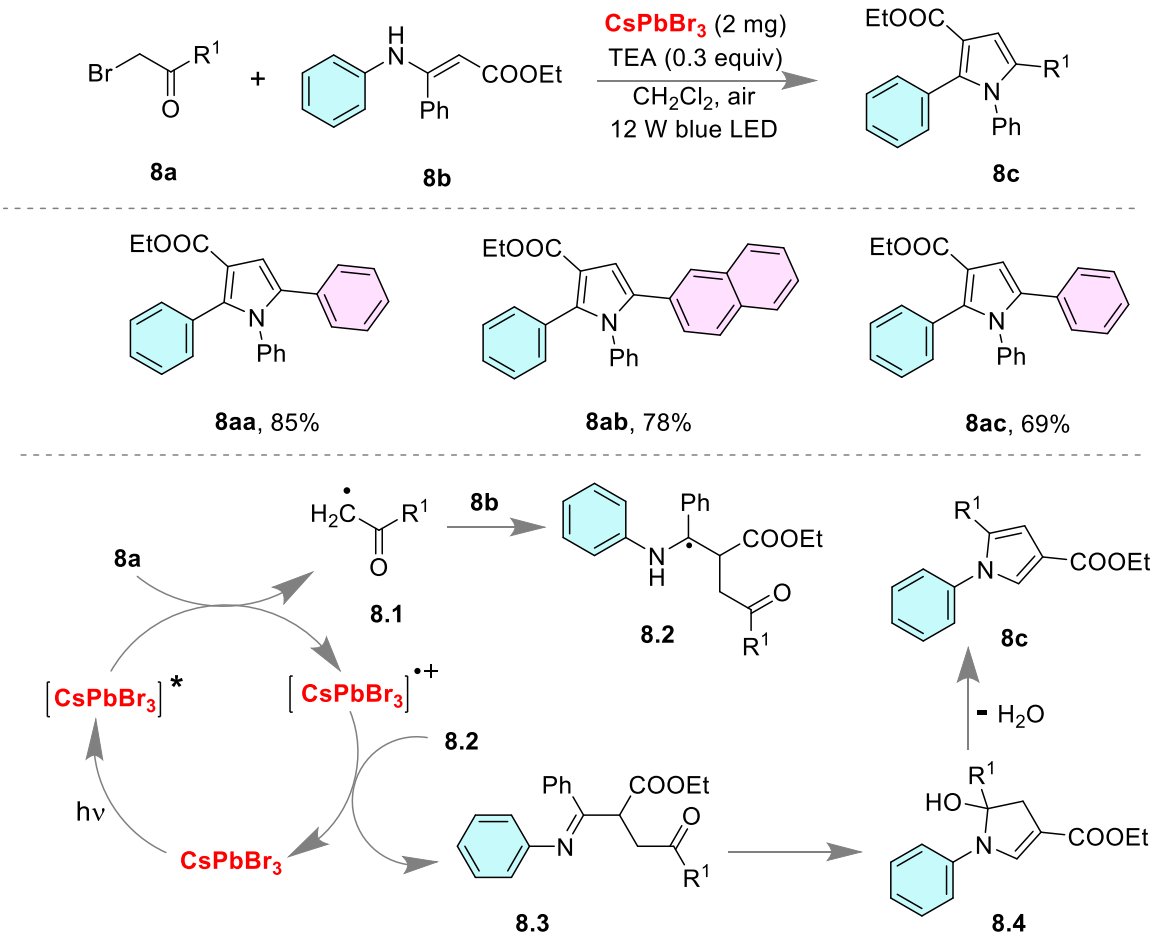

Scheme 8. Photochemical pyrrole synthesis utilizing LHP NCs by Yan's group.

1.9 $CsPbBr_3$ Perovskite sensitized Aryl C-O Cross-Coupling

Like Carbon-Nitrogen, Carbon-Oxygen bond formation is also one of the prime interests in organic chemistry[53-55]. On being exposed to light, a photocatalyst deals with electron donation or acceptance with the substrate, whereas a photosensitizer is related with the transfer of its energy to the substrate after being irradiated[56]. Not only $CsPbBr_3$ perovskite NCs are good photocatalysts to catalyze numerous fundamental organic transformations, but they are also an exceptional candidate to sensitize a transition metal complex in visible light[57-59]. In the same article, Yan and coworkers extended their work to a nickel-catalyzed aryl C-O cross-coupling using LHP NCs as the photosensitizer in CFL illumination at 40 ºC (Scheme 9)[44]. This visible light-induced synthetic protocol typically requires one Ni(0) co-catalyst like [dtbbpyNiCl_2] with 5 mol % loading, which is involved in anion-metathesis with $CsPbBr_3$ NCs and forms a much more effective mixed halide perovskite nanocrystals with different bromine and chlorine ratios ($CsPbBr_xCl_y$). This anion metathesis propelled the reaction forward, and the use of [dtbbpyNiBr_2] instead of [dtbbpyNiCl_2] couldn't deliver the expected aryl C-O cross-coupled product. Here, diisopropyl ethylamine (DIPEA) offered the role of acid quencher during the mechanistic cycle in THF solvent. This developed protocol successfully tolerates a broad range of substitutions (**9aa-9ad**) and was also operative for highly strained three or four-membered rings (**9ae-9af**). The mechanistic investigation suggested an energy transfer between the excited state perovskite NCs and organometallic Ni(0) co-catalyst. Initially, the Ni(0) based co-catalyst goes through oxidative addition with aryl bromide to form a Ni(II) species (**9.1**) which interacts with carboxylic acid to form another Ni(II) intermediate (**9.2**) by elimination of HBr. Now, the CFL-irradiated perovskite nanocrystals transfer energy from its triplet energy state ($\mathbf{T_1}$) to this Ni(II) species. After energy transfer, this (**9.2**) intermediate is excited to another much higher energy species (**9.3**), which makes effective reductive elimination to produce the anticipated C-O cross-coupled product and transform Ni(II) to its ground state.

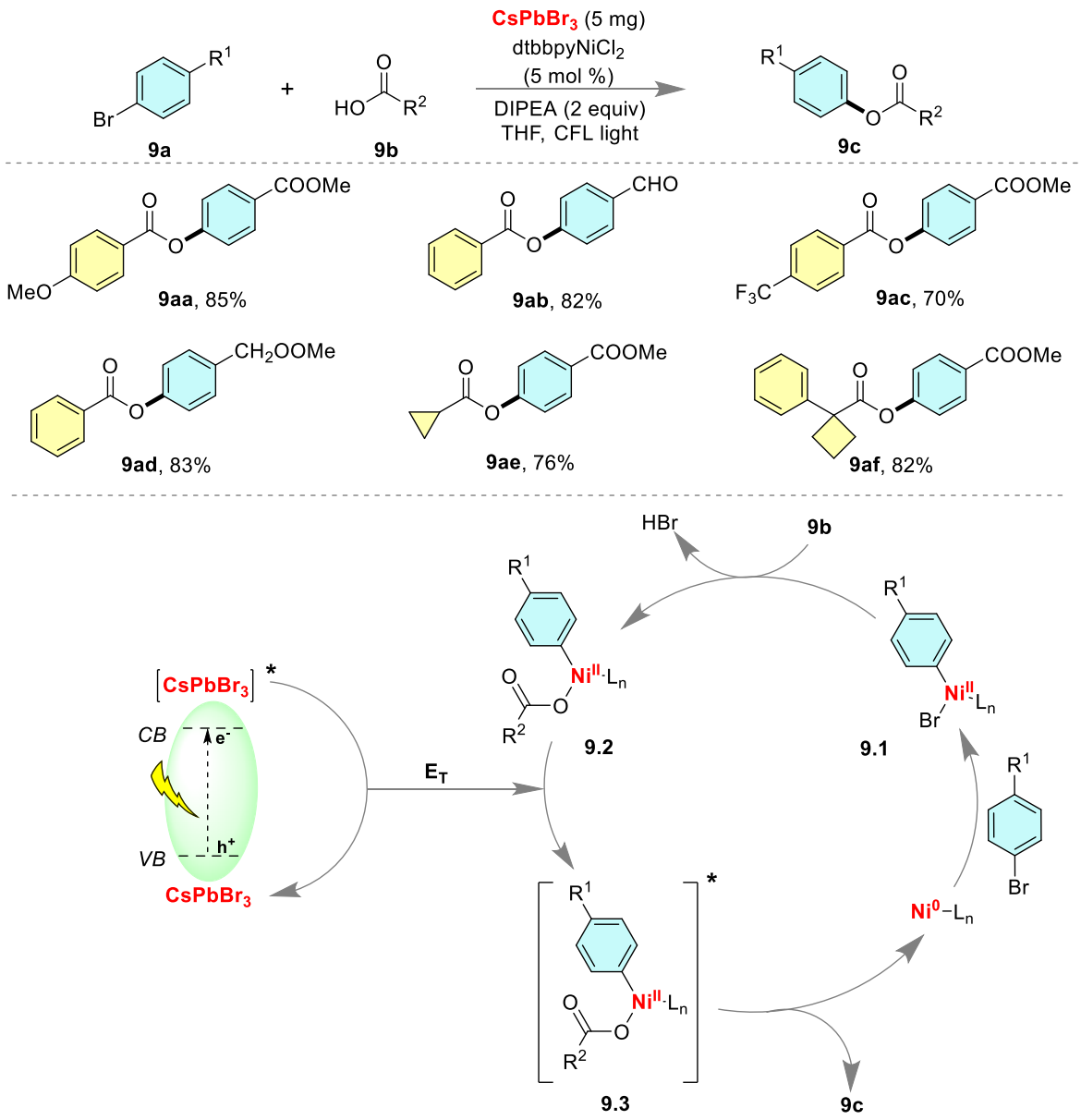

Scheme 9. $CsPbBr_3$ sensitized aryl C-O cross-coupling by Yan's group.

1.10 Photocatalytic dimerization using C-C coupling in aryl halides

There are some vacant places in the three-dimensional framework of lead halide perovskite nanocrystals, which may arise from the deficiency of a halide-ion in the corner, leading to the formation of 'anion-deficient perovskite' or it may arise due to the absence of a Pb(II) ion which is termed as 'cation-deficient perovskite'[60-62]. These deficiencies of ions offered a very crucial parameter behind $CsPbX_3$ perovskite's enormous potential. And, this enchanting feature

helps LHP NCs to abstract halide ions from any nearby external source to fill their vacancy, leading to the generation of a unique way of catalytic activity. So, the PL emission spectra of LHP NCs are often largely blue- or red-shifted in any halide-based solvent like DCM, DBM, DCE, etc., or in the presence of any halide-based reagents[26, 31, 63-64].

In 2020, Pardo *et. al*. revealed a photochemical homo- or hetero-coupling of aryl bromides at room temperature using colloidal $CsPbBr_3$ perovskite NCs as the photocatalyst in the presence of an organic nitrogen-based base like DIPEA (Scheme 10)[49]. The turnover number (TON) for this specific conversion reached up to 15000 with 447 nm blue LED irradiation in toluene solvent and undoubtedly anion-metathesis played a significant role behind this conversion. The synergy between the ligand and the NC surface plays a crucial role in this synthetic protocol, where dodecylamine (DDA) was employed as the capping agent to form the colloidal LHP NCs with a concentration of 1.44 μM. Several C-C coupled products were furnished using DIPEA with a stoichiometric ratio ranging between 10 and 20 equivalents, where DIPEA served the role of the terminal reductant, bringing back excited perovskite NCs to its ground state by accepting a photogenerated hole from its valance band (VB). Several homo-coupled products (**10aa-10ad**) were delivered with a very good reaction yield and also, a few unsymmetrical C-C coupled products (**10ae-10ag**) were successfully synthesized with moderate reaction yield. On the interpretation of mechanistic investigation, it was found that $CsPbBr_3$ perovskite NCs worked as an excited state reductant here, reducing benzyl bromides to a stable benzylic radical cation (**10.1**) by donating one excited electron from its conduction band. This highly stable benzylic radical dimerizes with itself or another benzylic system to produce symmetric and unsymmetric C-C coupled products.

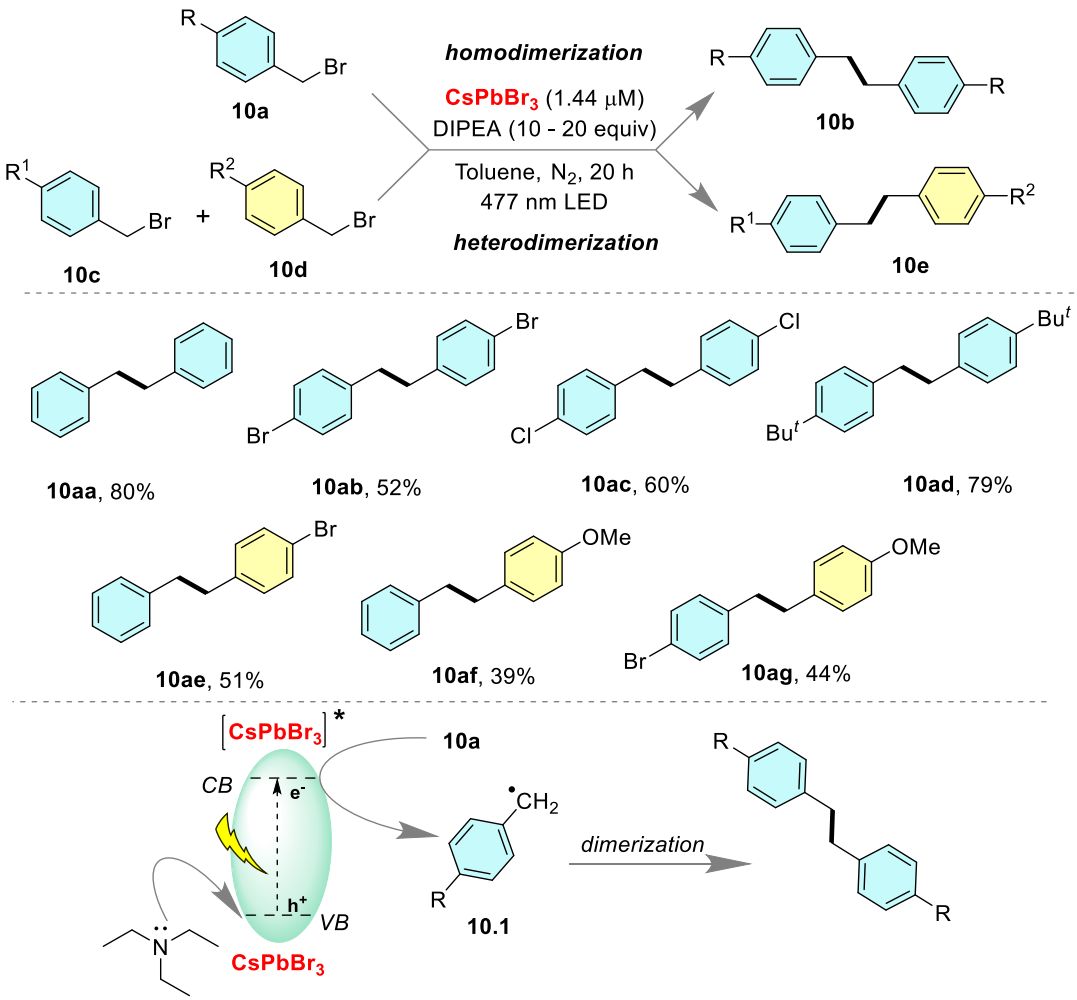

Scheme 10. Dimerization of benzylic bromides by Pardo *et al*.

1.11 Photochemical amino-methylation in imidazole-fused heterocycles

Like thiols, amines, or carboxylic acids, zwitterions are also outstanding capping agents for lead halide perovskite nanocrystals[65-68]. And, in this perspective, using an amino acid as a reactant in perovskite catalysis receives additional benefits over any other substrate due to surface-passivation of the nanocrystals by working as a ligand[69-71].

In 2020, Shi *et. al.* reported an aminomethylation reaction in an imidazole-fused heterocyclic system by using a modified amino acid as a coupling partner and a highly recyclable $CsPbBr_3$ perovskite nanocrystal as the heterogeneous photocatalyst in visible light irradiation (Scheme

11)[72]. After optimizing with several solvents, it was found that dichloroethane (DCE) was the optimum choice for their developed protocol and achieved up to 90% isolated reaction yield in white LED irradiation. Not only external LED, this specific protocol was also possible to carry out in the sunlight, producing almost the same reaction yield as a white LED with just 1 mol % of the catalyst loading in 12 h reaction duration. This strategy is capable of performing both in air and in an inert nitrogen atmosphere, but the yield in the N_2 atmosphere is somehow less compared to the oxygen-mediated pathway. Here, *N*-phenyl glycine, a modified amino acid, was used as the coupling partner and after a decarboxylation process, it became the precursor of aminomethyl functionality. Numerous heterocyclic products successfully delivered with a broad range of substitutions on the imidazole fused heterocyclic part (**11aa-11af**) with very good to average reaction yield and was also operative for a heterocycle containing multiple heteroatoms (**11ah**). Changing substitution on the coupling partner, also furnished the expected product (**11ag**) with a 68% reaction yield. The mechanistic cycle for the N_2-mediated pathway is slightly different compared to the O_2-based pathway. Excited perovskite NCs donate one photogenerated hole to the *N*-phenyl glycine (**11b**), leading to the formation of a carboxylate radical (**11.1**) which goes via decarboxylation to generate an aryl radical intermediate (**11.2**). Next, this aryl radical (**11.2**) couples with imidazole fused heterocyclic substrate (**11a**) to furnish a highly stable radical intermediate (**11.3**), which is oxidized to a carbocation (**11.4**) with molecular oxygen and finally delivers the coupled product by eliminating one proton (H^+). Here, also molecular oxygen serves the role of terminal oxidant for returning excited-state perovskite nanocrystals to their ground state by accepting an excited electron from the conduction band of the nanocrystals.

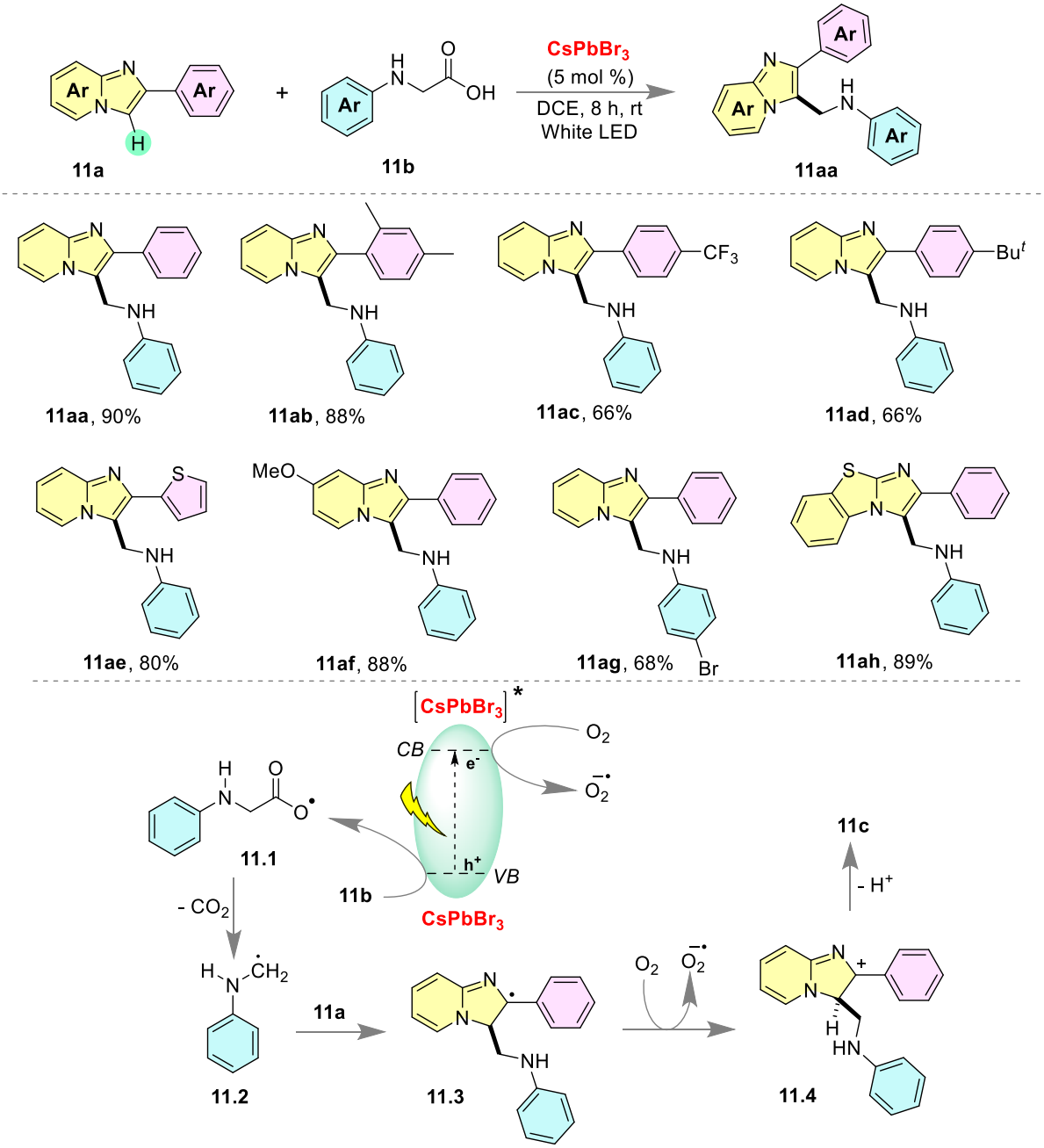

Scheme 11. Aminomethylation in imidazole-fused heterocycles by Shi *et. al.*

1.12 Cascade cyclization on Quinoxalines with *N*-alkyl glycines

Quinoxalinones are very essential structural motifs to synthesize numerous drugs and bio-active compounds[73]. Numerous methods have been developed in organic chemistry to synthesize or modify such organic frameworks in bench-stable conditions[74-77].

In 2020, Yu's group reported another LHP NCs catalyzed radical cyclization on quinoxalinone using *N*-phenyl glycine as the coupling partner with visible light irradiation (Scheme 12)[78]. This cascade cyclization successfully operated to furnish numerous quinoxalin-2(1*H*)-one derivative (**12aa-12af**) using dimethyl carbonate (DMC) as a non-polar media in white LED irradiation. Simple quinoxalinone (**12aa**) or *N*-alkyl quinoxalinone (**12ab-12ac**) both performed with satisfactory reaction yield and substitution of the nitrogen center with ethynyl (**12ad**) or a much larger group (**12ae-12af**) also delivered satisfactory reaction yield in this synthetic protocol. Multiple substitutions on the benzenoid part of the quinoxaline framework (**12ag**) also furnished the expected product with more than 75% of the reaction yield. The mechanistic cycle follows a similar trend as of previous one, excited perovskite NCs donate a photogenerated hole to the *N*-phenyl glycine (**12b**), leading to the formation of a carboxylate radical (**12.1**), which generates a stable aryl radical intermediate (**12.2**) on spontaneous decarboxylation. This radical intermediate couples with quinonoxalione (**12a**) and furnished (**12.3**) radical species. Again, (**12.3**) radical couples with another aryl radical intermediate (**12.2**) to form (**12.4**) intermediate. After that, protonation followed by an elimination produces a cationic species (**12.6**), which goes through a nucleophilic attack from the existing nitrogen center inside its framework to furnish the ultimate cascade cyclized product (**12c**).

The *N*-phenyl glycine is a derivatized amino acid, that exists in the form of a zwitter ion and is a typical radical initiator for numerous photocatalyzed organic transformations[79]. It also has a very high affinity for surface capping of perovskite nanocrystals and plays some unrevealed role in the stabilization of perovskite NCs[80]. So designing such a reactant is very important for perovskite catalysis, which will have a stable radical species masked inside and on the other hand it will gear up the perovskite's stability by capping them in the colloidal dispersed phase.

The outline of this work depicts that a zwitterion may be a reagent of choice for designing organic reaction schemes on perovskite catalysis in the future.

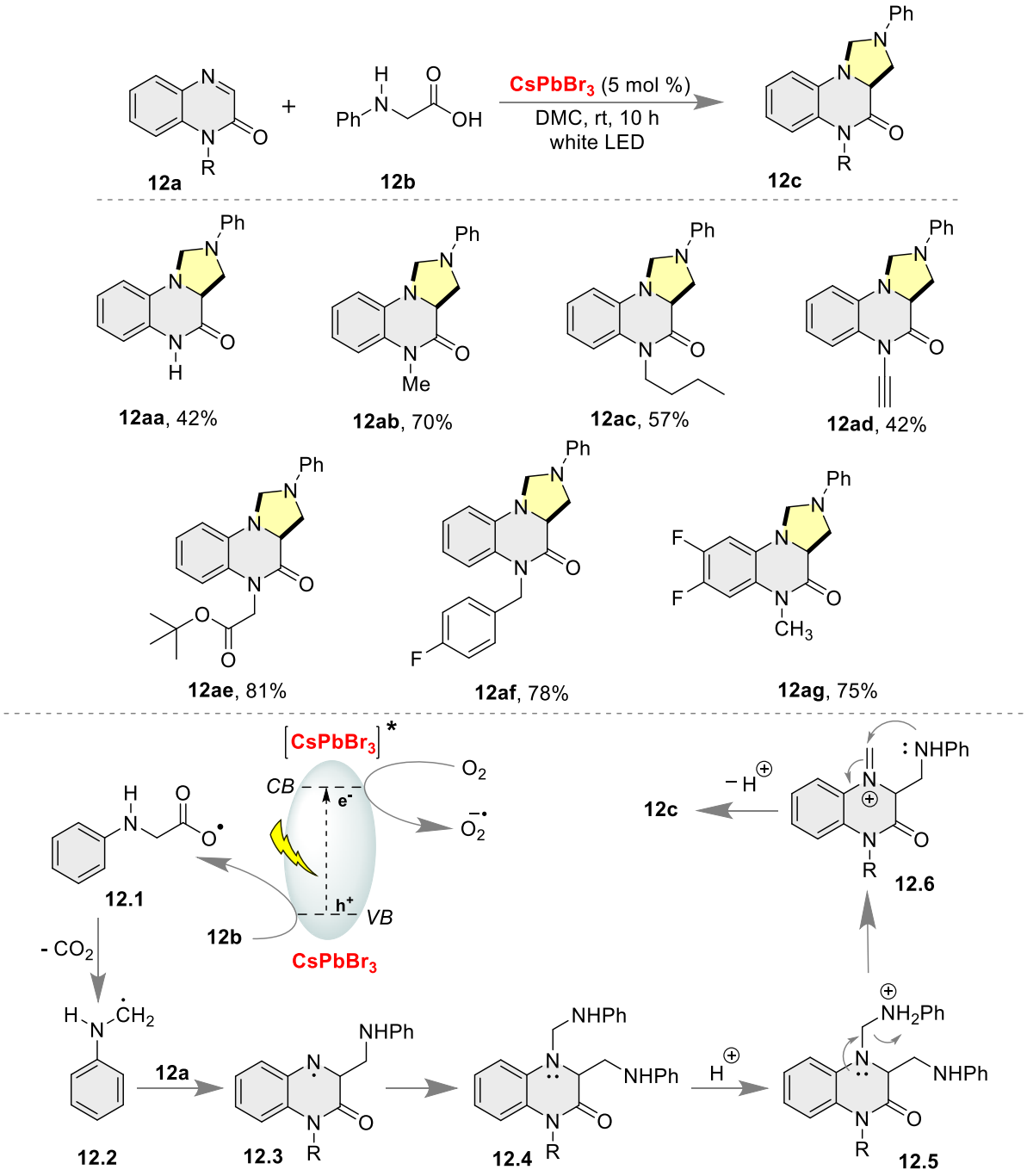

Scheme 12. Photochemical cascade cyclization on Quinoxalinone by Yu's group

1.13 Perovskite-catalyzed stereoselective C-C coupling on *α*-aryl keto nitriles

Zwitterion-capped perovskite NC is known not only for its higher stability in the colloidal phase but also for its outstanding selectivity toward a photochemical reaction[81].

In 2020, Chen's group reported a highly efficient stereoselective C-C oxidative homo-coupling of *α*-aryl keto nitriles using a zwitterionic ligand capped $CsPbBr_3$ perovskite QDs in visible light illumination (Scheme 13)[81]. This protocol was generalized to different starting materials with various substituents on the aromatic framework (**13aa-13ag**), producing stereoselective *dl*-isomers with more than 99 % selectivity. This specific strategy was performed using various non-expensive quantum dot photocatalysts like CdSe, CdS, and various ligand-capped LHP NCs. And, it was found that 3-(*N*,*N*-dimethyloctadecylammonio)propanesulfonate (DMOA-PS), a zwitterion, capped colloidal $CsPbBr_3$ NC QDs are the best candidate among all, which were synthesized using a method developed by the Kovalenko group[82]. Through the surface modification of $CsPbBr_3$ perovskite QDs with DMOA-PS, the stability of QDs and homocoupling reaction rate were dramatically increased, and the stereoselectivity also improved significantly. The $CsPbBr_3$ QDs capped with DMOA-PS, which are called Zwitter-ion capped QDs (ZW-$CsPbBr_3$ QDs) were recycled up to three catalytic cycles and the reaction duration was also dramatically decreased with a very high product selectivity. This protocol performed at its best on a mixture of THF and toluene media with an average optical density of the photocatalyst 7.7 at 470 nm wavelength. A reaction scope investigation depicted that electron-donating groups (EDGs) or large conjugated π-systems are necessary for efficient dimerization. After a bunch of control experiments, a radical-mediated pathway was proposed where colloidal ZW-$CsPbBr_3$ perovskite QDs act as an excited state oxidant, oxidize (**13a**) to a radical cationic species (**13.1**) which further loses one proton to furnish a very stable *α*-cyano benzylic radical (**13.2**). This stable radical species dimerizes to form the expected homocoupled

product (**13b**). Here, molecular oxygen serves the role of terminal oxidant for stabilizing excited ZW-$CsPbBr_3$ perovskite QDs to their ground state by reducing itself into a super-oxide radical anion.

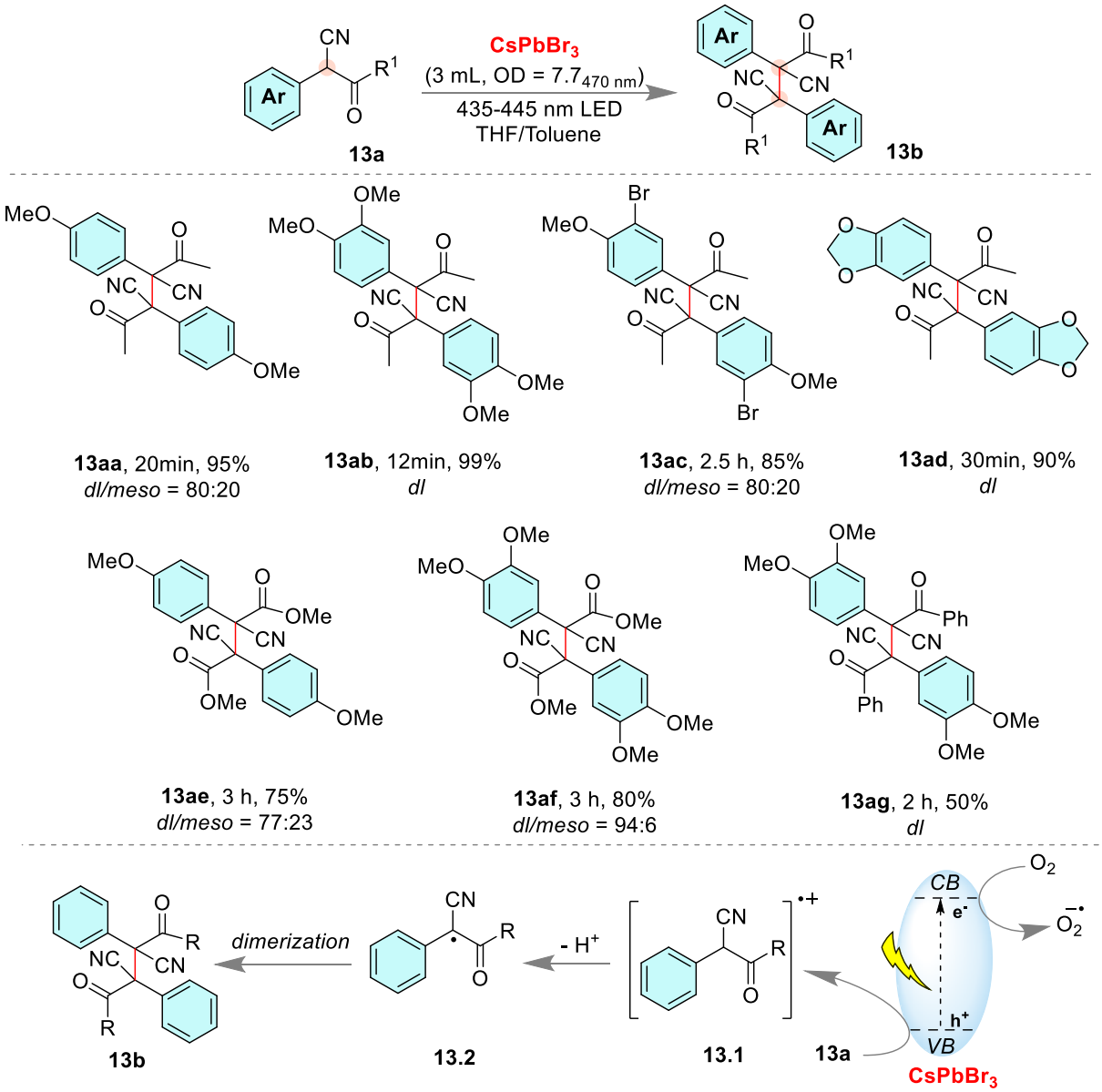

Scheme 13. Stereoselective C-C homocoupling in *α*-aryl keto nitriles by Chen's group.

1.14 Perovskite catalyzed photochemical thioether synthesis

Organosulfur derivatives are essential because of their omnipresence in biochemistry. Selectively, thioether-based heterocyclic frameworks are a class of compounds with very high

anti-cancer activity[83]. So, numerous synthetic protocols have been developed to synthesize such important structural motifs by employing metal-free[84-86], or metal-based pathway[87-89]. Thioethers or organic sulfides can be prepared from thiols, which are a very good candidate for surface passivation of LHP NCs by acting as a capping ligand[90].

In 2021, Xing's group reported a photochemical thioether synthesis from thiol and olefins using 1 mol % loading of $CsPbBr_3$ perovskite NCs as the photocatalyst in the presence of 32 W blue LED irradiation (Scheme 14)[91]. This protocol was operated in an inert atmosphere using acetonitrile as the optimized solvent to synthesize several organic sulfides within a 3 h reaction duration. The strategy effectively worked for various aromatic olefins (**14aa-14ad**) with outstanding yield, and also, some acyclic olefins (**14ag-14ah**) responded to this strategy with an average reaction yield. A few aliphatic cyclic olefins (**14ae-14af**) also obeyed the protocol with moderate reaction yield. Mechanistic investigation elucidates that the conduction band and the valance band of $CsPbBr_3$ NCs are located at - 1.49 V (vs. SCE) and +0.93 V (vs. SCE) respectively[38]. So, the oxidation potential of $CsPbBr_3$ perovskite nanocrystal is much more positive than the majority of the thiols like benzyl mercaptan (+0.45 V vs. SCE)[92], indicating LHP NCs are capable of oxidizing thiol systems (**14b**) into thiyl radical (**14.1**). This thiyl radical is added to the terminal alkenes to form a highly stable benzylic radical (**14.2**). This radical intermediate can be quenched in two ways, it may take one hydrogen radical from the existing thiol molecule and start a chain reaction, or it may accept one excited electron from the conduction band of the nanocrystals to form the anticipated thioether derivative.

Previously in 2018, Wu's group explored a $CsPbBr_3$ perovskite NCs catalyzed disulfide formation from thiols (Scheme 2), and here, in this protocol, thiols have been used in different stoichiometry to make a radical addition in terminal olefins by suppressing the disulfide generation. At least, 2.5 equiv of thiols are needed for effective addition in alkenes, and to stop

the dimerization of thiols in the presence of perovskite photocatalyst in visible light. This is one of the beautiful examples of how stoichiometry play a significant role on the selectivity of the reaction.

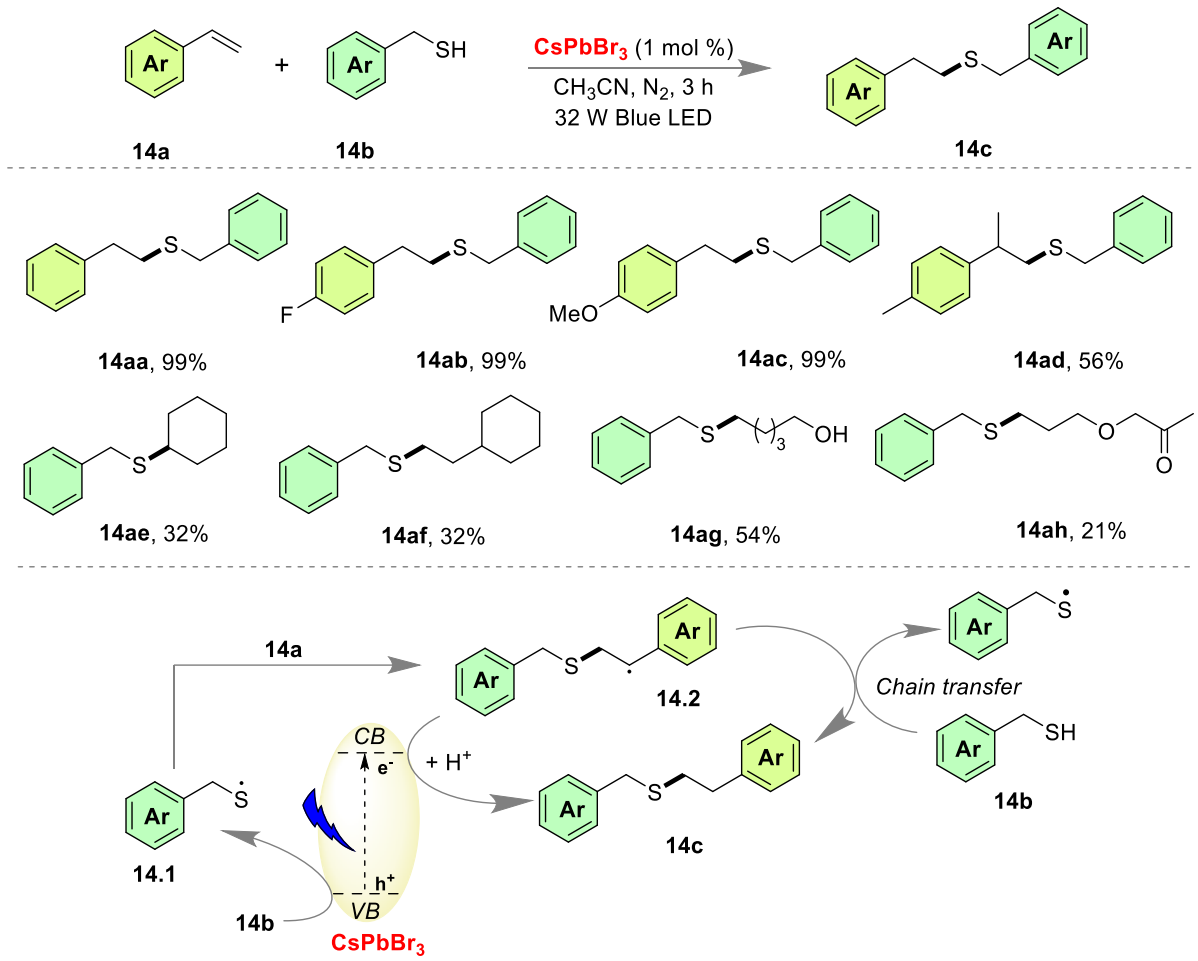

Scheme 14. Photochemical thioether synthesis from terminal alkenes by Xing's group.

1.15 Photochemical aromatization of Hantzsch esters using colloidal $CsPbBr_3$

Radical-mediated catalytic dehydrogenative aromatization has emerged as a beautiful route to furnish several highly substituted aromatic architectures from cyclic aliphatic skeleton[93-96]. In this perspective, Hantzsch esters, which were previously used as reductants in thermal transformations, have evolved as a versatile class of reagents in photo-organic chemistry with extraordinary demands[97-100]. However, photocatalytic dehydrogenative aromatizations of

nitrogen-based heterocycles like 1,2-dihydropyridines (1,2-DHP), or 1,4-dihydropyridines (1,4 DHP) are kinetically slow reactions, often requiring a potent oxidant.

In 2021, Tamang's group reported the dehydrogenative aromatization of various 1,4-Dihydropyridines (1,4-DHPs) or Hantzsch esters (**15a**) using halide passivated colloidal $CsPbBr_3$ perovskite-quantum dots (CQD $CsPbBr_3$) in visible light (Scheme 15)[101]. A library of pyridine derivatives (**15aa-15ad**) was synthesized with just 1 mg of bromide-rich CQD $CsPbBr_3$ perovskite NCs loading using DCE solvent in an aerial atmosphere. Here, molecular oxygen from the air acts as a benign source of oxidant by surpassing the degradative nature of conventional $CsPbBr_3$ perovskite NCs in an oxygen and moisture environment[102]. And, somehow, these newly formed colloidal $CsPbBr_3$ perovskite QDs are not that sensitive to moisture or oxygen. Blue LED irradiated CQD $CsPbBr_3$ perovskite NCs worked as an excited state reductant, reducing molecular oxygen to a superoxide radical anion by donating an excited electron from its conduction band. The excited perovskite oxidizes the dihydropyridine system (**15a**) to an *N*-centered radical cationic system (**15.1**) by donating one photogenerated hole, which further interacts with superoxide radical anion to make another *N*-centred radical species (**15.2**). This radical species again reacts with hydroperoxide radical to form another diradical (**15.3**) which rearranges to furnish the final aromatized pyridine product.

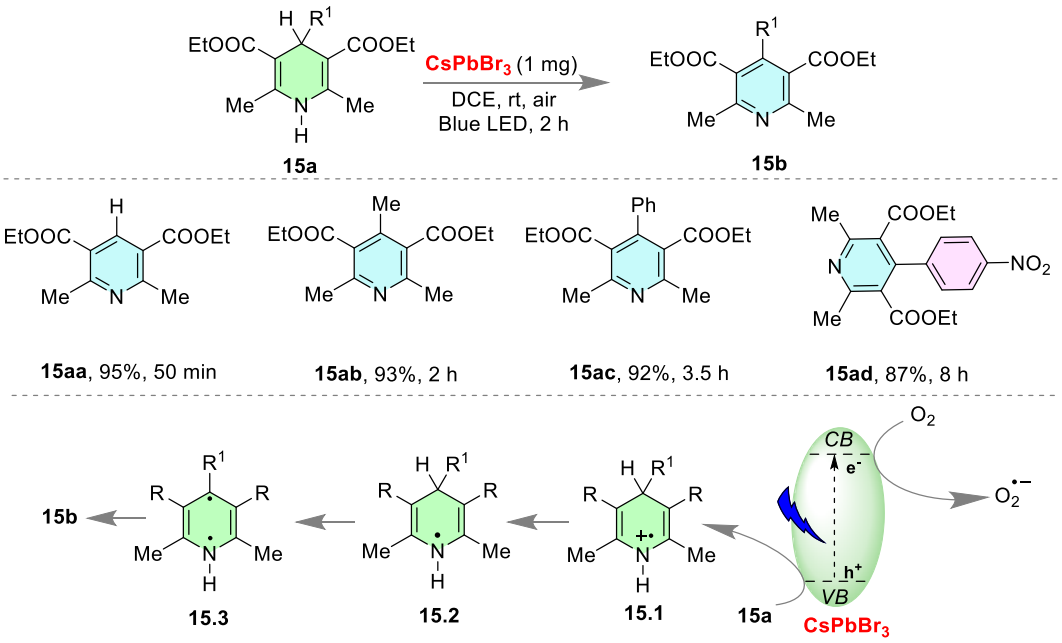

Scheme 15. Oxidative aromatization of Hantzsch esters by Tamang's group.

1.16 CQD $CsPbBr_3$ catalyzed aromatization of Hexahydro-acridine systems

Following this report, Tamang's group extended their protocol for oxidative aromatization of a much more complicated 3,4,6,7,9,10-hexahydroacridine-1,8(2H,5H)-dione systems (Scheme 16) with the utilization of a bromide rich $CsPbBr_3$ CQDs in DCE solvent in 40 W Blue LED[101]. This monodispersed, air-stable, and halide-rich $CsPbBr_3$ CQDs were prepared using a 'three precursors method' where a halide source was added externally in Oleyl amine unlike most of the 'two precursors method'[18] where the halide source is lead salt itself like PbX_2. Due to the utilization of individual Cs, Pb, and Br sources, desired halide-rich $CsPbBr_3$ CQDs have a very small amount of vacant sites where moisture or oxygen can penetrate and the resulting NCs become very resistant to conventional destabilizing factors. And, this bromide-rich perovskite NCs is used for oxidative aromatization of several 3,4,6,7,9,10-hexahydroacridine-1,8(2H,5H)-diones (**16a**) by following the previous mechanistic cycle. And, the strategy performed well for a broad range of substrates (**16aa-16ac**) with satisfactory reaction yield.

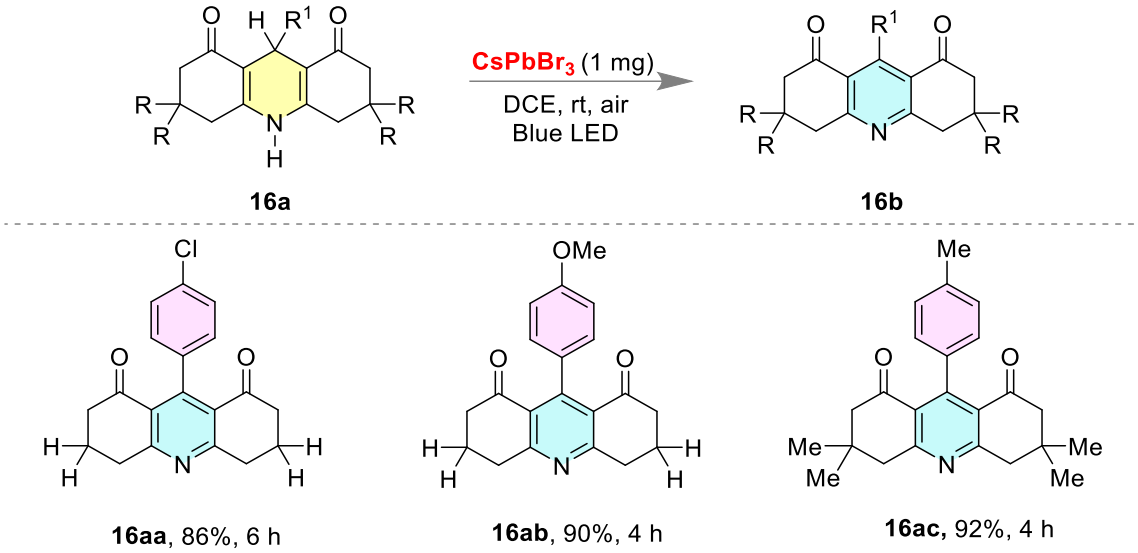

Scheme 16. Aromatization of cyclohexanone-fused 1,4-DHPs by Tamang's group.

1.17 CQD $CsPbBr_3$ catalyzed oxidative aromatization of 1,2-DHPs

The investigation on dihydropyridines was first started by Hantzsch in 1882 in the course of developing various pyridine derivatives[103]. The interest in these molecules outbreak with the discovery of NADH, a natural reducing agent, containing a dihydropyridine framework attached to the sugar ring. Like 1,4-DHPs, 1,2- Dihydropyridines are also significant structural motifs to synthesize various pharmaceutically active pyridine and piperidine derivatives by working as reactive synthons[104]. 1,2-DHPs and 1,4-DHPs may look structurally similar but differ very much in reactivity[105].

Tamang's group extended their oxidative aromatization technique to the 1,2-Dihydropyridines (1,2-DHPs) using the same colloidal $CsPbBr_3$ perovskite quantum dots as the non-expensive photocatalyst in the presence of 40 W blue LED irradiation (Scheme 17)[101]. Various azaheterocycles (**17aa-17ad**) were synthesized within a few hours with an excellent reaction yield in an aerial atmosphere using DCE as the optimized solvent in visible light irradiation. Several control experiments indicated a SET reaction mechanism as previously for 1,4-DHPs.

Blue LED irradiated CQD $CsPbBr_3$ perovskite nanocrystals behave as excited state reductants, reducing molecular oxygen to a superoxide radical anion. The excited state perovskite radical cation oxidizes the substrate (**17a**) to an *N*-centered radical cationic system (**17.1**) by photogenerated hole transfer, which further interacts with superoxide radical anion to make another *N*-centred radical intermediate (**17.2**). This radical intermediate again reacts with hydroperoxide radical to form a diradical species (**17.3**), which eventually furnishes the final pyridine product, and a stable molecule of hydrogen peroxide is eliminated from the system as a byproduct.

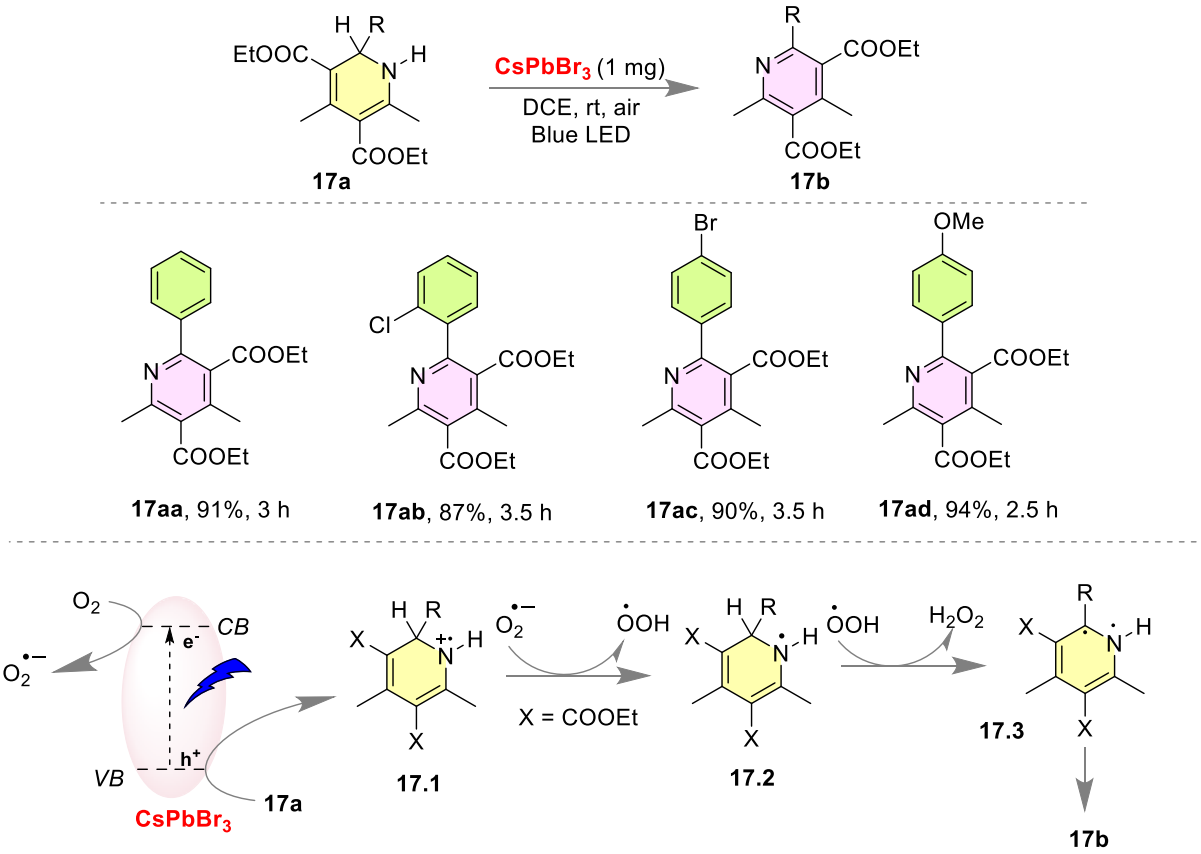

Scheme 17. Dehydrogenative aromatization of 1,2-DHPs by Tamang's group

1.18 CQD $CsPbBr_3$ catalyzed oxidative aromatization of 4,5-dihydro pyrazoles

Pyrazoles are one of the most important structural motifs to synthesize several bioactive drug molecules and natural products[106]. And, the most benign source to aromatize the

dihydropyrazole to aromatic pyrazole is singlet oxygen. Oxygen-sensitive colloidal perovskite QDs are capable of reducing molecular oxygen to a superoxide radical anion which plays the vital oxygenation source for this oxidative aromatization. Tamang and coworkers developed a protocol to oxidize several 1,2-DHPs and 1,4-DHPs which also worked for 4,5-dihydro pyrazole systems (Scheme 18) and synthesized several pyrazole derivatives with excellent reaction yields (**18aa-18ad**)[101]. This aromatization procedure is also mechanistically similar to the previous one, where molecular oxygen dominates over the catalytic cycle.

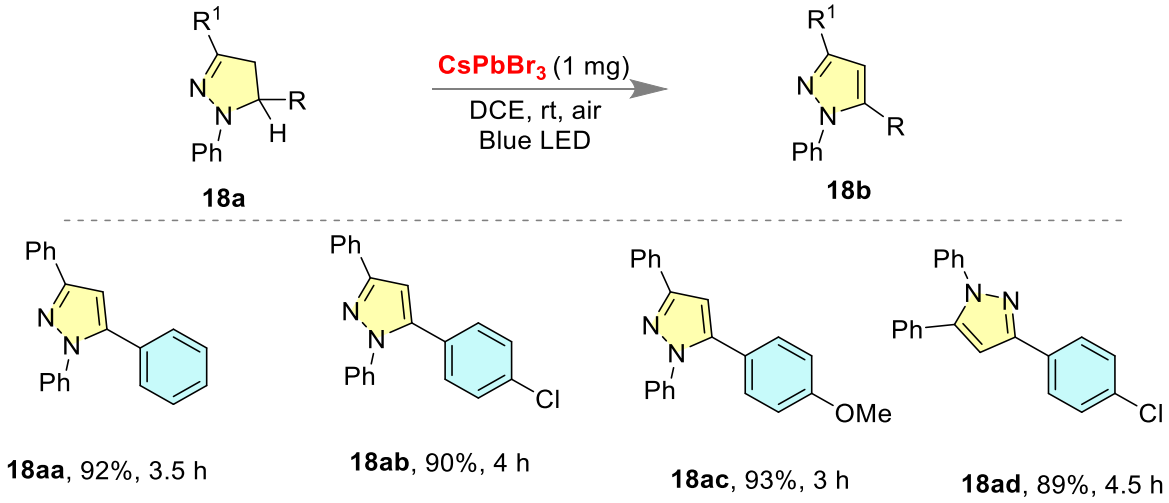

Scheme 18. Oxidative aromatization of 4,5-Dihydro pyrazoles by Tamang's group

1.19 $CsPbBr_3$ catalyzed oxidative aromatization of 1,2-dihydro benzothiazoles

After that, Tamang's group extended their strategy to dihydro-benzothiazole systems (**19a**) and synthesized several benzothiazole derivatives with an excellent reaction yield within a few hours in the presence of 40 W blue LED irradiation (Scheme 19)[101]. This synthesizing strategy also follows the same mechanistic way, where aerial molecular oxygen dominates over the catalytic cycle. Both *para*- and *ortho*-substituted phenyl rings obeyed the protocol and furnished the benzothiazole derivatives using bromide-rich colloidal CsPbBr3 perovskite QDs.

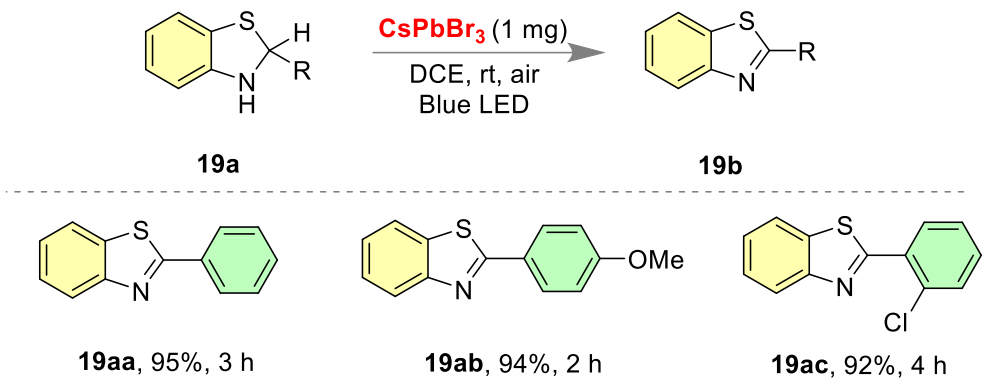

Scheme 19. Oxidative aromatization of dihydro benzothiazoles by Tamang's group.

1.20 $CsPbBr_3$ catalyzed photochemical oxidation of sulfide to sulfoxide

Organosulfur compounds are immensely important in organic as well as medicinal chemistry due to their omnipresence. So, numerous methodologies have been developed to synthesize such important structural motifs in both metal-free[86] and metal-based pathways[89]. Among all, organo-sulfur compounds, sulfur(IV) center-containing motifs are very prominent, and have been a subject of research for several decades[107]. Organic sulfoxide contains a sulfinyl functionality (S=O) which makes it chiral by separation of charges between two atoms, and is used broadly to serve numerous medicinal purposes[108].

In 2021, Ding and coworkers reported a facile protocol for the photocatalytic oxidation of a series of sulfides to their corresponding sulfoxides with excellent yields and selectivity using 10 mg of solid $CsPbBr_3$ perovskite nanocrystal as a visible-light photocatalyst in DCM solvent with 100 W blue LED irradiation (Scheme 20)[109]. The strategy successfully furnishes several sulfoxide derivatives (**20aa-20ad**) within 8 h at room temperature in an aerial atmosphere. Checking the reaction with different quenchers, the mechanistic investigation revealed that molecular oxygen plays a pivotal role in the catalytic cycle. Initially, perovskite nanocrystals are excited with 100 W blue LED irradiation and reduce molecular oxygen to a superoxide

radical anion by liberating an excited electron from its conduction band. Then, the excited perovskite nanocrystals came back to the ground state by oxidation of thiols to thiyl radical cation (**20.1**), donating a photogenerated hole, which reacts with superoxide radical anion to form another intermediate (**20.2**). This intermediate species reacts with the original thiol substrate (**20a**) to make the final sulfoxide product (**20b**). Here, it's suspected that an energy transfer mechanism may also be operated with an equal probability as electron transfer. The $CsPbBr_3$ perovskite nanocrystals, which were used as the visible-light photocatalyst, were synthesized from $PbBr_2$ and CsBr by using a 'two-precursor method' developed by Zhu[30].

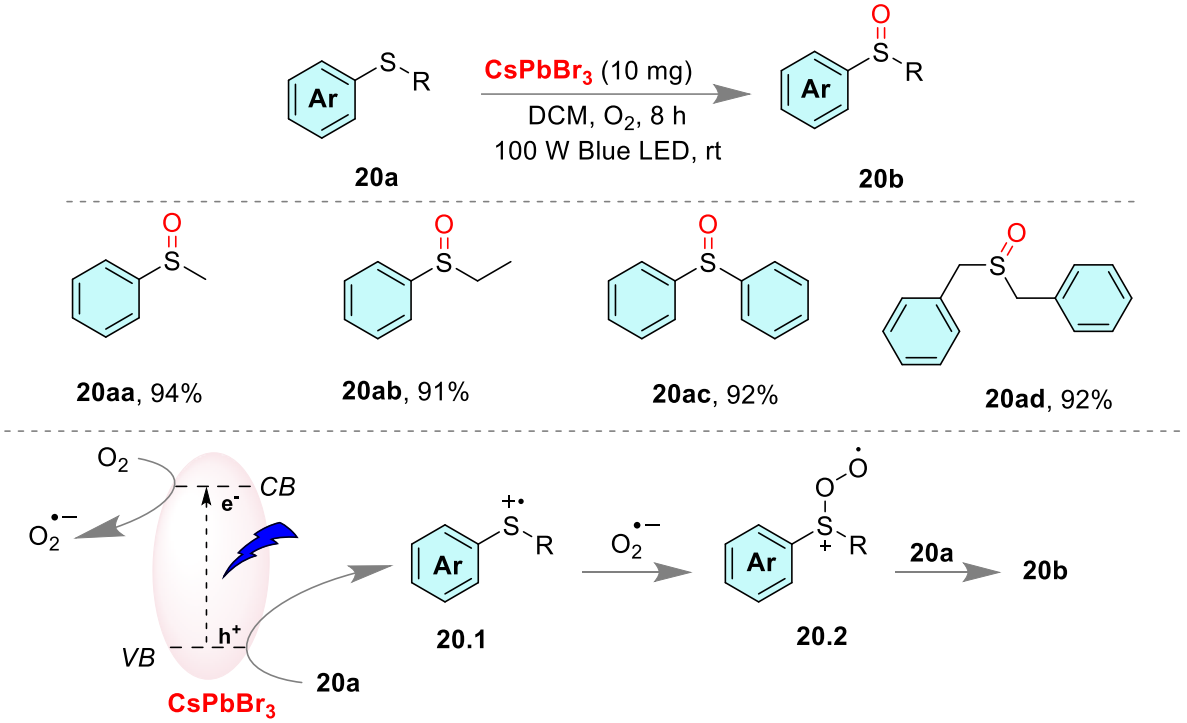

Scheme 20. Photochemical oxidation of sulfides to sulfoxides by Ding's group.

1.21 Photochemical imine and aldehyde synthesis from primary amine

Ding and coworkers developed another facile protocol to synthesize various imines and aldehydes from primary amines with excellent yields using $CsPbBr_3$ perovskite NCs in visible light irradiation (Scheme 21)[109]. It was observed that amines bearing electron-donating groups

(EDGs) furnished aldehydes as the final products, while amines with electron-withdrawing groups (EWGs) afforded imines as the major products. This synthetic protocol was executed in DCE solvent with very good selectivity of aldehydes for strong EDGs (**21aa-21ad**) and imines with strong EWGs (**21ae-21ag**) in 100 W blue LED irradiation. Mechanistic investigation revealed that blue LED irradiated perovskite NCs worked as an excited state oxidant, oxidizing benzyl amines (**21a**) to a benzylic cationic species (**21.1**) which reacts with superoxide radical anion to form another intermediate (**21.2**). Then the intermediate (**21.2**) releases hydrogen peroxide as a stable molecule to form an imine intermediate (**21.3**) which readily hydrolyses in the presence of water to produce aldehydes (**21a**). Now, this aldehyde may go further to attack electron-deficient amine systems to produce imines (**21b**) as the selective product.

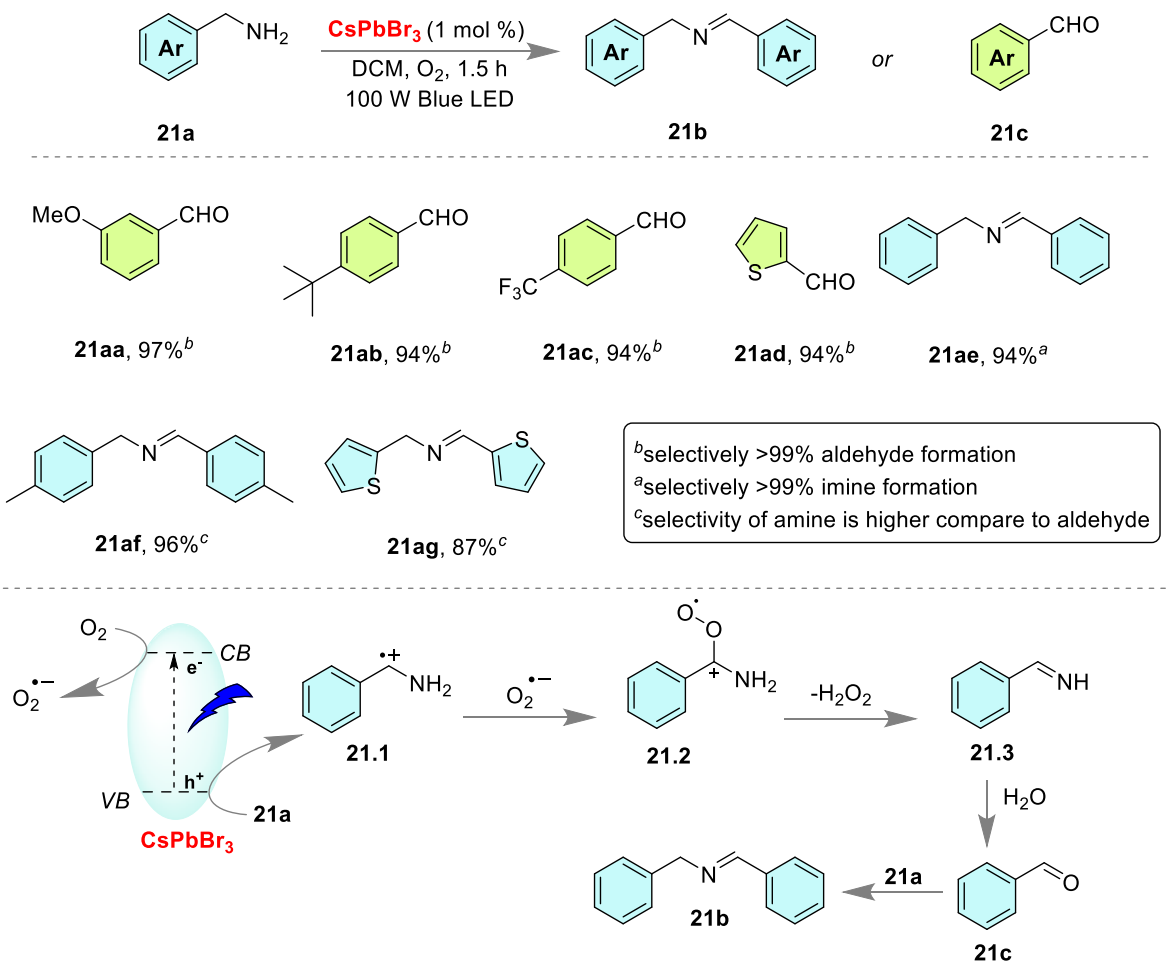

Scheme 21. Photochemical imine and aldehyde synthesis by Ding's group.

1.22 Cu-doped $CsPbBr_3$ catalyzed N-N hetero cyclization by MET pathway

The major difficulty in the use of $CsPbBr_3$ perovskite NCs in photocatalysis is its instability towards moisture, heat, oxygen, polar solvent, etc. The destabilizing factor may be altered by doping of appropriate impurity inside its framework. In this perspective, metal doping has emerged as a brand-new strategy to overcome the instability factors of LHP NCs, high charge carrier recombination rate, and fill the vacant sites in the ionic lattice[110-112]. Also, metal doping in perovskite's three-dimensional framework provides an avenue to boost their potential in terms of various features like enhancement in light emission, nano-scale magnetism, polarization control, or enhanced photocatalytic activity[113-116].

In 2021, Yan's group first reported that a copper-doped $CsPbBr_3$ has the potential for multielectron transfer (MET) and unlocked an attractive N-N hetero-cyclization using surface copper-doped $CsPbBr_3$ perovskite nanocrystals under 450 nm blue LED irradiation with TON over 44600 in four reusable catalytic cycles (Scheme 22)[117]. The photocatalytic $CsPbBr_3$ perovskite NCs were prepared by exposing as-prepared $CsPbBr_3$ NCs to a very dilute solution of CuBr in toluene at room temperature, resulting in lightly doped (Cu:$CsPbBr_3$) NCs where the concentration of the Cu(I) ions are considered to be less than 1% so its atomic ratio is depicted as ($Cu_{0.01}$:$CsPbBr_3$). The $CsPbBr_3$ perovskite nanocrystal (NC) was used to capture photons first and direct photogenerated holes to a surface-bound transition metal Cu-site, resulting in a N−N heterocyclization reaction. Mechanistic investigation revealed that the reaction starts from Cu-doped $CsPbBr_3$ surface-coordinated diamine substrates (**22.1**) and with blue LED irradiation holes are generated inside NCs which funneled to the Cu(I)-surface. This photogenerated hole in the perovskite NCs helps to oxidize surface-anchored Cu(I) to a Cu(II) species (**22.2**), which is further reduced by co-ordinated diamine substrate to another Cu(I) species (**22.3**). Again, the process repeated to form Cu(II) intermediate (**22.4**), and finally

another co-ordinated amine group reduces the Cu(II) and regenerates the catalyst by forming an N-centered diradical species (**22.5**) which dimerizes to form the final anticipated N-N heterocyclized compound. And, the excited perovskite nanocrystal came back to the ground state by reducing molecular oxygen to a superoxide radical anion which eventually transformed into stable hydrogen peroxide in the presence of acidic protons. Here Cu-site serves two important functions, coordinates the diamine substrate and attracts photogenerated holes from the valence band (VB) of the perovskite NCs leading to the multi-electron transfer (MET) to the bound substrate.

The DFT simulations suggested that Cu(I) is the substitute for the Cs-metal center and Cu(II) would substitute for Pb(II). From the EPR experiment, no Cu(II) was detected which eliminates the idea of photocatalytic Cu(I) to Cu(II) oxidation in the presence of light. They have proved also that only Cu cations residing near or at the NC surface are active for this photochemical oxidation while cations diffuse to the center of the NCs or external Cu(I) ions are not catalytically active. Most photocatalysts are capable of only a photoexcited single electron transfer (SET) but this is a rare example of challenging photoexcited multiple electron transfer (MET). And, for that reason, a photocatalytic diradical intermediate (**22.5**) was possible to form using this specific Cu-doped $CsPbBr_3$ NCs. Another interesting fact about these Cu-doped perovskite NCs is that only ~1% Cu(I) doped perovskite performed as the optimized catalyst confirmed by ICP-OES. A higher Cu-loading does not necessarily correspond to a higher reactivity whereas greater than 5% Cu-incorporation resulted in less catalytic activity. Also, >1% Cu-loading corresponds to a lower number of Cu-catalytic sites and the reaction yield was declined. The strategy was successfully performed for a library of substrates leading to the formation of various hexahydro pyridazines (**22aa-22ad**) with various substitutions and also worked for various pyrazolidines (**22ae-22ah**) with an excellent yield.

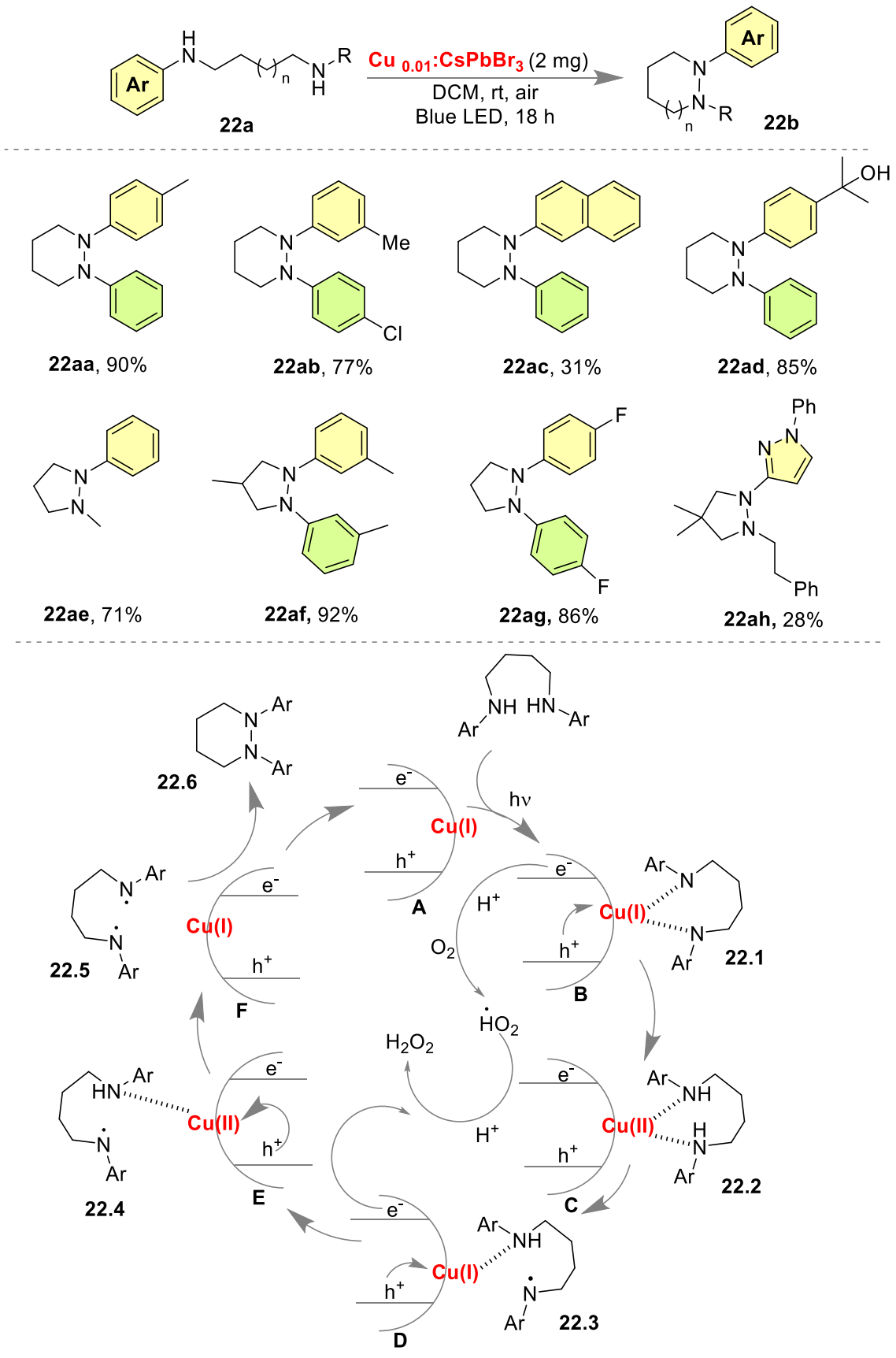

Scheme 22. Cu-doped $CsPbBr_3$ catalyzed N-N hetero cyclization by Yan's group.

1.23 Perovskite catalyzed stereo-specific photocatalytic [2+2] cycloaddition

Oleic acid or Oleylphosphonic is used as the capping agent during the hot-injection synthesis of $CsPbBr_3$ NCs because the carboxylate or phosphate group has a very high anchoring affinity towards these nanocrystals[118]. And, by capping on the surface of the nanocrystals, these ions play a pivotal role in the nucleation stage during the perovskite's bottom-up synthesis[119]. So, a substrate containing an acid group gave extra stability to the perovskite photocatalyst[120].

In 2022, Yan's group revealed a highly stereospecific [2+2] photocatalytic cycloaddition in surface-capped α,β-unsaturated aryl carboxylic acid derivatives by utilizing $CsPbBr_3$ NCs with 14 W household blue LED bulb (Scheme 23)[121]. This is a beautiful example of an energy transfer from the triplet state (TET) of $CsPbBr_3$ NCs to the substrate directly. This reaction proceeds by anchoring the carboxylate anion on the surface of the nanocrystal photocatalyst. This anchoring phenomenon was probably the major reason for the stereospecificity in this cycloaddition reaction. Only the syn-addition product was observed with moderate to high reaction yield, and the protocol performed very well for almost all types of substitution on α,β-unsaturated aryl carboxylic acid (**23aa-23ac**). This reaction perfectly demonstrates stereospecific photocatalytic [2+2] cyclo-added syn-product formation with energy transfer from the triplet state of the nanocrystal. Mechanistic investigation illustrates that carboxylate anion gets anchored on the surface of $CsPbBr_3$ perovskite NPs and provides a perfect geometry to the substrate for cycloaddition maintaining 'syn' formate. The $CsPbBr_3$ NCs irradiated with blue LED emission and made an electronic transition from the singlet ground state ($\mathbf{S_0}$) to its first singlet excited state ($\mathbf{S_1}$). And, after perfect intersystem crossing (ISC) the electron jumps from the first singlet excited state ($\mathbf{S_1}$) to the first triplet excited state ($\mathbf{T_1}$). Triplet to singlet transition is symmetrically forbidden so in practice a triplet state contains a higher lifetime than that of a singlet state, so energy transition becomes more physible from the long-lasted triplet

excited state ($\mathbf{T_1}$) to the anchored substrate. This triplet state energy transfer ($\mathbf{E_T}$) supplies energy for activation to the substrate for achieving a higher excited state (**23a***), where it couples with itself or with another 'ene' analog to furnish the anticipated cyclobutane derivative (**23b**). Large LHP nanocrystals (size > 10 nm) or quantum-confined smaller nanocrystals both are capable of performing this triplet-state energy transfer.

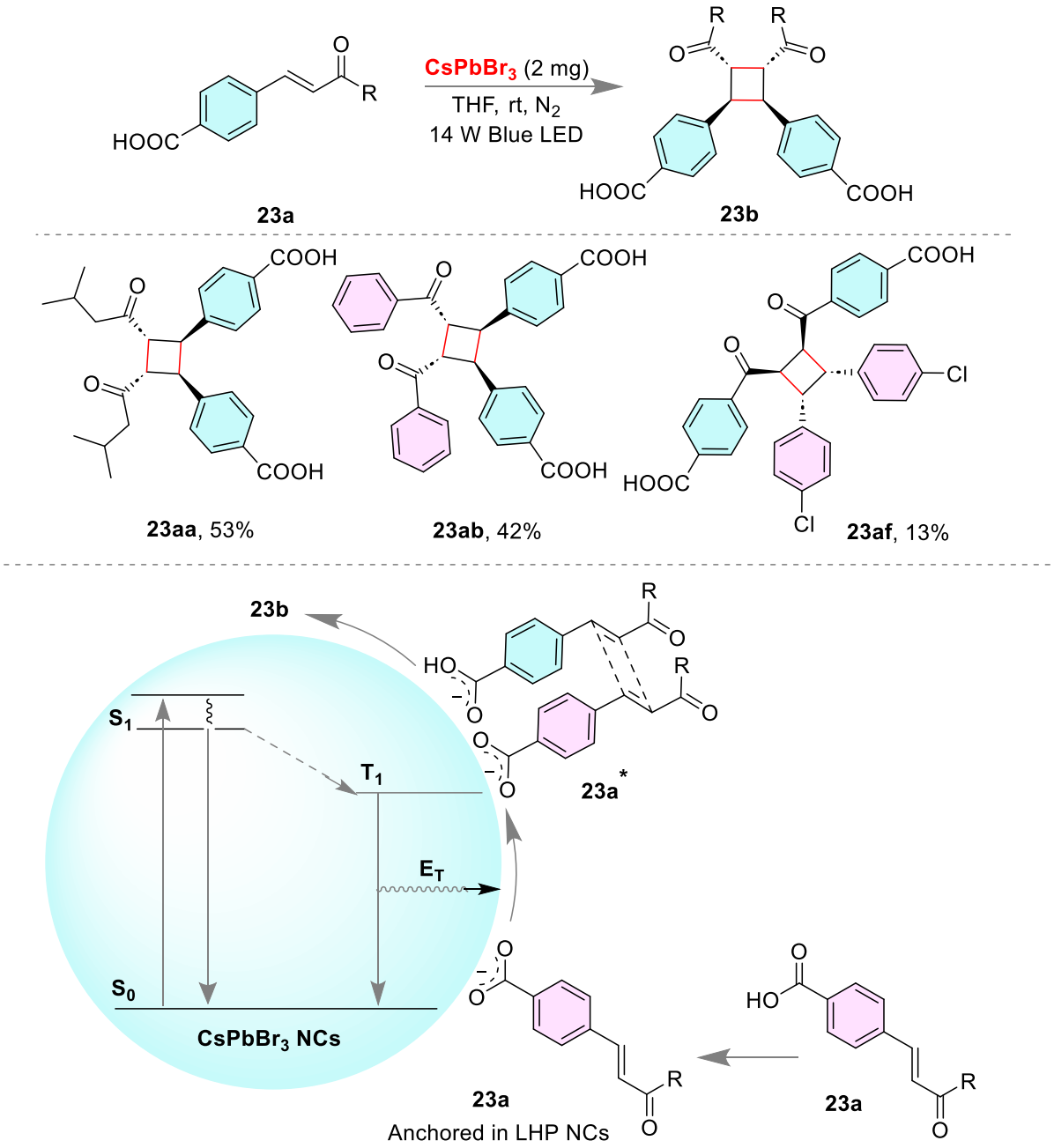

Scheme 23. $CsPbBr_3$ NCs catalyzed stereospecific [2+2] cycloaddition by Yan's group.

1.24 Perovskite catalyzed cascade cyclization on *N*-sulfonyl ketimines

Zwitterions are a class of compounds with extraordinary features, its extensive use covers every pioneer field of research due to presence of two different charges on it[122-126]. Natural amino acids, monomers of peptide or protine in animals, exist as zwitterionic form[x]. So, these ions find an enormous application in multiple organic synthesis.

In 2023, Yu's group reported a $CsPbBr_3$ NCs catalyzed cascade cyclization on *N*-sulfonyl ketimines using a zwitterionic radical precursor in acetonitrile (Scheme 24)[127]. The protocol was executed with 10 mol % of the catalyst loading in the presence of white LED or sunlight and within 10 hours of reaction duration, cascade cyclized product was furnished with an outstanding yield in acetonitrile solvent. Although acetonitrile is a polar solvent, very prone towards lead leaching from perovskite framework, still LHP NCs can hold their fluorescence in this solvent for a very long time. From simple mononuclear systems to polynuclear systems or allyl-substituted aromatic systems (**24aa-24ad**), this strategy performs nicely with a satisfactory reaction yield. Like previously, here also, *N*-phenyl glycine plays the role of a capping ligand, which may have an unexplored role behind the stabilization of these perovskite nanocrystals. The mechanistic investigation shows a similar kind of trend as of the previous (Scheme 11). Initially, the perovskite NCs irradiated with sunlight and work as an excited state oxidant, oxidize *N*-phenyl glycine (**24b**) to form a carboxylate radical which further goes through decarboxylation to form another stable radical intermediate (**24.2**). This radical attacks *N*-sulfonyl ketimines (**24a**) twice to form an intermediate (**24.4**), which goes through protonation and is followed by elimination to form a cationic species (**24.6**). Then nucleophilic attack from the existing nitrogen center inside the organic framework furnished the ultimate cascade cyclized product (**24c**).

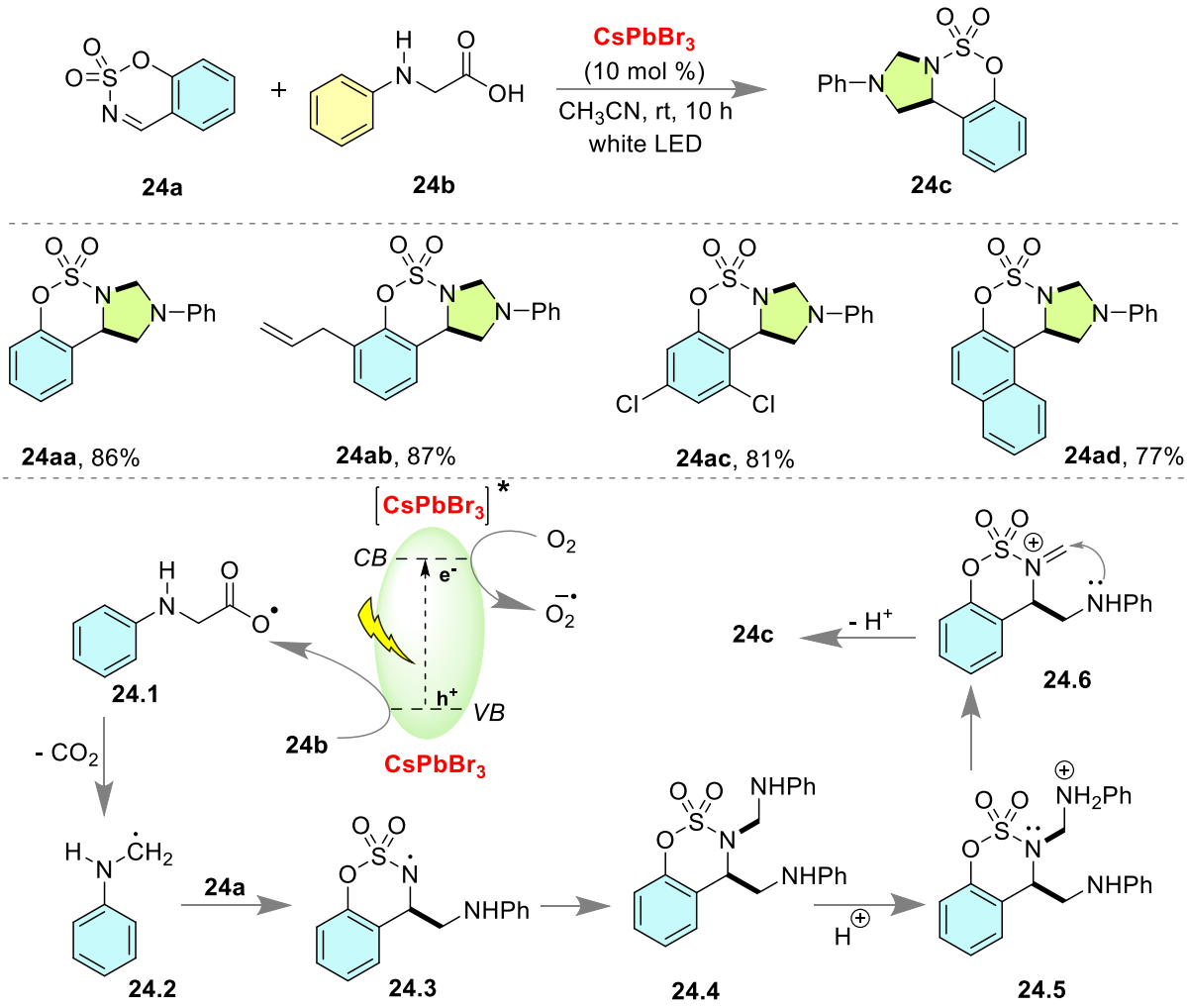

Scheme 24. $CsPbBr_3$ catalyzed cascade cyclization on *N*-sulfonyl ketimines by Yu's group

1.25 Perovskite catalyzed intramolecular cyclization of protected diamines

More than 70% of FDA approved drugs and bio-active natural products contains atleast one heterocyclic framework in its core[128]. So, carbon-heteroatom bond generation is very much crusial in organic chemistry, and a plentiful pathways have been designed to synthesize such highly demanded structural motifs[129-131]. Nitrogen-based skeletons are very common in bio-based heterocyclic chemistry, illustrating the importance of C-N bond generation in synthetic tool box[132-136].

In 2022, Tamang's group reported another fascinating intramolecular cyclization of *N*-protected diamines by generating C-N bond to furnish several enantiopure bioactive imidazolidines using DBI-generated $CsPbBr_3$ perovskite nanocrystal in the presence of 40 W blue LED irradiation (Scheme 25)[137]. Here, Gurung *et al.* revealed the synthesis of much more stable $CsPbBr_3$ perovskite quantum dots compared to the conventional $CsPbBr_3$ perovskite NCs using dibromoisocyanuric acid (DBI) as a benign and effective bromide source. This specific scalable protocol was simply executed in the open air at room temperature using 40 W Kessil blue LED irradiation source. But, surprisingly a very low turnover number of around 177 was achieved compared to previous perovskite-based reactions. The intramolecular cyclization performed with excellent yields for various substitutions on the aromatic part irrespective of their electronic nature (**25aa-25ad**). The most plausible mechanism states that blue LED irradiated bromide-rich $CsPbBr_3$ perovskite NCs behave as an excited state reductant, reducing molecular oxygen to a superoxide radical anion. And, the diamine substrate accepts (**25a**) one photogenerated hole from the valance band of the nanocrystals and itself oxidizes into a *N*-centered radical cation (**25.1**). The superoxide radical anion reduces this species and also abstracts one proton from the diamine substrate leading to the formation of an *N*-centered cationic intermediate (**25.2**). This cationic species loses again one acidic proton in the presence of a hydroperoxide anion to form another intermediate (**25.3**) and a stable molecule of hydrogen peroxide was produced. This intermediate (**25.3**) furnished the final product by intramolecular nucleophilic attack from the nitrogen centre to the electrophilic carbon center.

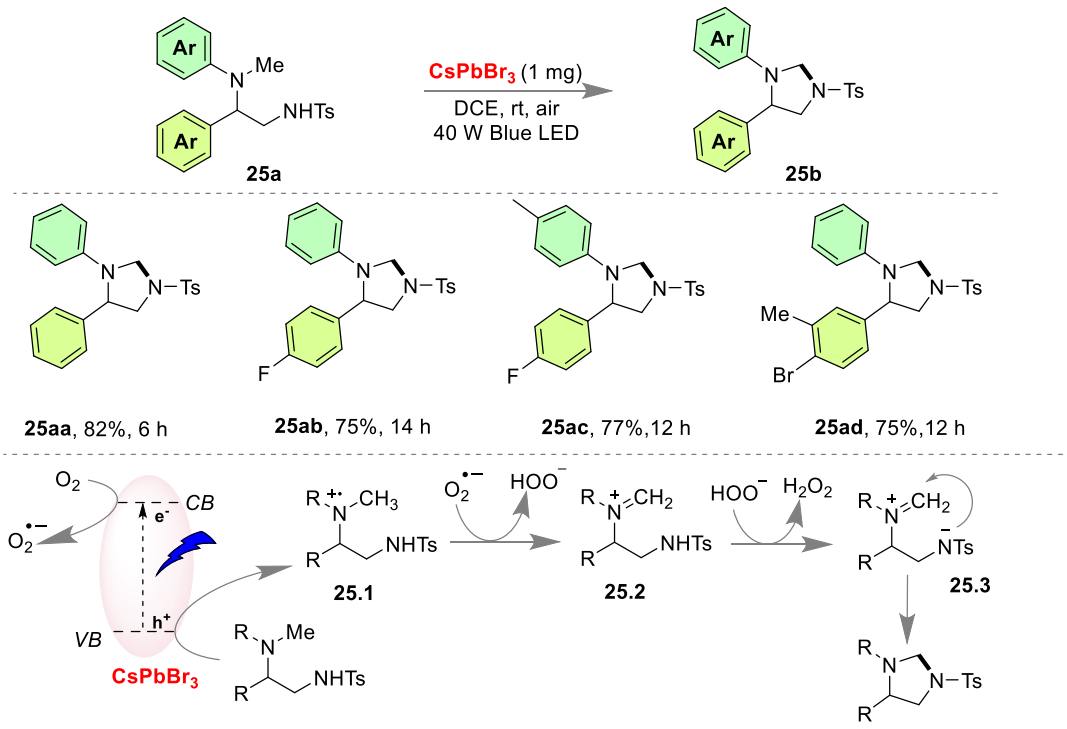

Scheme 25. Intramolecular cyclization of diamines by Tamang's group

1.26 $CsPbBr_3$ catalyzed intramolecular cyclization to form fused imidazolidinies

Tamang's group extended their strategy to another familiar system to explore the structural diversity of their developed synthetic protocol (Scheme 26)[137]. The strategy smoothly worked for several tetrahydroisoquinoline derived 1,2-diamines (**26a**) and furnished several aliphatic six-membered fused imidazolidines (**26b**) with excellent yields within 3 h using 40 W blue LED irradiation. They have investigated their strategy with various substitutions on the aromatic ring (**26aa-26ad**) and reached up to 80% of the reaction yield with just 1 mg of $CsPbBr_3$ perovskite loading.

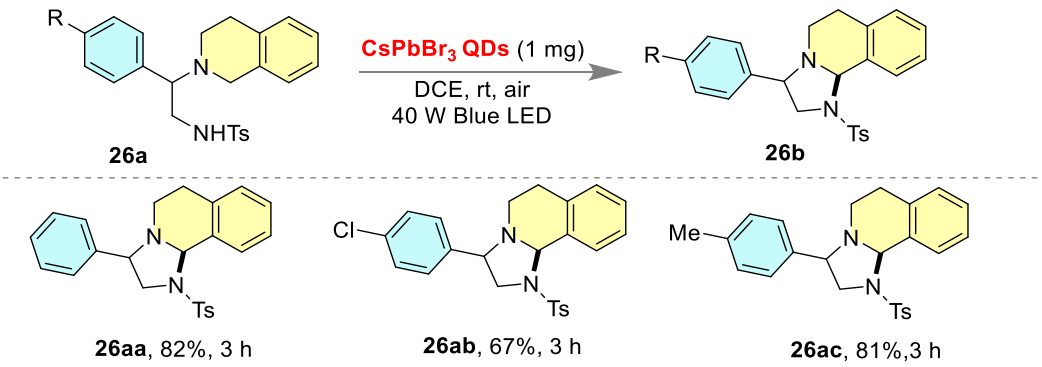

Scheme 26. Six-membered ring fused imidazolidine synthesis by Tamang's group

1.27 Photochemical synthesis of 1, 3-oxazolidine by intramolecular cyclization

Oxazolidine is a five-member heterocyclic system containing a nitrogen and oxygen atom inside the ring. It has three isomers among which 2-oxazolidinone is the most investigated one. These organic moities surprised people from ancient time with their potential applications in the field of anticancer, antibacterial, antituberculosis, anti-inflammatory, etc[138-139].

To further explore the substrate scope and structural diversity, Tamang's group extended their optimal reaction conditions to 1,2-amino alcohols (**27a**) and achieved the anticipated 1,3-oxazolidine derivatives (**27b**) with very good yield within 12 h using DBI-generated orthorhombic $CsPbBr_3$ perovskite NCs in 40 W blue LED irradiation (Scheme 27)[137]. The developed strategy was followed by several 1,2-diamino alcohols and several 1,3-oxazolidine derivatives (**27aa-27ad**) were synthesized in the open air at room temperature with just 1 mg loading of bromide-rich $CsPbBr_3$ perovskite NCs dust. These specific $CsPbBr_3$ perovskite nanocrystal were developed using a 'three-precursor method' containing cesium oleate, Pb(II) salts like PbO or $PbBr_2$, and dibromoisocyanuric acid (DBI) as brominating source. Any solvent containing halide like DCE, DCM, DBM, chloroform, etc. is an expert in doing 'anion-metathesis' with the halide vacancy inside the perovskite NCs which is easily detectable by a blue or red shift in fluorescence emission spectra of the nanocrystal. Rao *et al.* revealed this

anion exchange rate is connected with the stability of the perovskite NCs as well as the surface passivating ligands what we provide externally during perovskite synthesis like OA/OAm, TOP, TOPO, etc.[140].

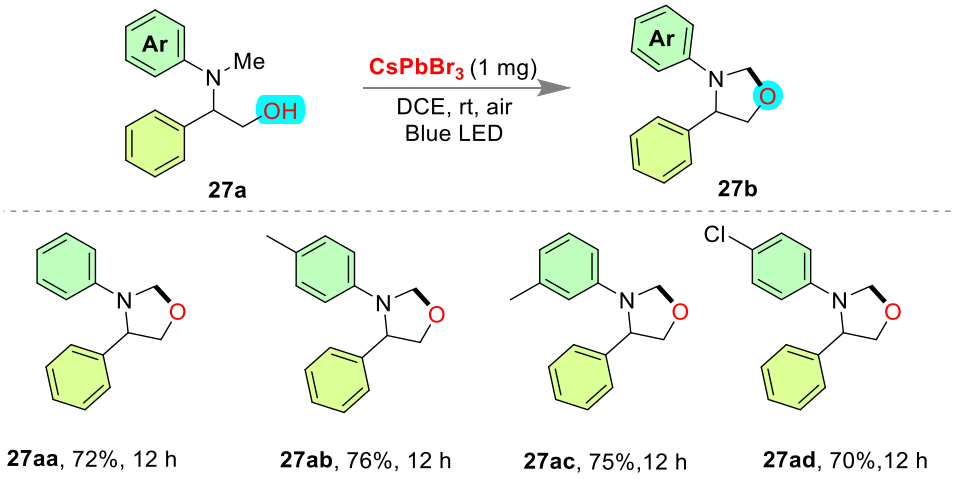

Scheme 27. Photochemical 1,3-oxazolidine synthesis by Tamang's group

1.28 Electrophilic solvolysis halogenation in an aromatic system

A chemical reaction where solvent itself play a role of nucleophile or electrophile is termed as 'solvolysis reaction'[141]. Halogenated solvents posses several halth risk including its carcionogenecity and hematotoxicity[142-143]. But, these solvents are also very cheap and can be utilized efficiently to derive a plentiful environmentally benign structural frameworks[144]. In ancient times, people often used dihalogen for halogenation reaction, but due to extreme toxicity and hazardous nature of dihalogens (except iodine)[145-146], several sustainable methods have been developed in the synthetic tool box to halogenate hydrocarbons in visible light using benign halogenation source[147-148]. And, enormous application of these compounds in several fields[149], still employing researchers around the globe to find a much more safer way.

In 2022, Xie's group discovered an elegent technique to make electrophilic substitution in an electron-rich aromatic system by utilizing different electrophilic source including solvents and inorganic salts in the visible light irradiation (Scheme 28)[150]. Electrophilic bromination and

chlorination was executed using dibromomethane (DBM) and dichloromethane (DCM) solvent respectively, where anion metathesis plays a pivotal role in the catalytic cycle. The halide deficiency on vacant sites in $CsPbBr_3$ perovskite's three-dimensional framework helps to make anion-exchange with the solvent molecules, which is responsible for tunability in the energy gap between the valance band and the conduction band of the NCs. After several control experiments, it was observed that excited state $CsPbBr_3$ NCs reduces dihalomethane solvent to its radical anion (**28.1**) by liberating an electron from its conduction band. This radical anion species further cleaved to form a radical (**28.2**) and a halide anion. This halide ion again being oxidized to a halide radical by acceping a photogenerated hole from the valace band of the perovskite NCs. Subsequently, halide radical dimerizes to form stable halogen molecule which act as electrophile towards electron rich aromatic system. By using electron shuttle in perovskite's surface, they successfully synthesized numerous halogenated product (**28aa-28ad**) with satisfactory yield in all the cases. They have also observed that their protocol has a very broad funtional group toleration including -Cl, -I, -Bpin, $-COOCH_3$, -CN, $-NO_2$, -NHAc, etc. After halogenation, Xie's group have extended their protocol to check the diversity of electrophiles for their protocol and successfully installed thiocyanate (-SCN), triflet ($-CF_3$), iodide (-I), and nitro ($-NO_2$) functionality in the aromatic system with excellent to average reaction yield using sodium thiocyanate, sodium triflet, sodium iodide and silver nitrate respectively.

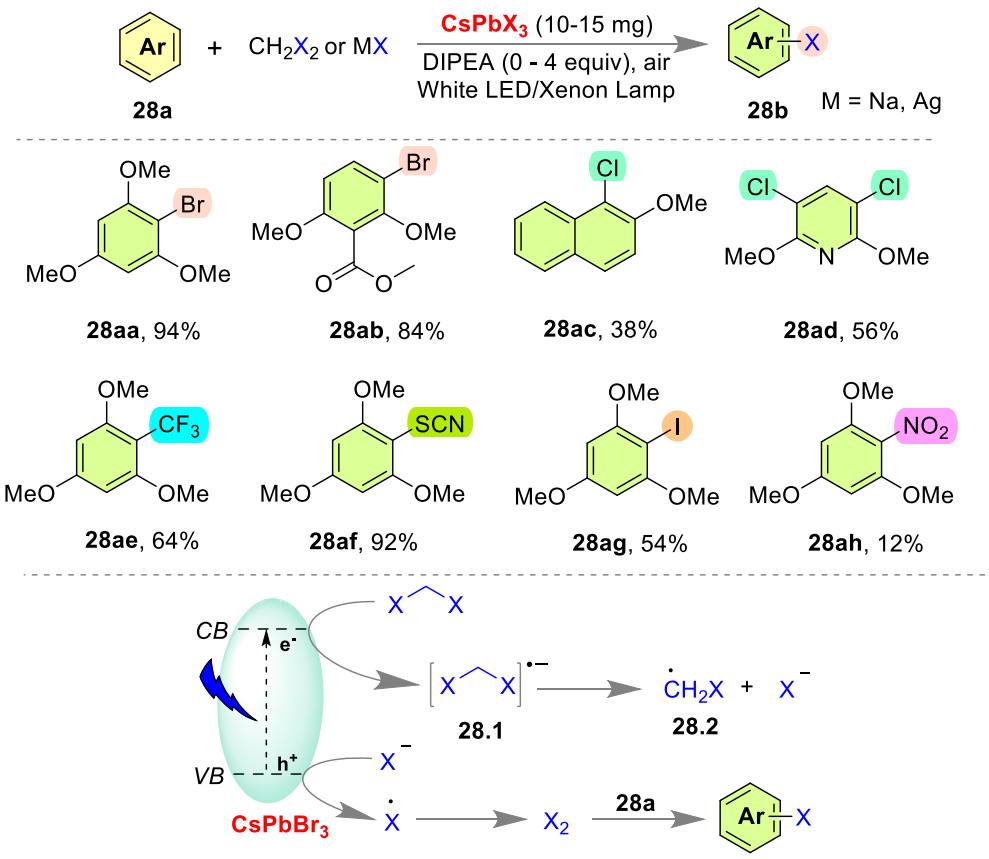

Scheme 28. Electrophilic aromatic substitution in an electron-rich system by Xie's group.

1.29 Perovskite catalyzed simultaneous C-O and C-X bond formation

Like the previous work, Mal's group revealed another small molecule activation technique by utilizing DBI-generated $CsPbBr_3$ perovskite NCs, previously made by Tamang's group[137]. In 2023, Mal's group explored simultaneous C-O and C-X bond formation by activationg small saturated aliphatic molecule in visible light using perovskite catalysis (Scheme 29)[151]. This typical synthetic protocol was accomplished within 3 h in 3W blue LED irradiation with just 0.6 mol % of catalyst loading in DCE solvent. And, more interestingly, the yield of the reaction depends very much on the morphology of the perovskite NCs. The morphology of the unit cell of $CsPbBr_3$ was tuned from cubic to orthorhombic which leads to an enormous change in the yield of *gem*-dihaloenones (**29b**). The brominating source in the synthesis of $CsPbBr_3$ nanocrystal plays a vital role in the nucleation stage of those nanocrystal hence changing the

brominating source affects the morphology of the perovskite nanocrystals. By changing the brominating source from *N*-bromo succinimide (NBS), 1,3-Dibromo-5,5-dimethylhydantoin (DBDMH) to Dibromo-isocyanuric acid (DBIA), the morphology of $CsPbBr_3$ perovskite also changes from cubic to orthorhombic. These orthorhombic nanocrystals have an average excited state lifetime of 12 nanoseconds and an elevated oxidation potential at +1.6 V, proved to be much more potent compared to normal cubic perovskite NCs. The strategy furnishes a broad spectrum of *gem*-dichloroenone substrates (**29aa-29ad**) and successfully performs for a library of *gem*-dibromoenone compounds (**29ae-29af**). On mechanistic elucidation, it has been observed that excited $CsPbBr_3$ NCs act as the excited state reductant, reducing carbon tetrahalide to a radical anion species that loses one bromide anion to form a stable trihalo methane radical (**29.1**). This radical is enough stable to attack a carbon-carbon triple bond in arylacetylenes (**29a**) to make another stable benzylic radical (**29.2**) which plays the role of the terminal reductant, stabilizes perovskite NCs to its ground state and itself oxidizes to a carbocationic species (**29.3**) by accepting a photogenerated hole from the valance band of the nanocrystals. Moisture present in the solvent molecule attacks this carbocation and makes another organic molecule (**29.4**), which eliminates a stable HBr molecule to produce the anticipated *gem*-dibromoenones. Often moisture present in a solvent plays a very crucial role in the catalytic cycle and leads to the formation of oxidized products[152]. To accomplish this protocol also, moisture in the solvent was necessary so this reaction can't furnish expected *gem*-dihaloenones in dry acetonitrile solvent. The outline of the work is perovskite may be unstable in water but a very small amount of water may be reactive for perovskite catalysis.

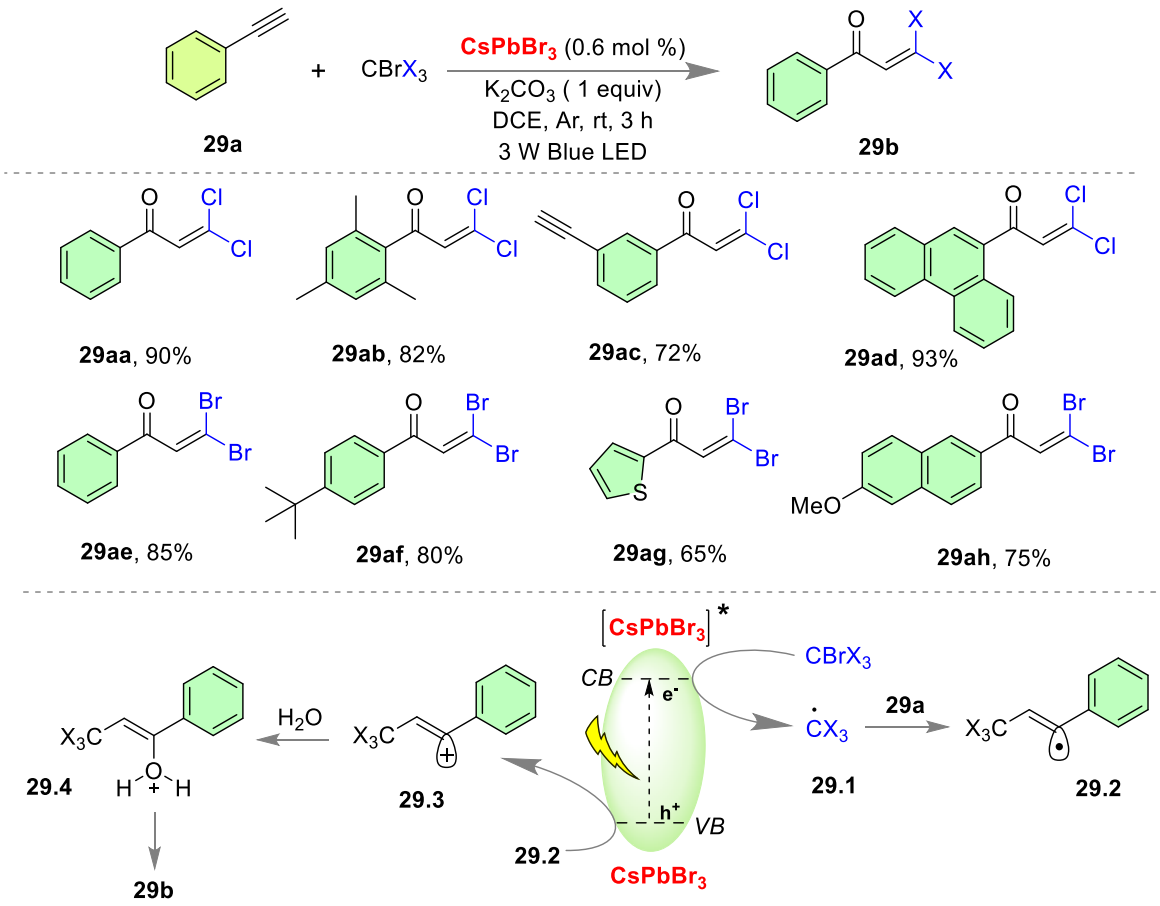

Scheme 29. $CsPbBr_3$ NCs catalyzed photocatalytic C-X bond activation by Mal's group.

1.30 Perovskite-catalyzed chemo-divergent cascade cyclization using CBr_4

The assembling of high reactivity and high selectivity makes radical chemistry ideal for cascade reactions[153]. Cascade radical cyclization is a cutting-edge technique to furnish numerous large organic frameworks in a single step by diminishing the duration, cost, and wastage of the reaction[154-155].

Following this report, Mal's group reported another $CsPbBr_3$ perovskite catalyzed chemo-divergent tandem cyclization in *N*-alkyl alkanamides using carbon tetrabromide as the aliphatic brominating precursor (Scheme 30)[156]. Cascade cyclizations have always been of prime interest in organic chemistry due to their fascinating features, which lead to the target molecule by

skipping several steps[157]. This reaction was performed nicely with orthorhombic $CsPbBr_3$ perovskite nanocrystals originating from the dibromoisocyanuric acid (DBIA). This chemo-divergent protocol furnished three different types of cascade-cyclized products depending on the *para*-substitution on the *N*-alkyl substituted framework. When a very bulky tertiary group occupies the para position of the aromatic ring, a '*6-endo-trig*' way of cyclization leads to the formation of a quinoline type of nucleus (**30aa-30ad**) with a satisfactory reaction yield. However, when a methoxy group (-OMe) occupies the para position, or for unsubstituted rings, a '*5-exo-trig*' spiro cyclization was observed leading to the formation of various spiro-cyclized products (**30ae-30ah**). The reaction was performed at its best in acetonitrile solvent using 3 W blue LED irradiation. Initially, blue LED irradiated $CsPbBr_3$ NCs excite one electron from its valance band to the conduction band, which reduces carbon tetrabromide (CBr_4) to make a bromine free radical. This bromine radical attacks the substrate (**30a**) and a stable benzylic radical intermediate (**30.1**) forms. Now, depending on the substitution of the *para*-position, this radical intermediate goes through different types of ring closure leading to the formation of different intermediates (**30.2-30.7**) and leading to the generation of three different types of products. The Formation of a specific type of cyclized product was largely dependent on the *para*-substitution of the existing aromatic ring in the *N*-alkyl alkanamide.

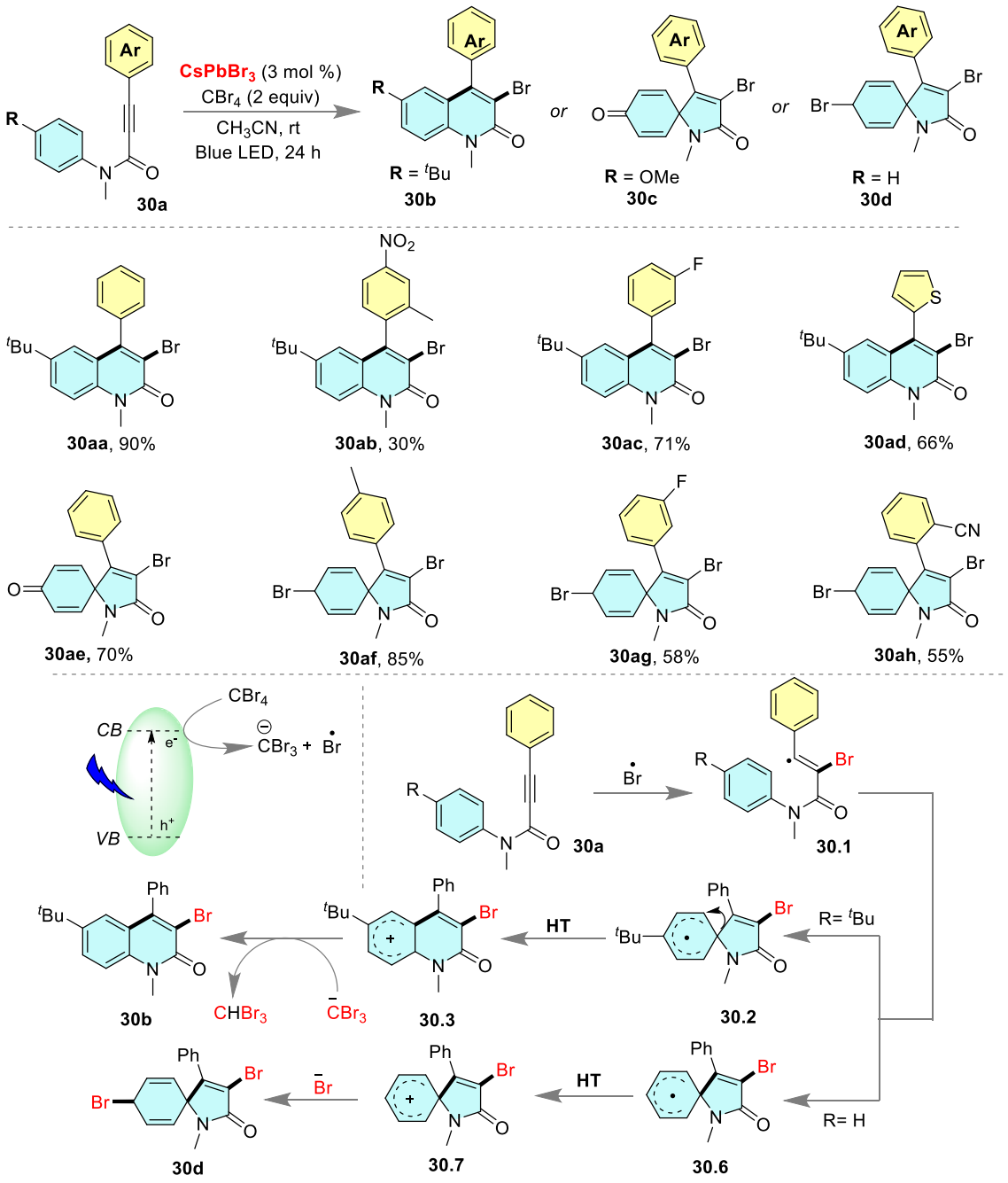

Scheme 30. Chemo-divergent cascade cyclization in *N*-alkyl alkanamides by Mal's group.

1.31 Photocatalytic [3+2] cycloaddition using $CsPbBr_3$ NCs

Cycloaddition reactions remained the most investigated and widely used in synthetic organic chemistry for the construction of a plentiful organic framework in a single-step operation[158-159]. In 2024, Yan and coworkers reported another $CsPbBr_3$ perovskite-based photochemical

[3+2] cycloaddition between vinyl cyclopropanes and alkenes in the presence of 40 W blue LED irradiation using dibromo methane (DBM) solvent as the radical initiator (Scheme 31)[160]. Anion metathesis between halides vacant sites of perovskite and the organohalide solvent is the major driving force for this reaction. Here in this reaction, $CsPbBr_3$ perovskite NCs in dibromo methane generate a 'Br' radical from the hole oxidation, which is the active key intermediate for photocatalytic [3+2] cyclo-addition leading to the synthesis of various vinylcyclopentanes (**31c**). The nanocrystal photocatalyst was highly recyclable due to its self-healing in a bromine-rich environment by anion-exchange strategy, and the solvent was considered as the co-catalyst in this synthetic strategy. The protocol was smoothly obeyed by various substituted styrene systems (**31aa-31ad**) and also worked for various other olefinic systems (**31ae-31ah**) with moderate yield. Mechanistic investigation revealed that dibromo methane forms a bromide anion by accepting an excited electron from the conduction band of the nanocrystal photocatalyst. Then, the bromide anion again oxidized to bromine radical by a photogenerated hole transfer from the valance band of the NCs. This Br radical plays a key role in the whole catalytic cycle by acting as a radical initiator. Initially, it attacks the vinyl group in cyclopropane and cleaves the highly strained cyclopropane ring to form an intermediate (**31.1**), which again reacts with terminal alkenes to form another stable benzylic intermediate (**31.2**). Subsequently, this intermediate rearranges itself to form a stable five-membered ring system and eliminates a bromine radical from the framework.

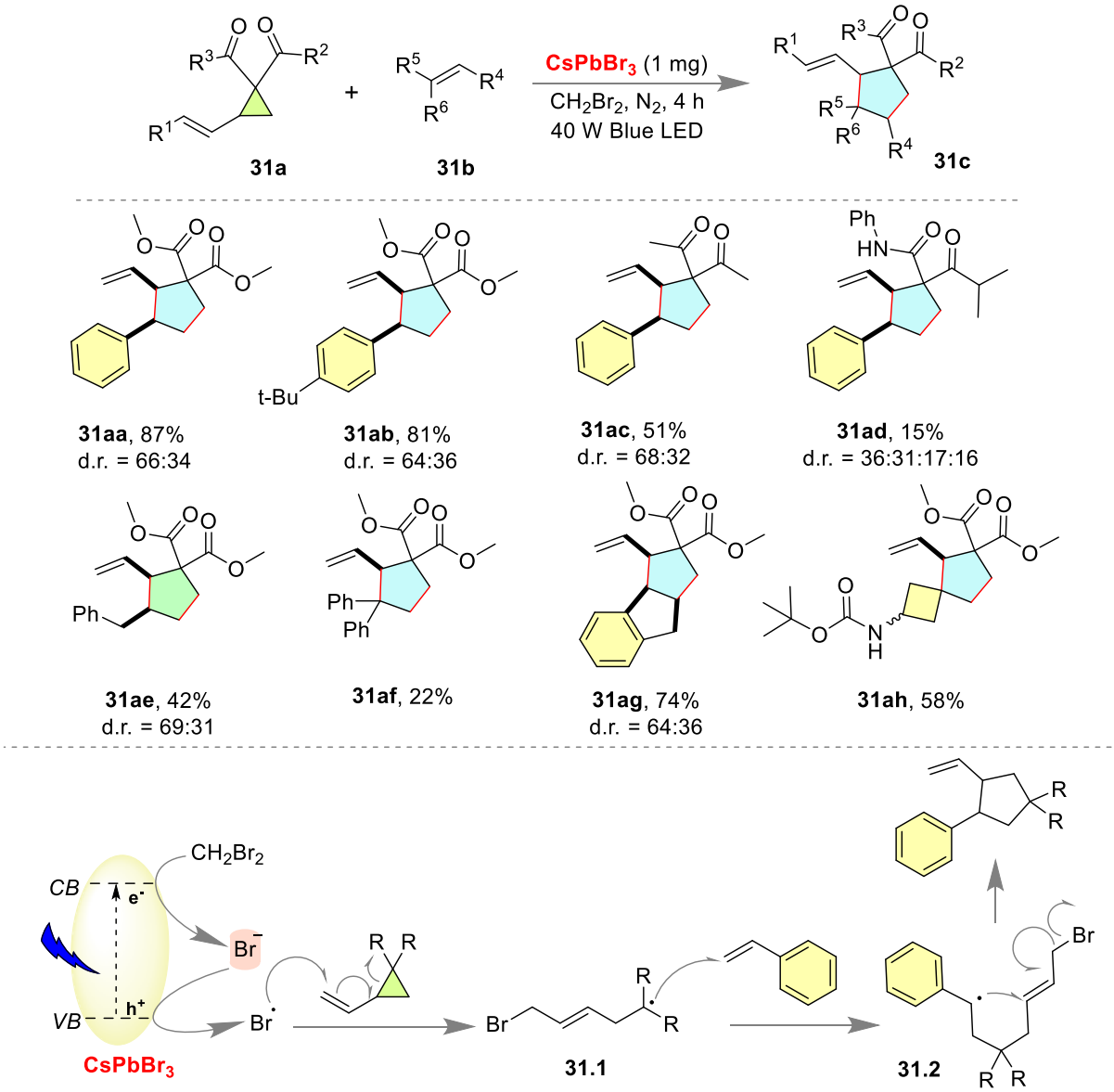

Scheme 31. Photochemical [3+2] cycloaddition by Yan's group.

1.32 Perovskite-catalyzed oxidation of terminal olefins with aerial oxygen

Another group from China, explored $CsPbBr_3$ catalyzed oxidation of terminal olefin leading to the formation of numerous carbonyl moieties in visible light using the same DCE solvent (Scheme 32)[161]. Le *et al.* discovered that with just 6 mol % of the catalyst loading and 50 W blue LED irradiation in an oxygen environment, this strategy successfully furnished aldehyde for various substitutions in the aromatic ring (**32aa-32ab**). It is also capable of performing for

production of ketones with very high reaction yields from different substitutions and heteroaromatic frameworks (**32ac-32af**). Blue LED irradiates perovskite nanocrystals to an excited state where it works as an excited-state reductant, reducing molecular oxygen to a superoxide radical anion. This radical anion reacts with an unsaturated 'ene' framework (**32a**) to produce a dioxo radical anion (**32.1**) which serves the role of a terminal reductant, bringing perovskite nanocrystals to the ground state from the excited state and itself oxidizes to a dioxetane derivative (**32.2**). Dioxetanes are highly unstable species, that immediately eliminate a stable formaldehyde molecule to furnish the anticipated carbonyl compound.

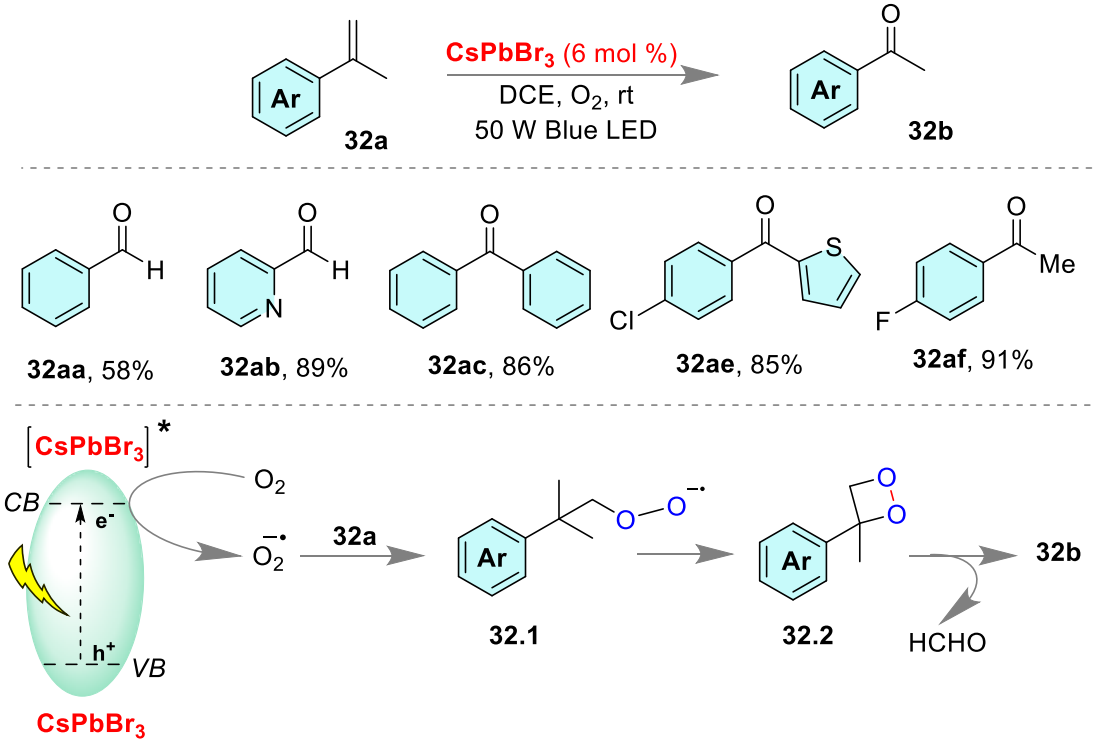

Scheme 32. Photochemical oxidation of terminal olefins by Le *et al*.

1.33 Perovskite catalyzed oxidation of alcohols to carbonyls

Oxidation of alcohols or olefins to carbonyl compounds is one of the prime interests in organic chemistry due to the large requirement of ketonic substrates to fulfill various synthetic demands[162]. All over the world, demand for such fundamental organic transformation using

much more ambient conditions is increasing day by day[163]. Cesium lead halide perovskite NCs are capable of catalyzing these conversions with very high efficiency in visible light. In 2023, Fan and coworkers activated the 'O-H' bond of primary and secondary alcohols and synthesized numerous aldehydes and ketones (Scheme 33)[164]. This $CsPbBr_3$ perovskite nanocrystal catalyzed strategy performed at its best in dichloroethane (DCE) solvent with blue LED irradiation in an aerial atmosphere. This strategy was performed with outstanding yield for various substitutions on aromatic rings (**33aa-33ac**) and also worked very well for heteroaromatic (**33ad**) and multiple non-aromatic systems (**33ae-33ag**). Aerial oxygen plays a very crucial role in the catalytic cycle, initially perovskite molecule gets excited on visible light irradiation and acts as an excited state reductant which reduces molecular oxygen to a superoxide radical anion. This radical anion reacts with substrate (**33a**) to make radical species (**33.1**) which rearranges to produce carbonyl compounds. The oxygen radical anion also serves the role of terminal reductant to complete the catalytic cycle. And, here also this specific chlorinated solvent is found to be the best performer of the reaction, probably due to anion metathesis with bromide perovskite nanocrystal, leading to the formation of a much more potent mix-halide perovskite structure.

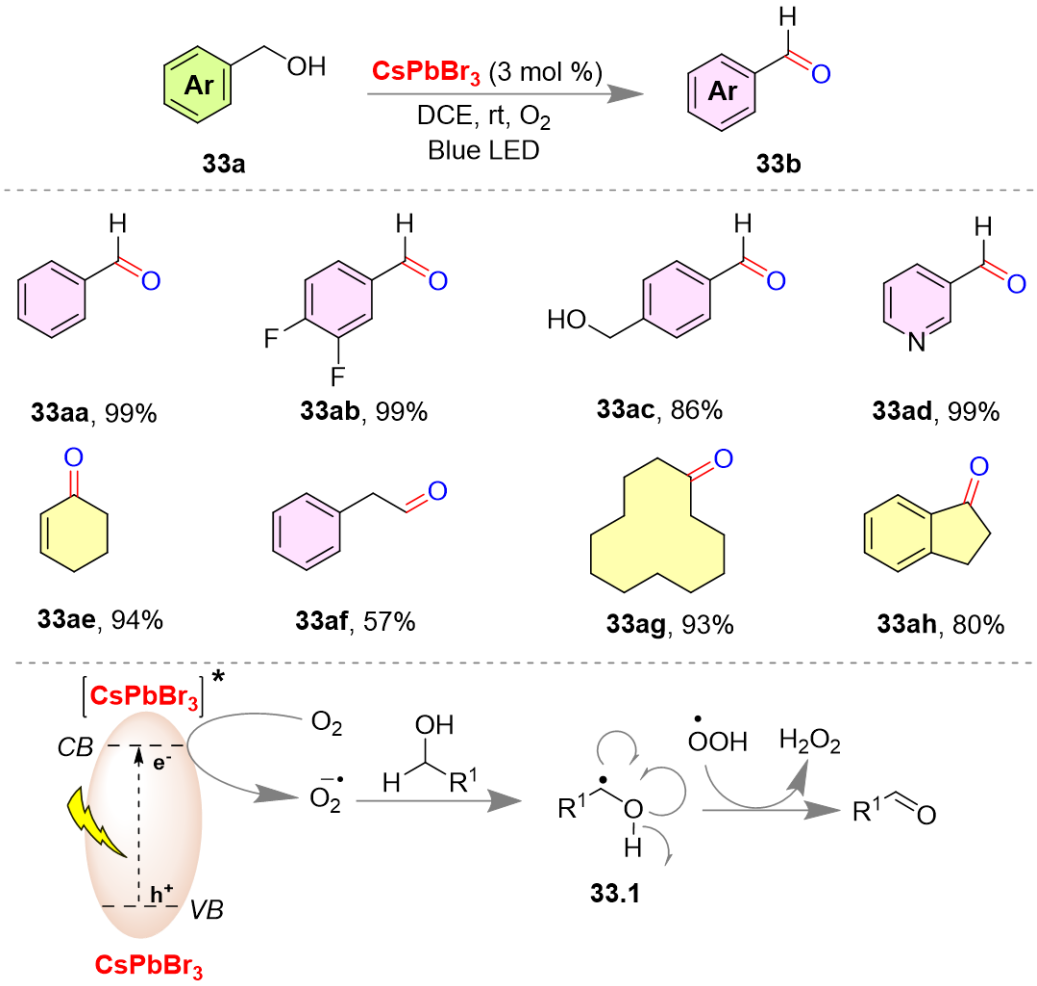

Scheme 33. $CsPbBr_3$ catalyzed oxidation of alcohol by Fan *et al.*

1.34 A gram-scale synthesis of 3,4-dihydropyrimidin-2-(1H)-ones in air atmosphere

Multicomponent reactions (MCR) in organic chemistry have a unique identity with very high atom economy[165], where three or more substrates react to generate a novel product in a single reaction vessel[166-169]. Strecker synthesis was the first example of that kind in the early nineteen decades. After that, Mannich[170], Biginelli[171], Passerini[172], and Ugi reactions[173] become extremely useful in the pharmaceutical industry as a cutting-edge technique.

In 2023, F. Mohamadpour unlocked a scalable synthesis of 3,4-dihydropyrimidin-2-(1H)-ones/thiones (**34d**) using $CsPbBr_3$ perovskite catalysis in blue LED irradiation with a TON

around 90 (Scheme 34)[174]. Like the Biginelli reaction[175], this multicomponent synthesis protocol contains *β*-ketoesters, aryl aldehydes, and urea/thiourea. The protocol was executed with just 1 mol % catalyst loading in ethanol solvent at room temperature with 7 W blue LED irradiation. The strategy was applied to generate a library of substrates, various 3,4-dihydropyrimidin-2(1H)-one derivative (**34aa-34ab**) and 3,4-dihydropyrimidin-2(1H)-thiones (**34ac-34ad**) were synthesized with excellent reaction yield. The catalyst is found quite stable in this strategy and reusable up to six catalytic cycles with declined reaction yield and significant structural changes or activity loss. Also, the applicability of the protocol was extended to a larger scale to make it suitable for industrial use. The author proved a single electron transfer (SET) mechanism by several control experiments. The blue LED irradiated perovskite NCs donate a photogenerated hole from its valance band to the *β*-ketoesters and oxidize it to a radical cation (**34.1**). Then the excess one electron in the conduction band was taken by aldehyde to form a radical anion of aldehyde (**34.2**). This radical anion reacts with urea/thiourea to form another radical anionic species (**34.3**). Now, one radical anion and another radical cationic species added up to form a covalent neutral molecule (**34.4**), which rearranges to form the final product.

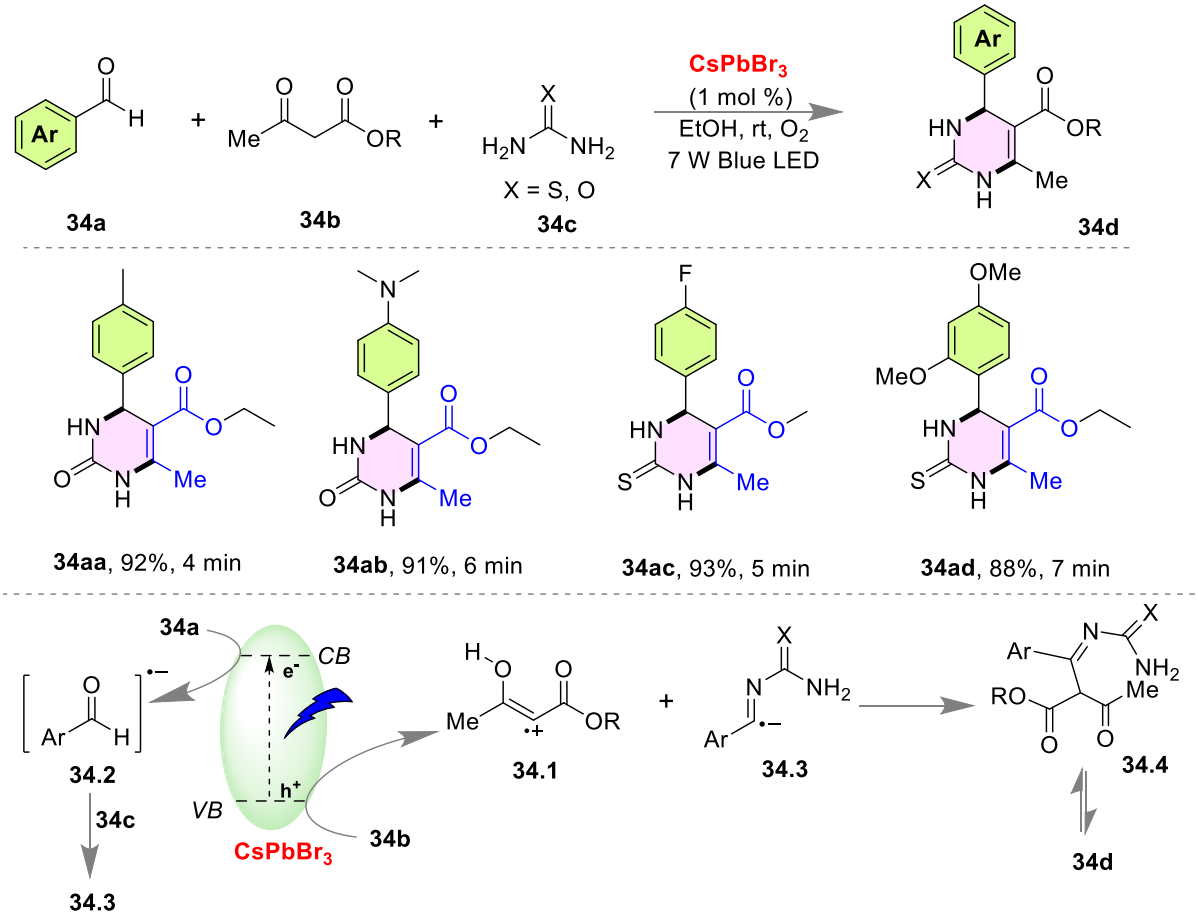

Scheme 34. Scalable synthesis of 3,4-dihydropyrimidin-2-(1H)-ones by F. Mohamadpour.

1.35 Perovskite-catalyzed thio or seleno-etherification in electron-rich arenes

Organosulfur compounds are immensely important in organic chemistry due to their omnipresence in nature. More specifically, thioether-based heterocyclic frameworks belong to a unique class of compounds with very high anti-cancer activity[83]. So, numerous synthetic protocols have been addressed to furnish such important structural motifs by employing metal-free[84-86], or metal-based routes[87-89].

Recently, in 2024, Mal's group reported another $CsPbBr_3$ perovskite catalyzed C-H functionalization on *tri*-methoxy benzenes using *di*-sulfide or *di*-selenide as the chalcogenating source (Scheme 35)[176]. This LHP NCs catalyzed reaction was performed at its best on

acetonitrile solvent using 3W blue LED irradiation in an aerial atmosphere. The C-H functionalization on *tri*-methoxy benzene (**35a**) by activating the 'S-S' or 'Se-Se' bond in *di*-chalcogenides (**35b**), resulting in the formation of chalco-ether derivative (**35c**) in an oxygen environment. This reaction was investigated on a broad range of *di*-sulfide or *di*-selenide substrates considering *tri*-methoxy benzene as the constant nucleophilic aromatic site for anchoring of thiol or selenol group. The reaction performed with satisfactory yield regardless of the number or type of substitution in the aromatic part of the *di*-sulfides (**35aa-35ae**). Also, the protocol was able to furnish several selenol functionalized *tri*-methoxy benzene (**35af-35ah**) with average reaction yield. Mechanistic investigation illustrates the necessity of oxygen to complete the catalytic cycle. Cesium lead bromide perovskite NCs excited in the presence of blue LED emission and this irradiation excites an electron from the valence band to the conduction band. After that, excited perovskite nanocrystals reduce molecular oxygen to superoxide radical anion by an electronic transition from its conduction band to the $\mathbb{\Pi}^*$ molecular orbital of dioxygen. And, the electron deficiency in the perovskite NCs is compensated by the *di*-sulfide (**35b**) compound, accepting a photogenerated hole from the valance band of the nanocrystal. This leads to the formation of a *di*-sulfide radical cation (**35.1**) which gets attached to *tri*-methoxy benzene to form another oxygen-centered radical cation (**35.2**) which gets reduced with superoxide radical anion and subsequently, removal of a stable molecule of hydrogen peroxide generates the anticipated thio or seleno-ether product (**35c**).

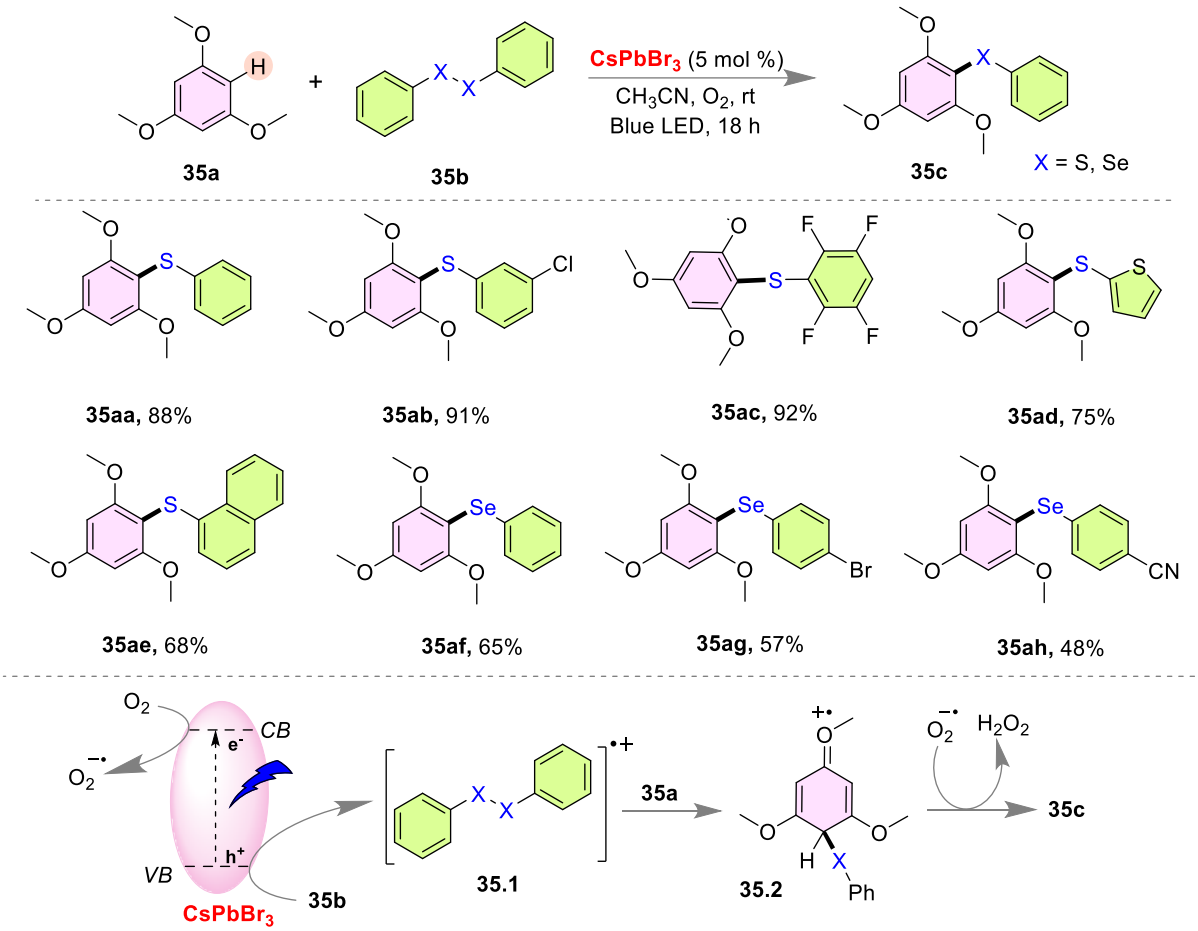

Scheme 35. Thio or seleno-etherification in electron-rich arenes by our group.

1.36 Decarboxylative alkylation via C_{sp}^3- H bond activation of unactivated ethers

Photocatalytic C-H activation is an extremely powerful strategy to functionalize small aliphatic molecules like methane, ethane, butane, etc, derived from fossil fuels[177]. The C-H activation reaction in tetrahydrofuran has been known for the last few decades but not accessible effectively in a bench-stable photocatalytic condition[178-180].

In 2024, Ghosh *et al.* reported an elegant photocatalytic C-H activation in aliphatic cyclic ethers to synthesize various *γ*-keto cyclic aryl ethers using 1 mg of dodecahedral $CsPbBr_3$ NCs as the photocatalyst in 456 nm blue LED irradiation using *α,β*-unsaturated acids as the keto-alkyl source (Scheme 36)[181]. They have explored this protocol by optimizing it in a bunch of

differently shaped $CsPbBr_3$ perovskite polyhedral nanocrystals e.g. rhombicuboctahedron, hexapod, dodecahedron, cubic, Pd-$CsPbBr_3$, Pt-$CsPbBr_3$, $Pb_4S_3Br_2$-$CsPbBr_3$, etc. Among them, the dodecahedron was found to be efficient due to its higher capability of anchoring the carboxylate anion in the 40 W blue LED with a TON around 32200. The protocol initiated with the decarboxylative coupling of cinnamic acid at the α-position of tetrahydrofuran solvent and then extended to several α,β-unsaturated acid derivatives with excellent reaction yield (**36aa-36ah**). The dodecahedral $CsPbBr_3$ NCs have a reduction potential value of E_{red} (PC^*/PC^+ = −1.3 V vs SCE)[121], whereas cinnamic acid has (E_{red} = −1.09 V vs SCE)[182] and oxygen (E_{red} O_2/O_2^- = −0.35 V vs SCE) suggest that $CsPbBr_3$ will reduce molecular oxygen to superoxide radical anion in the mechanistic cycle. Then, the superoxide radical anion helps to form a radical adjacent to the hetero-center in THF solvent (**36.1**), which was added to the α,β-unsaturated system to form another radical intermediate (**36.2**). Blue LED irradiated photogenerated hole was transferred to this intermediate to form a cationic species (**36.3**) which was added to the existing hydroperoxide anion to form a hydroperoxide derivative (**36.4**). This intermediate again accepts one electron from excited LHP NCs and forms another intermediate (**36.6**) by hydroxide anion. A photogenerated hole was transferred to this intermediate (**36.6**) again to form a radical intermediate (**36.7**) which furnished the final product by decarboxylation and a hydrogen atom transfer (HAT).

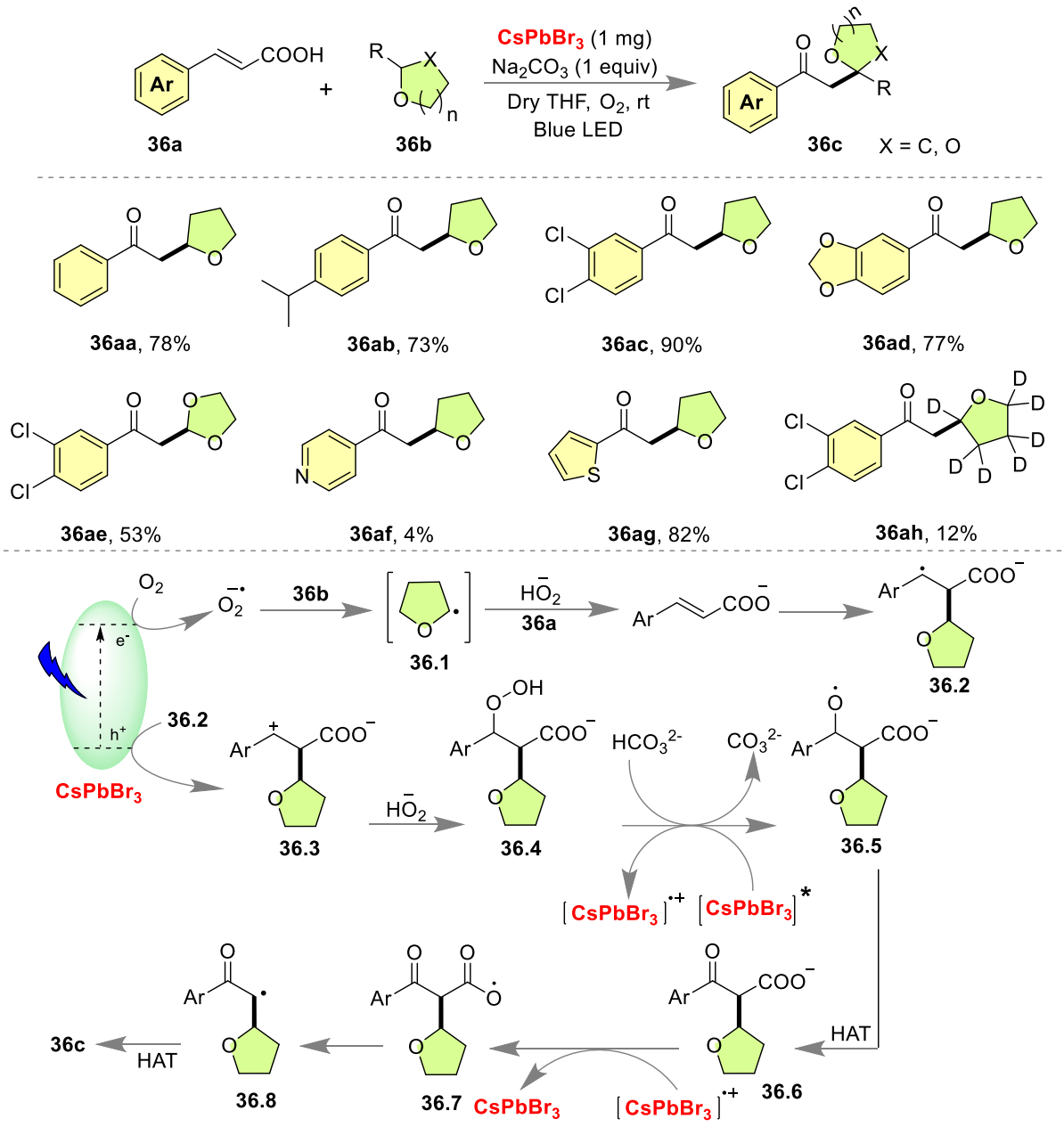

Scheme 36. The decarboxylative C_α - alkylation of aliphatic cyclic ethers by Ghosh *et al.*

1.37 Anti-Markovnikov Sulfinylsulfonation of Terminal Alkynes

Organo-sulfur compounds are very important because of their potent pharmaceutical application in medicinal chemistry[183]. Numerous drugs, natural products, and bio-molecules contain sulfur atoms in their core[184-185]. So, the C-S bond formation is also one of the prime interests in organic synthesis[186]. Recently, Mal's group disclosed another report on C-S cross-

coupling using cesium lead halide perovskite catalysis where sodium azide (NaN_3) served the role of a stoichiometric additive. The protocol established *E*-selective anti-markonikov sulfinyl sulfonation (**37c**) of terminal alkynes (**37a**) using an ultra-small $CsPbBr_3$ nanocrystal (~5.6 nm) as the photocatalyst and *p*-aryl sulfonyl cyanide (**37b**) as the source of sulfone functionality with a product conversion rate of 62,500 μmol g^{-1} h^{-1} (Scheme 37)[187]. A three-precursor method was utilized to synthesize ultra-small $CsPbBr_3$ nanocrystals with an extended excited state lifetime and a very high surface area, where *tri*-bromo isocyanuric acid (TBIA) was employed as the bromide precursor. These newly reported perovskite nanocrystals have a near-unity quantum yield with an elevated oxidation potential of +1.80 V, which can be reused up to several mechanistic cycles. The protocol was well obeyed by various substitutions on the aromatic ring of the terminal alkyne part and delivered a very good reaction yield in all the cases (**37aa-37ac**). Polyaromatic (**37ad**), and heterocyclic systems (**37ae**) also responded to this strategy by surpassing the expectation. The result of several control experiments depicted that a single electron transfer (SET) pathway may be operated here and sodium azide possibly played a scavenger role in abstracting the cyanide functionality from the *p*-aryl sulfonyl cyanide (**37b**) by forming cyanogen azide (N_3CN). TBIA-generated perovskite nanocrystals behaved as an excited state oxidant, oxidizing *p*-aryl sulfonyl cyanide (**37b**) to its radical cationic species. After the reaction with sodium azide, a sulfur-centered sulfonyl radical species formed (**37.1**), which directly reacts with terminal alkyne to make a benzylic type of radical (**37.2**), and also rearranges itself through several consecutive steps to make another sulfinyl radical species (**37.6**). Then, this sulfinyl radical was added with (**37.2**) species to furnish the *E*-selective and anti-markonikov sulfinyl sulfonyl-added product (**37c**).

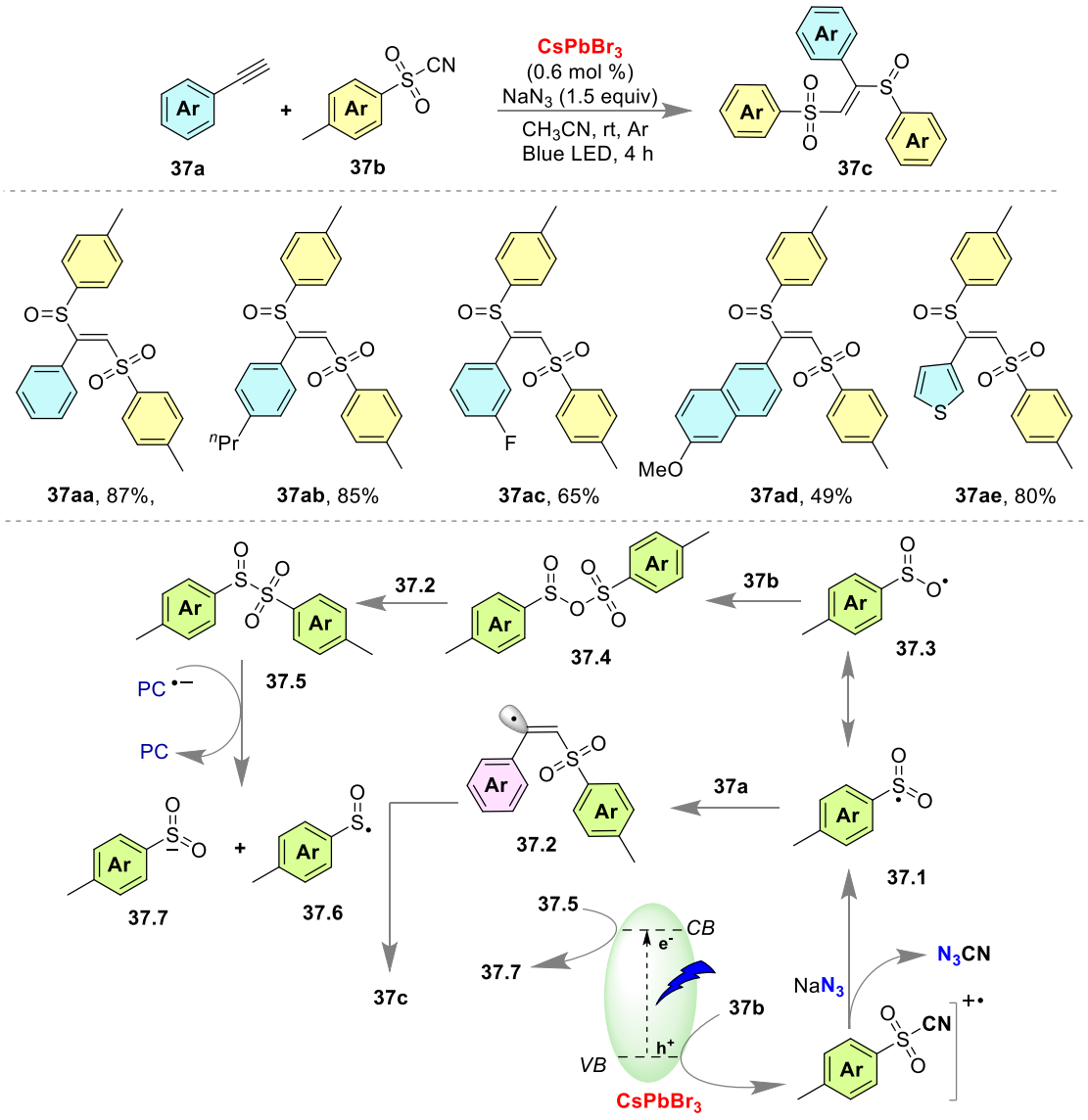

Scheme 37. Anti-merkonikov sulfinyl sulfonation in terminal alkynes by Mal's group

Procedure to synthesize Cesium Lead halide ($CsPbX_3$) perovskite nanocrystal

There are various reported strategies available for synthesizing Lead Halide Perovskite nanocrystals including solvothermal[188], ultrasonication[189], ball-milling[190], chemical vapor deposition (CVD)[191], ligand-assisted reprecipitation (LARP)[192], or microwave-mediated synthesis[193]. Among them, the most prevalent and easiest synthetic approach is the 'Hot-injection' method developed by Protesescu *et. al.*[18]

Preparation of Cs-oleate. Initially, cesium carbonate (0.814g) was taken into a 100 mL 3-neck flask along with octadecene (ODE) (40 mL, TCI), and oleic acid (OA, 2.5 mL), dried for 30 min at 120 ºC under high vacuum, and then heated 1h at 150 ºC under N_2. Since freshly prepared cesium oleate precipitates out of ODE at room temperature, so every time it has to be pre-heated to 100 ºC before use in the hot-injection method.

Synthesis of $CsPbX_3$ NCs. In a 25 mL three-neck flask octadecene (ODE, 5 mL), lead halide (PbX_2, 0.188 mmol) was taken and dried under a high vacuum for 1h at 120 ºC. Then, pre-dried oleylamine (OAm, 0.5 mL) and oleic acid (OA, 0.5 mL) were injected at 120 ºC under a nitrogen atmosphere. Then, the temperature was raised to 140-200 ºC and kept for 1h under an inert atmosphere. After that, pre-heated cesium oleate solution (0.4 mL, 0.125 M in ODE) was quickly injected and the reaction mixture was frozen in an ice-water bath.

Isolation and purification of $CsPbX_3$ NCs. The crude solution was cooled down in a water bath and the aggregated NCs were separated by centrifuging. For smaller NCs synthesized below 160 ºC, centrifugation at 0 ºC or the addition of tert-butanol to the crude solution (ODE:tBuOH=1:1 by volume) were found to be helpful for a complete precipitation. After centrifugation, the supernatant was discarded and the particles were redispersed in toluene or hexane forming long-term colloidally stable solutions. Nowadays, methyl acetate is being used as an anti-solvent instead of tert-butanol to wash the impurities in the purification stage.

Recent advances on the stability of metal halide perovskite NCs

Cage shaped supramolecular framework may regulate the stability of smaller molecules trapped inside its cavity[194-195]. Utilizing this idea, a few pioneering steps have been taken to stabilize LHP NCs by covering them with polymer-like material or molecular assemblies.

Metal halide perovskite NCs combined with polymers may create nanocomposites that bestow an array of advantageous characteristics including higher stability, solution-based processability, and stretchability by maintaining the basic morphology of the nanocrystals intact[196-204].

CONCLUSION AND OUTLOOK

In summary, this review illustrates the systematic development made over $CsPbX_3$ perovskite catalysis in the last few years by assembling a bunch of recent literature that outlines various effective organic syntheses nicely performed utilizing $CsPbX_3$ catalysis in visible-light irradiation. The astonishing array of reactivity of these highly fluorescent $CsPbBr_3$ perovskite nanocrystal will offer practitioners of organic synthesis a new route to apply in numerous photo-redox catalysis. The mild nature of the reaction environment is capable of tolerating a wide and complex functionality, and it is expected this newly developed photocatalyst will surely leave a significant impact on the face of future photo-organic chemistry. Although some developments have been made in perovskite-based photocatalysts in the last few years, we strongly believe there are still many unexplored hidden reactivity of these materials that remain untouched. These promising nanocrystal will play the role of a bridge to connect photo redox chemistry with material science. This compilation of literature, highlighting methodologies of perovskite-mediated photo-organic synthesis is anticipated to contribute uniquely and significantly to the domain of photochemistry. The adoption of perovskite photocatalysis can lead beginners toward much more complicated organic synthesis revealing new opportunities for constructing a variety of organic frameworks with potential applications. Furthermore, hybrid catalysts with improved performance might be produced by combining perovskite nanocrystals with other nanostructured materials like CNTs, graphene, MOFs, COFs. We

expect that this comprehensive review will enable beginners in this field to design new routes to synthesize numerous unknown organic compounds.

Authors' Biographies

Pravat Nayek (ORCID id: 0009-0001-7881-646X) was born in East Medinipuir, West Bengal, India. He earned his B.Sc. degree from Midnapore Autonomous College, Midnapore, and his M.Sc. from IIEST, Shibpur. He qualified for CSIR-NET in 2022 and GATE in 2021 and is currently pursuing his doctoral studies under Prof. Prasenjit Mal at NISER, Bhubaneswar. His research interests focus on the development and morphology control of $CsPbBr_3$ perovskite nanocrystal and utilizing them in fascinating organic synthesis.

Buddhadeb Pal (ORCID id: 0009-0008-1440-6825) was born in Haldia, East Medinipuir, West Bengal, India. He earned his B.Sc. degree from Haldia Govt. College, and M.Sc. degree from Vidyasagar University. He qualified for CSIR-NET in 2021 and GATE in 2021 and is currently pursuing his doctoral studies under Prof. Prasenjit Mal at NISER, India. His research interests focus on Visible light-mediated homogeneous and heterogeneous photocatalysis.

Prof. Prasenjit Mal (ORCID id: 0000-0002-7830-9812) was born at Lokhesole, Bankura, West Bengal, India. He obtained his M.Sc. degree from the Indian Institute of Technology (IIT) Kharagpur and PhD at the Indian Institute of Technology (IIT) Kanpur in 2005. Then he undertook postdoctoral studies at the University of Siegen in Germany as an Alexander von Humboldt Fellow (2006-2007) and at the University of Cambridge in the UK as a Marie Curie Fellow (2008-2009). He started an independent research career at NISER Bhubaneswar in December 2009. Currently, he is pursuing research in a diverse field including supramolecular catalysis, solventless ball-milling reactions, visible light photocatalysis, hypervalent iodine, lead-free and lead-containing perovskite synthesis, and application in organic chemistry.

ACKNOWLEDGEMENTS

PN thanks UGC (INDIA) and BP thanks NISER for the fellowship. We also thank the Department of Atomic Energy, Government of India (DAE) for financial support (grant number RIN 4002).

NOTES AND REFERENCES

1. D. Gust and T. A. Moore, Mimicking Photosynthesis, *Science*, 1989, **244**, 35-41. 10.1126/science.244.4900.35.
2. K. Wenderich and G. Mul, Methods, Mechanism, and Applications of Photodeposition in Photocatalysis: A Review, *Chem. Rev.*, 2016, **116**, 14587-14619. 10.1021/acs.chemrev.6b00327.
3. N. A. Romero and D. A. Nicewicz, Organic Photoredox Catalysis, *Chem. Rev.*, 2016, **116**, 10075-10166. 10.1021/acs.chemrev.6b00057.

4. S. Zhu and D. Wang, Photocatalysis: Basic Principles, Diverse Forms of Implementations and Emerging Scientific Opportunities, *Advanced Energy Materials*, 2017, **7**, 1700841. https://doi.org/10.1002/aenm.201700841.
5. H. Cano-Yelo and A. Deronzier, Photocatalysis of the Pschorr reaction by tris-(2,2′-bipyridyl)ruthenium(II) in the phenanthrene series, *Journal of the Chemical Society, Perkin Transactions 2*, 1984, 1093-1098. 10.1039/P29840001093.
6. A. Bauer, F. Westkämper, S. Grimme and T. Bach, Catalytic enantioselective reactions driven by photoinduced electron transfer, *Nature*, 2005, **436**, 1139-1140. 10.1038/nature03955.
7. M. Nakamura, R. Dohno and T. Majima, Intramolecular Binaphthyl Formation from Radical Cations of Tri-1-naphthyl Phosphate and Related Compounds in Photoinduced Electron-Transfer Reactions Sensitized by 9,10-Dicyanoanthracene, *J. Org. Chem.*, 1998, **63**, 6258-6265. 10.1021/jo9805706.
8. C. Vila, J. Lau and M. Rueping, Visible-light photoredox catalyzed synthesis of pyrroloisoquinolines via organocatalytic oxidation/[3 + 2] cycloaddition/oxidative aromatization reaction cascade with Rose Bengal, *Beilstein J. Org. Chem.*, 2014, **10**, 1233-1238. 10.3762/bjoc.10.122.
9. K. Kalyanasundaram, Photophysics, photochemistry and solar energy conversion with tris(bipyridyl)ruthenium(II) and its analogues, *Coord. Chem. Rev.*, 1982, **46**, 159-244. https://doi.org/10.1016/0010-8545(82)85003-0.
10. A. Juris, V. Balzani, F. Barigelletti, S. Campagna, P. Belser and A. von Zelewsky, Ru(II) polypyridine complexes: photophysics, photochemistry, eletrochemistry, and chemiluminescence, *Coord. Chem. Rev.*, 1988, **84**, 85-277. https://doi.org/10.1016/0010-8545(88)80032-8.
11. K. Kalyanasundaram and M. Grätzel, Applications of functionalized transition metal complexes in photonic and optoelectronic devices, *Coord. Chem. Rev.*, 1998, **177**, 347-414. https://doi.org/10.1016/S0010-8545(98)00189-1.
12. C. K. Prier, D. A. Rankic and D. W. C. MacMillan, Visible Light Photoredox Catalysis with Transition Metal Complexes: Applications in Organic Synthesis, *Chem. Rev.*, 2013, **113**, 5322-5363. 10.1021/cr300503r.
13. C. Han, X. Zhu, J. S. Martin, Y. Lin, S. Spears and Y. Yan, Recent Progress in Engineering Metal Halide Perovskites for Efficient Visible-Light-Driven Photocatalysis, *ChemSusChem*, 2020, **13**, 4005-4025. https://doi.org/10.1002/cssc.202000953.

14. P. Kanhere and Z. Chen, A Review on Visible Light Active Perovskite-Based Photocatalysts, *Molecules*, 2014, **19**, 19995-20022.
15. J. Jagielski, S. Kumar, M. Wang, D. Scullion, R. Lawrence, Y.-T. Li, S. Yakunin, T. Tian, M. V. Kovalenko, Y.-C. Chiu, E. J. G. Santos, S. Lin and C.-J. Shih, Aggregation-induced emission in lamellar solids of colloidal perovskite quantum wells, *Science*, 2017, **3**, eaaq0208. doi:10.1126/sciadv.aaq0208.
16. M. V. Kovalenko, L. Protesescu and M. I. Bodnarchuk, Properties and potential optoelectronic applications of lead halide perovskite nanocrystals, *Science*, 2017, **358**, 745-750. 10.1126/science.aam7093.
17. M. K. Panda, D. Acharjee, A. B. Mahato and S. Ghosh, Facet Dependent Photoluminescence Blinking from Perovskite Nanocrystals, *Small*, **n/a**, 2311559. https://doi.org/10.1002/smll.202311559.
18. L. Protesescu, S. Yakunin, M. I. Bodnarchuk, F. Krieg, R. Caputo, C. H. Hendon, R. X. Yang, A. Walsh and M. V. Kovalenko, Nanocrystals of Cesium Lead Halide Perovskites (CsPbX3, X = Cl, Br, and I): Novel Optoelectronic Materials Showing Bright Emission with Wide Color Gamut, *Nano Lett.*, 2015, **15**, 3692-3696. 10.1021/nl5048779.
19. H. Li, S. Li, Y. Wang, H. Sarvari, P. Zhang, M. Wang and Z. Chen, A modified sequential deposition method for fabrication of perovskite solar cells, *Solar Energy*, 2016, **126**, 243-251. https://doi.org/10.1016/j.solener.2015.12.045.
20. R. Zhu, Inverted devices are catching up, *Nature Energy*, 2020, **5**, 123-124. 10.1038/s41560-020-0559-z.
21. J. Wang, G. Wang and B. Chen, A review of recent progress on enhancing the stability of CsPbX3 perovskite solar cells, *Sustainable Energy & Fuels*, 2024. 10.1039/D4SE00914B.
22. M. L. Petrus, J. Schlipf, C. Li, T. P. Gujar, N. Giesbrecht, P. Müller-Buschbaum, M. Thelakkat, T. Bein, S. Hüttner and P. Docampo, Capturing the Sun: A Review of the Challenges and Perspectives of Perovskite Solar Cells, *Adv. Energy Mater.*, 2017, **7**, 1700264. https://doi.org/10.1002/aenm.201700264.
23. I. Lignos, S. Stavrakis, G. Nedelcu, L. Protesescu, A. J. deMello and M. V. Kovalenko, Synthesis of Cesium Lead Halide Perovskite Nanocrystals in a Droplet-Based Microfluidic Platform: Fast Parametric Space Mapping, *Nano Lett.*, 2016, **16**, 1869-1877. 10.1021/acs.nanolett.5b04981.

24. R. M. Maceiczyk, K. Dümbgen, I. Lignos, L. Protesescu, M. V. Kovalenko and A. J. deMello, Microfluidic Reactors Provide Preparative and Mechanistic Insights into the Synthesis of Formamidinium Lead Halide Perovskite Nanocrystals, *Chem. Mater.*, 2017, **29**, 8433-8439. 10.1021/acs.chemmater.7b02998.
25. O. Nazarenko, M. R. Kotyrba, S. Yakunin, M. Aebli, G. Rainò, B. M. Benin, M. Wörle and M. V. Kovalenko, Guanidinium-Formamidinium Lead Iodide: A Layered Perovskite-Related Compound with Red Luminescence at Room Temperature, *J. Am. Chem. Soc.*, 2018, **140**, 3850-3853. 10.1021/jacs.8b00194.
26. G. Nedelcu, L. Protesescu, S. Yakunin, M. I. Bodnarchuk, M. J. Grotevent and M. V. Kovalenko, Fast Anion-Exchange in Highly Luminescent Nanocrystals of Cesium Lead Halide Perovskites (CsPbX3, X = Cl, Br, I), *Nano Lett.*, 2015, **15**, 5635-5640. 10.1021/acs.nanolett.5b02404.
27. P. Papagiorgis, L. Protesescu, M. V. Kovalenko, A. Othonos and G. Itskos, Long-Lived Hot Carriers in Formamidinium Lead Iodide Nanocrystals, *J. Phys. Chem. C*, 2017, **121**, 12434-12440. 10.1021/acs.jpcc.7b02308.
28. R. Yadav, M. Roy, G. Banappanavar and M. Aslam, Growth of Hybrid Perovskite Films via Single-Source Perovskite Nanoparticle Evaporation, *Chemistry An Asian Journal*, 2022, **17**, e202200087. https://doi.org/10.1002/asia.202200087.
29. G. Wang, F. Zhang, Y. Wang and J. Ma, Research Progress on Photocatalytic Reduction of CO2 Based on CsPbBr3 Perovskite Materials, *ChemNanoMat*, 2022, **8**, e202200230. https://doi.org/10.1002/cnma.202200230.
30. X. Zhu, Y. Lin, Y. Sun, M. C. Beard and Y. Yan, Lead-Halide Perovskites for Photocatalytic α-Alkylation of Aldehydes, *J. Am. Chem. Soc.*, 2019, **141**, 733-738. 10.1021/jacs.8b08720.
31. D. Parobek, Y. Dong, T. Qiao, D. Rossi and D. H. Son, Photoinduced Anion Exchange in Cesium Lead Halide Perovskite Nanocrystals, *J. Am. Chem. Soc.*, 2017, **139**, 4358-4361. 10.1021/jacs.7b01480.
32. G. Ghosh, K. Marjit, S. Ghosh, D. Ghosh and A. Patra, Evidence of Hot Charge Carrier Transfer in Hybrid CsPbBr3/Functionalized Graphene, *ChemNanoMat*, 2022, **8**, e202200172. https://doi.org/10.1002/cnma.202200172.
33. A. Das, D. Acharjee, M. K. Panda, A. B. Mahato and S. Ghosh, Dodecahedron CsPbBr3 Perovskite Nanocrystals Enable Facile Harvesting of Hot Electrons and Holes, *The Journal of Physical Chemistry Letters*, 2023, **14**, 3953-3960. 10.1021/acs.jpclett.3c00661.

34. J. Shamsi, A. S. Urban, M. Imran, L. De Trizio and L. Manna, Metal Halide Perovskite Nanocrystals: Synthesis, Post-Synthesis Modifications, and Their Optical Properties, *Chem. Rev.*, 2019, **119**, 3296-3348. 10.1021/acs.chemrev.8b00644.

35. Q. Chen, J. Wu, X. Ou, B. Huang, J. Almutlaq, A. A. Zhumekenov, X. Guan, S. Han, L. Liang, Z. Yi, J. Li, X. Xie, Y. Wang, Y. Li, D. Fan, D. B. L. Teh, A. H. All, O. F. Mohammed, O. M. Bakr, T. Wu, M. Bettinelli, H. Yang, W. Huang and X. Liu, All-inorganic perovskite nanocrystal scintillators, *Nature*, 2018, **561**, 88-93. 10.1038/s41586-018-0451-1.

36. Q. A. Akkerman, G. Rainò, M. V. Kovalenko and L. Manna, Genesis, challenges and opportunities for colloidal lead halide perovskite nanocrystals, *Nat. Mater.*, 2018, **17**, 394-405. 10.1038/s41563-018-0018-4.

37. K. Chen, X. Deng, G. Dodekatos and H. Tüysüz, Photocatalytic Polymerization of 3,4-Ethylenedioxythiophene over Cesium Lead Iodide Perovskite Quantum Dots, *J. Am. Chem. Soc.*, 2017, **139**, 12267-12273. 10.1021/jacs.7b06413.

38. W.-B. Wu, Y.-C. Wong, Z.-K. Tan and J. Wu, Photo-induced thiol coupling and C–H activation using nanocrystalline lead-halide perovskite catalysts, *Catal. Sci. Technol.*, 2018, **8**, 4257-4263. 10.1039/c8cy01240g.

39. D. Ravelli, S. Protti and M. Fagnoni, Carbon–Carbon Bond Forming Reactions via Photogenerated Intermediates, *Chem. Rev.*, 2016, **116**, 9850-9913. 10.1021/acs.chemrev.5b00662.

40. A. Vijeta, C. Casadevall, S. Roy and E. Reisner, Visible-Light Promoted C–O Bond Formation with an Integrated Carbon Nitride–Nickel Heterogeneous Photocatalyst, *Angew. Chem. Int. Ed.*

2021, **60**, 8494-8499. https://doi.org/10.1002/anie.202016511.

41. U. S. Kanchana, E. J. Diana, T. V. Mathew and G. Anilkumar, Palladium- Catalyzed C−P Bond Forming Reactions: An Overview, *ChemistrySelect* 2021, **6**, 1579-1588. https://doi.org/10.1002/slct.202004433.

42. R. Bhanja, S. K. Bera and P. J. S. Mal, Transition-Metal-and Photocatalyst-Free Photoinduced Formation of Carbon–Pnictogen (–N,–P) Bonds, *Synthesis*, 2024.

43. D. A. Nicewicz and D. W. C. MacMillan, Merging Photoredox Catalysis with Organocatalysis: The Direct Asymmetric Alkylation of Aldehydes, *Science*, 2008, **322**, 77-80. 10.1126/science.1161976.

44. X. Zhu, Y. Lin, J. San Martin, Y. Sun, D. Zhu and Y. Yan, Lead halide perovskites for photocatalytic organic synthesis, *Nat. Commun.*, 2019, **10**, 2843. 10.1038/s41467-019-10634-x.

45. S. Bonabi Naghadeh, B. Luo, G. Abdelmageed, Y.-C. Pu, C. Zhang and J. Z. Zhang, Photophysical Properties and Improved Stability of Organic–Inorganic Perovskite by Surface Passivation, *J. Phys. Chem. C*, 2018, **122**, 15799-15818. 10.1021/acs.jpcc.8b03681.

46. Y. Tan, Y. Zou, L. Wu, Q. Huang, D. Yang, M. Chen, M. Ban, C. Wu, T. Wu, S. Bai, T. Song, Q. Zhang and B. Sun, Highly Luminescent and Stable Perovskite Nanocrystals with Octylphosphonic Acid as a Ligand for Efficient Light-Emitting Diodes, *ACS Appl. Mater. Interfaces*, 2018, **10**, 3784-3792. 10.1021/acsami.7b17166.

47. F. Zhang, D. Bi, N. Pellet, C. Xiao, Z. Li, J. J. Berry, S. M. Zakeeruddin, K. Zhu and M. Grätzel, Suppressing defects through the synergistic effect of a Lewis base and a Lewis acid for highly efficient and stable perovskite solar cells, *Energy Environ. Sci.*, 2018, **11**, 3480-3490. 10.1039/C8EE02252F.

48. S. Fustero, M. Sánchez-Roselló, P. Barrio and A. Simón-Fuentes, From 2000 to Mid-2010: A Fruitful Decade for the Synthesis of Pyrazoles, *Chem. Rev.*, 2011, **111**, 6984-7034. 10.1021/cr2000459.

49. I. Rosa-Pardo, C. Casadevall, L. Schmidt, M. Claros, R. E. Galian, J. Lloret-Fillol and J. Pérez-Prieto, The synergy between the CsPbBr3 nanoparticle surface and the organic ligand becomes manifest in a demanding carbon–carbon coupling reaction, *Chem. Commun.*, 2020, **56**, 5026-5029. 10.1039/D0CC01339K.

50. V. Bhardwaj, D. Gumber, V. Abbot, S. Dhiman and P. Sharma, Pyrrole: a resourceful small molecule in key medicinal hetero-aromatics, *RSC Adv.*, 2015, **5**, 15233-15266. 10.1039/C4RA15710A.

51. B. H. Ganesh, A. G. Raj, B. Aruchamy, P. Nanjan, C. Drago and P. Ramani, Pyrrole: A Decisive Scaffold for the Development of Therapeutic Agents and Structure-Activity Relationship, *ChemMedChem*, 2024, **19**, e202300447. https://doi.org/10.1002/cmdc.202300447.

52. N. Jeelan Basha, S. M. Basavarajaiah and K. Shyamsunder, Therapeutic potential of pyrrole and pyrrolidine analogs: an update, *Molecular Diversity*, 2022, **26**, 2915-2937. 10.1007/s11030-022-10387-8.

53. J. F. Hartwig, Carbon–heteroatom bond formation catalysed by organometallic complexes, *Nature*, 2008, **455**, 314-322. 10.1038/nature07369.

54. G. Evano, J. Wang and A. Nitelet, Metal-mediated C–O bond forming reactions in natural product synthesis, *Org. Chem. Front.*, 2017, **4**, 2480-2499. 10.1039/C7QO00671C.
55. H. Miyabe, Synthesis of Oxygen Heterocycles via Aromatic C-O Bond Formation Using Arynes, *Molecules*, 2015, **20**, 12558-12575.
56. C. Michelin and N. Hoffmann, Photosensitization and Photocatalysis—Perspectives in Organic Synthesis, *ACS Catal.*, 2018, **8**, 12046-12055. 10.1021/acscatal.8b03050.
57. A. Kojima, K. Teshima, Y. Shirai and T. Miyasaka, Organometal Halide Perovskites as Visible-Light Sensitizers for Photovoltaic Cells, *J. Am. Chem. Soc.*, 2009, **131**, 6050-6051. 10.1021/ja809598r.
58. Z. A. VanOrman, H. K. Drozdick, S. Wieghold and L. Nienhaus, Bulk halide perovskites as triplet sensitizers: progress and prospects in photon upconversion, *J. Mater. Chem. C*, 2021, **9**, 2685-2694. 10.1039/D1TC00245G.
59. J.-X. Wang, X. Wang, J. Yin, L. Gutiérrez-Arzaluz, T. He, C. Chen, Y. Han, Y. Zhang, O. M. Bakr, M. Eddaoudi and O. F. Mohammed, Perovskite-Nanosheet Sensitizer for Highly Efficient Organic X-ray Imaging Scintillator, *ACS Energy Lett.*, 2022, **7**, 10-16. 10.1021/acsenergylett.1c02173.
60. A. Pasha, P. Pramanik, J. K. George, N. Dhiman, H. Zhang, S. Sidhik, F. Mandani, S. Ranjan, A. T. Nagaraja, S. Umapathy, A. D. Mohite and R. G. Balakrishna, Cationic and Anionic Vacancy Healing for Suppressed Halide Exchange and Phase Segregation in Perovskite Solar Cells, *ACS Energy Lett.*, 2023, **8**, 3081-3087. 10.1021/acsenergylett.3c01024.
61. S. M. Liga, S. R. Kavanagh, A. Walsh, D. O. Scanlon and G. Konstantatos, Mixed-Cation Vacancy-Ordered Perovskites (Cs2Ti1–xSnxX6; X = I or Br): Low-Temperature Miscibility, Additivity, and Tunable Stability, *J. Phys. Chem. C*, 2023, **127**, 21399-21409. 10.1021/acs.jpcc.3c05204.
62. T. Yamamoto, A. Chikamatsu, S. Kitagawa, N. Izumo, S. Yamashita, H. Takatsu, M. Ochi, T. Maruyama, M. Namba, W. Sun, T. Nakashima, F. Takeiri, K. Fujii, M. Yashima, Y. Sugisawa, M. Sano, Y. Hirose, D. Sekiba, C. M. Brown, T. Honda, K. Ikeda, T. Otomo, K. Kuroki, K. Ishida, T. Mori, K. Kimoto, T. Hasegawa and H. Kageyama, Strain-induced creation and switching of anion vacancy layers in perovskite oxynitrides, *Nat. Commun.*, 2020, **11**, 5923. 10.1038/s41467-020-19217-7.

63. H. Jiang, S. Cui, Y. Chen and H. Zhong, Ion exchange for halide perovskite: From nanocrystal to bulk materials, *Nano Select*, 2021, **2**, 2040-2060. https://doi.org/10.1002/nano.202100084.

64. K. Sandeep, K. Padmakumar, K. U. Ambili, P. Jishnu, K. H. Fousia, A. R. Ramesh, J. P. Rappai, V. Santhi and M. Shanthil, Anion Exchange in Lead Halide Perovskites: An Overview, *physica status solidi (b)*, 2022, **259**, 2100600. https://doi.org/10.1002/pssb.202100600.

65. B. Hu, W. Zhang and Y. Chu, Hybrid Amino Acid Ligand-Regulated Excited Dynamics of Highly Luminescent Perovskite Quantum Dots for Bright White Light-Emitting Diodes, *Nanomaterials*, 2024, **14**, 1266.

66. Q. Chen, X. Yang, Y. Zhou and B. Song, Zwitterions: promising interfacial/doping materials for organic/perovskite solar cells, *New J. Chem.*, 2021, **45**, 15118-15130. 10.1039/D1NJ01605A.

67. C. Cueto, M. Hu, T. P. Russell and T. Emrick, Conjugated Zwitterionic Oligomers as Ligands on Perovskite Nanocrystals: Hybrid Structures with Tunable Interparticle Spacing, *J. Am. Chem. Soc.*, 2024, **146**, 8189-8197. 10.1021/jacs.3c12723.

68. K. Xiao, R. Lin, Q. Han, Y. Hou, Z. Qin, H. T. Nguyen, J. Wen, M. Wei, V. Yeddu, M. I. Saidaminov, Y. Gao, X. Luo, Y. Wang, H. Gao, C. Zhang, J. Xu, J. Zhu, E. H. Sargent and H. Tan, All-perovskite tandem solar cells with 24.2% certified efficiency and area over 1 cm2 using surface-anchoring zwitterionic antioxidant, *Nat. Energy*, 2020, **5**, 870-880. 10.1038/s41560-020-00705-5.

69. S. Ghosh and P. Kar, Aromatic Amino Acid-Mediated Perovskite Nanocrystals: Fluorescence Tuning and Morphological Evolution, *Inorg. Chem.*, 2022, **61**, 10079-10088. 10.1021/acs.inorgchem.2c01021.

70. N. Agarwal, D. Agarwal and T. Debnath, Amino Acid-Driven Dimensional Reduction of CsPbBr3 Nanocrystals, *ACS Omega*, 2024, **9**, 31026-31034. 10.1021/acsomega.4c04364.

71. A. Jancik Prochazkova, Y. Salinas, C. Yumusak, O. Brüggemann, M. Weiter, N. S. Sariciftci, J. Krajcovic and A. Kovalenko, Cyclic Peptide Stabilized Lead Halide Perovskite Nanoparticles, *Scientific Reports*, 2019, **9**, 12966. 10.1038/s41598-019-49643-7.

72. T. Shi, K. Sun, X.-L. Chen, Z.-X. Zhang, X.-Q. Huang, Y.-Y. Peng, L.-B. Qu and B. Yu, Recyclable Perovskite as Heterogeneous Photocatalyst for Aminomethylation of

Imidazo-Fused Heterocycles, *Adv. Synth. Catal.*, 2020, **362**, 2143-2149. https://doi.org/10.1002/adsc.201901324.

73. G. Yashwantrao and S. Saha, Recent advances in the synthesis and reactivity of quinoxaline, *Org. Chem. Front.*, 2021, **8**, 2820-2862. 10.1039/D0QO01575J.
74. S. Sau and P. J. T. J. o. O. C. Mal, Visible-Light Promoted Regioselective Oxygenation of Quinoxalin-2 (1 H)-Ones Using O2 as an Oxidant, *J. Org. Chem.*, 2022, **87**, 14565-14579.
75. S. Sau and P. J. E. J. o. O. C. Mal, C− H Hydroxylation of Quinoxalin-2 (1H)-ones through ipso-Substitution Using tert-Butyl Nitrite, *Eur. J. Org. Chem.*, 2022, **2022**, e202200425.
76. B. Pal, S. Sahoo and P. Mal, Atom Transfer Radical Addition Reactions of Quinoxalin-2(1H)-ones with CBr4 and Styrenes Using Mes-Acr-MeClO4 Photocatalyst, *J. Org. Chem.*, 2024, **89**, 1784-1796. 10.1021/acs.joc.3c02469.
77. S. Sau, S. Sahoo, A. Manna and P. Mal, Moisture-resistant radical anions of quinoxalin-2(1H)-ones in aerial dioxygen activation, *Org. Biomol. Chem.*, 2024, **22**, 4662-4666. 10.1039/D4OB00673A.
78. Y.-F. Si, K. Sun, X.-L. Chen, X.-Y. Fu, Y. Liu, F.-L. Zeng, T. Shi, L.-B. Qu and B. Yu, Arylaminomethyl Radical-Initiated Cascade Annulation Reaction of Quinoxalin-2(1H)-ones Catalyzed by Recyclable Photocatalyst Perovskite, *Org. Lett.*, 2020, **22**, 6960-6965. 10.1021/acs.orglett.0c02518.
79. J. Zhang, J. Lalevée, X. Mou, F. Morlet-Savary, B. Graff and P. Xiao, N-Phenylglycine as a Versatile Photoinitiator under Near-UV LED, *Macromolecules*, 2018, **51**, 3767-3773. 10.1021/acs.macromol.8b00747.
80. Y. Xu, W. Zhang, K. Su, Y.-X. Feng, Y.-F. Mu, M. Zhang and T.-B. Lu, Glycine-Functionalized CsPbBr3 Nanocrystals for Efficient Visible-Light Photocatalysis of CO2 Reduction, *Chem. Eur. J.*, 2021, **27**, 2305-2309. https://doi.org/10.1002/chem.202004682.
81. Y. Yuan, H. Zhu, K. Hills-Kimball, T. Cai, W. Shi, Z. Wei, H. Yang, Y. Candler, P. Wang, J. He and O. Chen, Stereoselective C−C Oxidative Coupling Reactions Photocatalyzed by Zwitterionic Ligand Capped CsPbBr3 Perovskite Quantum Dots, *Angew. Chem. Int. Ed.,* 2020, **59**, 22563-22569. https://doi.org/10.1002/anie.202007520.

82. F. Krieg, S. T. Ochsenbein, S. Yakunin, S. ten Brinck, P. Aellen, A. Süess, B. Clerc, D. Guggisberg, O. Nazarenko, Y. Shynkarenko, S. Kumar, C.-J. Shih, I. Infante and M. V. Kovalenko, Colloidal CsPbX3 (X = Cl, Br, I) Nanocrystals 2.0: Zwitterionic Capping Ligands for Improved Durability and Stability, *ACS Energy Lett.*, 2018, **3**, 641-646. 10.1021/acsenergylett.8b00035.

83. M. I. Han and Ŧ. J. C. d. t. Küçükgüzel, Thioethers: an overview, *Current drug targets*, 2022, **23**, 170-219.

84. Y. Lv, Z. Wang, J. Hao, X. Zhao and W. Wei, Visible-Light-Induced Synthesis of Thioethers through Three-Component Reactions of α-Diazoesters, Thiols, and Cyclic Ethers, *Asian J. Org. Chem.*, 2023, **12**, e202300290. https://doi.org/10.1002/ajoc.202300290.

85. A. Nandy, I. Kazi, S. Guha and G. Sekar, Visible-Light-Driven Halogen-Bond-Assisted Direct Synthesis of Heteroaryl Thioethers Using Transition-Metal-Free One-Pot C–I Bond Formation/C–S Cross-Coupling Reaction, *J. Org. Chem.*, 2021, **86**, 2570-2581. 10.1021/acs.joc.0c02672.

86. M. Pramanik, K. Choudhuri and P. Mal, Metal-free C–S coupling of thiols and disulfides, *Org. Biomol. Chem.*, 2020, **18**, 8771-8792. 10.1039/D0OB01741H.

87. V. J. Geiger, R. M. Oechsner, P. H. Gehrtz and I. J. S. Fleischer, Recent metal-catalyzed methods for thioether synthesis, *Synthesis*, 2022, **54**, 5139-5167.

88. I. P. Beletskaya and V. P. J. C. R. Ananikov, Transition-metal-catalyzed C–S, C–Se, and C–Te bond formations via cross-coupling and atom-economic addition reactions. Achievements and challenges, *Chem. Rev.*, 2022, **122**, 16110-16293.

89. D. Kaiser, I. Klose, R. Oost, J. Neuhaus and N. Maulide, Bond-Forming and -Breaking Reactions at Sulfur(IV): Sulfoxides, Sulfonium Salts, Sulfur Ylides, and Sulfinate Salts, *Chem. Rev.*, 2019, **119**, 8701-8780. 10.1021/acs.chemrev.9b00111.

90. H. Song, J. Yang, S. G. Lim, J. Lee, W. H. Jeong, H. Choi, J. H. Lee, H. Y. Kim, B. R. Lee and H. Choi, On the surface passivating principle of functional thiol towards efficient and stable perovskite nanocrystal solar cells, *Chem. Eng. J.*, 2023, **454**, 140224. https://doi.org/10.1016/j.cej.2022.140224.

91. X. Liu, R. Bai, Z. Guo, Y. Che, C. Guo and H. Xing, Photogeneration of thiyl radicals using metal-halide perovskite for highly efficient synthesis of thioethers, *Appl. Organomet. Chem.*, 2022, **36**, e6492. https://doi.org/10.1002/aoc.6492.

92. E. L. Tyson, M. S. Ament and T. P. Yoon, Transition Metal Photoredox Catalysis of Radical Thiol-Ene Reactions, *J. Org. Chem.*, 2013, **78**, 2046-2050. 10.1021/jo3020825.

93. X.-Y. Chen and W. Shu, Radical-Enabled Dehydrogenative Aromatization: Forging Functionalized Aromatics from Aliphatic Architectures at Ambient Temperature, *ChemCatChem*, **n/a**, e202400688. https://doi.org/10.1002/cctc.202400688.

94. Z. Qu, X. Ji, S. Tang, G.-J. Deng and H. Huang, Hydrogen-Borrowing Reduction/Dehydrogenative Aromatization of Nitroarenes through Visible-Light-Induced Energy Transfer: An Entry to Pyrimidoindazoles and Carbazoles, *Org. Lett.*, 2022, **24**, 7173-7177. 10.1021/acs.orglett.2c02894.

95. S. H. Son, J.-W. Shin, H.-J. Won, H.-S. Yoo, Y. Y. Cho, S. L. Kim, Y. H. Jang, B. Y. Park and N.-J. Kim, Synthesis of meta-(Indol-3-yl)phenols from Indoles and Cyclohexenone via Palladium(II)-Catalyzed Oxidative Heck Reaction and Dehydrogenative Aromatization in a One-Step Sequence, *Org. Lett.*, 2021, **23**, 7467-7471. 10.1021/acs.orglett.1c02679.

96. S. A. Girard, H. Huang, F. Zhou, G.-J. Deng and C.-J. Li, Catalytic dehydrogenative aromatization: an alternative route to functionalized arenes, *Org. Chem. Front.*, 2015, **2**, 279-287. 10.1039/C4QO00358F.

97. P.-Z. Wang, J.-R. Chen and W.-J. Xiao, Hantzsch esters: an emerging versatile class of reagents in photoredox catalyzed organic synthesis, *Org. Biomol. Chem.*, 2019, **17**, 6936-6951. 10.1039/C9OB01289C.

98. M. O. Konev, L. Cardinale and A. Jacobi von Wangelin, Catalyst-Free N-Deoxygenation by Photoexcitation of Hantzsch Ester, *Org. Lett.*, 2020, **22**, 1316-1320. 10.1021/acs.orglett.9b04632.

99. Y.-Y. Guo, Z.-H. Tian, Y.-C. Han, D. Ma, T. Shao and Z. Jiang, Hantzsch Ester as Efficient and Economical NAD(P)H Mimic for In Vitro Bioredox Reactions, *Chem. Eur. J.*, 2023, **29**, e202301180. https://doi.org/10.1002/chem.202301180.

100. D.-L. Zhu, Q. Wu, H.-Y. Li, H.-X. Li and J.-P. Lang, Hantzsch Ester as a Visible-Light Photoredox Catalyst for Transition-Metal-Free Coupling of Arylhalides and Arylsulfinates, *Chem. Eur. J.*, 2020, **26**, 3484-3488. https://doi.org/10.1002/chem.201905281.

101. S. Pradhan, D. Bhujel, B. Gurung, D. Sharma, S. Basel, S. Rasaily, S. Thapa, S. Borthakur, W. L. Ling, L. Saikia, P. Reiss, A. Pariyar and S. Tamang, Stable lead-

halide perovskite quantum dots as efficient visible light photocatalysts for organic transformations, *Nanoscale Adv.*, 2021, **3**, 1464-1472. 10.1039/D0NA00992J.

102. C. C. Boyd, R. Cheacharoen, T. Leijtens and M. D. McGehee, Understanding Degradation Mechanisms and Improving Stability of Perovskite Photovoltaics, *Chem. Rev.*, 2019, **119**, 3418-3451. 10.1021/acs.chemrev.8b00336.
103. A. J. J. L. A. d. C. Hantzsch, Ueber die synthese pyridinartiger verbindungen aus acetessigäther und aldehydammoniak, *Justus Liebigs Ann. Chem.*, 1882, **215**, 1-82.
104. B.-S. Mu, X.-Y. Cui, X.-P. Zeng, J.-S. Yu and J. Zhou, Modular synthesis of chiral 1,2-dihydropyridines via Mannich/Wittig/cycloisomerization sequence that internally reuses waste, *Nat. Commun.*, 2021, **12**, 2219. 10.1038/s41467-021-22374-y.
105. J.-Y. Zhang and X.-Q. Zhu, Comparison between 1,2-Dihydropyridine and 1,4-Dihydropyridine on Hydride-Donating Ability and Activity, *Molecules*, 2022, **27**, 5382.
106. A. Ansari, A. Ali, M. Asif and Shamsuzzaman, Review: biologically active pyrazole derivatives, *New J. Chem.*, 2017, **41**, 16-41. 10.1039/C6NJ03181A.
107. R. V. J. J. C. R. Kupwade, A concise review on synthesis of sulfoxides and sulfones with special reference to oxidation of sulfides, *J. Chem. Rev.*, 2019, **1**, 99-113.
108. I. Fernández and N. Khiar, Recent Developments in the Synthesis and Utilization of Chiral Sulfoxides, *Chem. Rev.*, 2003, **103**, 3651-3706. 10.1021/cr990372u.
109. Q. Fan, L. Zhu, X. Li, H. Ren, H. Zhu, G. Wu and J. Ding, Visible-light photocatalytic selective oxidation of amine and sulfide with CsPbBr3 as photocatalyst, *New J. Chem.*, 2021, **45**, 13317-13322. 10.1039/D1NJ02595C.
110. J. Yin, G. H. Ahmed, O. M. Bakr, J.-L. Brédas and O. F. Mohammed, Unlocking the Effect of Trivalent Metal Doping in All-Inorganic CsPbBr3 Perovskite, *ACS Energy Lett.*, 2019, **4**, 789-795. 10.1021/acsenergylett.9b00209.
111. Y. Xie, B. Peng, I. Bravić, Y. Yu, Y. Dong, R. Liang, Q. Ou, B. Monserrat and S. Zhang, Highly Efficient Blue-Emitting CsPbBr3 Perovskite Nanocrystals through Neodymium Doping, *Adv. Sci.*, 2020, **7**, 2001698. https://doi.org/10.1002/advs.202001698.
112. M. Liu, G. Zhong, Y. Yin, J. Miao, K. Li, C. Wang, X. Xu, C. Shen and H. Meng, Aluminum-Doped Cesium Lead Bromide Perovskite Nanocrystals with Stable Blue Photoluminescence Used for Display Backlight, *Adv. Sci.*, 2017, **4**, 1700335. https://doi.org/10.1002/advs.201700335.

113. Y. Lin, Y. Shao, J. Dai, T. Li, Y. Liu, X. Dai, X. Xiao, Y. Deng, A. Gruverman, X. C. Zeng and J. Huang, Metallic surface doping of metal halide perovskites, *Nat. Commun.*, 2021, **12**, 7. 10.1038/s41467-020-20110-6.

114. Y. Zhou, J. Chen, O. M. Bakr and H.-T. Sun, Metal-Doped Lead Halide Perovskites: Synthesis, Properties, and Optoelectronic Applications, *Chem. Mater.*, 2018, **30**, 6589-6613. 10.1021/acs.chemmater.8b02989.

115. N. Phung, R. Félix, D. Meggiolaro, A. Al-Ashouri, G. Sousa e Silva, C. Hartmann, J. Hidalgo, H. Köbler, E. Mosconi, B. Lai, R. Gunder, M. Li, K.-L. Wang, Z.-K. Wang, K. Nie, E. Handick, R. G. Wilks, J. A. Marquez, B. Rech, ... and A. Abate, The Doping Mechanism of Halide Perovskite Unveiled by Alkaline Earth Metals, *JACS*, 2020, **142**, 2364-2374. 10.1021/jacs.9b11637.

116. F. Zhong, Y. He, Y. Sun, F. Dong and J. Sheng, Metal-doping of halide perovskite nanocrystals for energy and environmental photocatalysis: challenges and prospects, *J. Mat. Chem. A*, 2022, **10**, 22915-22928. 10.1039/D2TA06851F.

117. J. S. Martin, X. Zeng, X. Chen, C. Miller, C. Han, Y. Lin, N. Yamamoto, X. Wang, S. Yazdi, Y. Yan, M. C. Beard and Y. Yan, A Nanocrystal Catalyst Incorporating a Surface Bound Transition Metal to Induce Photocatalytic Sequential Electron Transfer Events, *J. Am. Chem. Soc.*, 2021, **143**, 11361-11369. 10.1021/jacs.1c00503.

118. B. Zhang, L. Goldoni, C. Lambruschini, L. Moni, M. Imran, A. Pianetti, V. Pinchetti, S. Brovelli, L. De Trizio and L. Manna, Stable and Size Tunable CsPbBr3 Nanocrystals Synthesized with Oleylphosphonic Acid, *Nano Lett.*, 2020, **20**, 8847-8853. 10.1021/acs.nanolett.0c03833.

119. V. K. Ravi, P. K. Santra, N. Joshi, J. Chugh, S. K. Singh, H. Rensmo, P. Ghosh and A. Nag, Origin of the Substitution Mechanism for the Binding of Organic Ligands on the Surface of CsPbBr3 Perovskite Nanocubes, *J. Phys. Chem. Lett.*, 2017, **8**, 4988-4994. 10.1021/acs.jpclett.7b02192.

120. T. Kosugi, Y. Iso and T. Isobe, Effects of Oleic Acid on the Stability of Perovskite CsPbBr3 Quantum Dot Dispersions, *Chem. Lett.*, 2019, **48**, 349-352. 10.1246/cl.180998 %J Chemistry Letters.

121. Y. Lin, M. Avvacumova, R. Zhao, X. Chen, M. C. Beard and Y. Yan, Triplet Energy Transfer from Lead Halide Perovskite for Highly Selective Photocatalytic 2 + 2 Cycloaddition, *ACS Appl. Mater. Interfaces*, 2022, **14**, 25357-25365. 10.1021/acsami.2c03411.

122. Q. Li, C. Wen, J. Yang, X. Zhou, Y. Zhu, J. Zheng, G. Cheng, J. Bai, T. Xu, J. Ji, S. Jiang, L. Zhang and P. Zhang, Zwitterionic Biomaterials, *Chem. Rev.*, 2022, **122**, 17073-17154. 10.1021/acs.chemrev.2c00344.

123. M. Yoshizawa-Fujita and H. Ohno, Applications of Zwitterions and Zwitterionic Polymers for Li-Ion Batteries, *Chem. Rec.*, 2023, **23**, e202200287. https://doi.org/10.1002/tcr.202200287.

124. L. Beverina and G. A. Pagani, π-Conjugated Zwitterions as Paradigm of Donor–Acceptor Building Blocks in Organic-Based Materials, *Acc. Chem. Res.*, 2014, **47**, 319-329. 10.1021/ar4000967.

125. R. Chauvin, Zwitterionic Organometallates, *Eur. J. Inorg. Chem.*, 2000, 577-591. https://doi.org/10.1002/(SICI)1099-0682(200004)2000:4<577::AID-EJIC577>3.0.CO;2-F.

126. Y.-H. Chiao, A. Sengupta, M. B. M. Y. Ang, S.-T. Chen, T. Y. Haan, J. Almodovar, W.-S. Hung and S. R. J. P. Wickramasinghe, Application of zwitterions in forward osmosis: A short review, *Polymers*, 2021, **13**, 583.

127. A. Shi, K. Sun, X. Chen, L. Qu, Y. Zhao and B. Yu, Perovskite as Recyclable Photocatalyst for Annulation Reaction of N-Sulfonyl Ketimines, *Org. Lett.*, 2022, **24**, 299-303. 10.1021/acs.orglett.1c03960.

128. N. Kerru, L. Gummidi, S. Maddila, K. K. Gangu and S. B. Jonnalagadda, A Review on Recent Advances in Nitrogen-Containing Molecules and Their Biological Applications, *Molecules*, 2020, **25**, 1909.

129. J. F. J. N. Hartwig, Carbon–heteroatom bond formation catalysed by organometallic complexes, *Nature*, 2008, **455**, 314-322.

130. R. Bhanja, S. Kanti Bera and P. Mal, Sustainable Synthesis through Catalyst-Free Photoinduced Cascaded Bond Formation, *Chem. Asian J.*, 2024, **19**, e202400279. https://doi.org/10.1002/asia.202400279.

131. R. Bhanja, S. K. Bera and P. Mal, Photocatalyst- and Transition-Metal-Free Light-Induced Formation of Carbon-Chalcogen Bonds, *Adv. Synth. Catal.*, 2024, **366**, 168-182. https://doi.org/10.1002/adsc.202301094.

132. J. Bariwal and E. Van der Eycken, C–N bond forming cross-coupling reactions: an overview, *Chem. Soc. Rev.*, 2013, **42**, 9283-9303. 10.1039/C3CS60228A.

133. S. Kathiravan and I. A. Nicholls, Recent advances in electrochemical C–N bond formation via C–H/N–H activation with hydrogen evolution, *Curr. Res. Green Sustain.*, 2024, **8**, 100405. https://doi.org/10.1016/j.crgsc.2024.100405.

134. C. Lee, H.-J. Kang and S. Hong, NiH-catalyzed C–N bond formation: insights and advancements in hydroamination of unsaturated hydrocarbons, *Chem. Sci.*, 2024, **15**, 442-457. 10.1039/D3SC05589B.

135. J. Luo and W.-T. Wei, Recent Advances in the Construction of C–N Bonds Through Coupling Reactions between Carbon Radicals and Nitrogen Radicals, *Adv. Synth. Catal.*, 2018, **360**, 2076-2086. https://doi.org/10.1002/adsc.201800205.

136. M. Ju and J. M. Schomaker, Nitrene transfer catalysts for enantioselective C–N bond formation, *Nat. Rev. Chem.*, 2021, **5**, 580-594. 10.1038/s41570-021-00291-4.

137. B. Gurung, S. Pradhan, D. Sharma, D. Bhujel, S. Basel, S. Chettri, S. Rasaily, A. Pariyar and S. Tamang, CsPbBr3 perovskite quantum dots as a visible light photocatalyst for cyclisation of diamines and amino alcohols: an efficient approach to synthesize imidazolidines, fused-imidazolidines and oxazolidines, *Catal. Sci. Technol.*, 2022, **12**, 5891-5898. 10.1039/D2CY00799A.

138. G. F. S. Fernandes, C. B. Scarim, S.-H. Kim, J. Wu and D. Castagnolo, Oxazolidinones as versatile scaffolds in medicinal chemistry, *RSC Medicinal Chemistry*, 2023, **14**, 823-847. 10.1039/D2MD00415A.

139. J. F Branco-Junior, D. RC Teixeira, M. C Pereira, I. R Pitta and M. J. C. B. C. R Galdino-Pitta, The role of oxazolidine derivatives in the treatment of infectious and chronic diseases, *Current Bioactive Compounds*, 2017, **13**, 292-304.

140. S. Singh, S. Sahu, D. Mittal, S. De and V. Govind Rao, Metal Halide Perovskite Nanocrystals for C–X Activation: Role of Halide Vacancies, *ACS Appl. Nano Mater.*, 2024, **7**, 16913-16921. 10.1021/acsanm.4c03013.

141. A. J. C. S. R. Thibblin, Mechanisms of solvolytic alkene-forming elimination reactions, *Chem. Soc. Rev.*, 1993, **22**, 427-433.

142. P. Perocco, S. Bolognesi and W. Alberghini, Toxic activity of seventeen industrial solvents and halogenated compounds on human lymphocytes cultured in vitro, *Toxicol. Lett.*, 1983, **16**, 69-75. https://doi.org/10.1016/0378-4274(83)90012-7.

143. M. Mercier, M. Lans and J. De Gerlache, Mutagenicity, carcinogenicity, and teratogenicity of halogenated hydrocarbon solvents. In *Mutagenicity, carcinogenicity, and teratogenicity of industrial pollutants*, Springer: 1984; pp 281-324.

144. J. L. Raucy, J. C. Kraner and J. M. Lasker, Bioactivation of Halogenated Hydrocarbons by Cytochrome P4502E1, *Crit. Rev. Toxicol.*, 1993, **23**, 1-20. 10.3109/10408449309104072.

145. D. R. Addis, J. A. Lambert, D. A. Ford, T. Jilling and S. Matalon, Halogen gas exposure: toxic effects on the parturient, *Toxicology Mechanisms and Methods*, 2021, **31**, 272-287. 10.1080/15376516.2020.1736702.

146. S. Deflora and F. D'Agostini, Halogen lamp carcinogenicity, *Nature*, 1992, **356**, 569-569. 10.1038/356569a0.

147. A. A. Festa, O. A. Storozhenko, L. G. Voskressensky and E. V. Van der Eycken, Visible light-mediated halogenation of organic compounds, *Chem. Soc. Rev.*, 2023, **52**, 8678-8698. 10.1039/D3CS00366C.

148. H. Yekkezare, H. Tajik and N. M. Mahmoodi, Green halogenation of aromatic compounds using environmentally friendly synthesized rod-like metal-organic framework (MIL-88A) catalyst, *J. Mol. Struct.*, 2023, **1285**, 135454. https://doi.org/10.1016/j.molstruc.2023.135454.

149. R. Wilcken, M. O. Zimmermann, A. Lange, A. C. Joerger and F. M. Boeckler, Principles and Applications of Halogen Bonding in Medicinal Chemistry and Chemical Biology, *J. Med. Chem.*, 2013, **56**, 1363-1388. 10.1021/jm3012068.

150. Y. Li, T. Wang, Y. Wang, Z. Deng, L. Zhang, A. Zhu, Y. Huang, C. Zhang, M. Yuan and W. Xie, Tunable Photocatalytic Two-Electron Shuttle between Paired Redox Sites on Halide Perovskite Nanocrystals, *ACS Catal.*, 2022, **12**, 5903-5910. 10.1021/acscatal.2c01044.

151. A. Manna, T. K. Dinda, S. Ghosh and P. Mal, $CsPbBr_3$ in the Activation of the C–Br Bond of $CBrX_3$ (X = Cl, Br) under Sunlight, *Chem. Mater.*, 2023, **35**, 628-637. 10.1021/acs.chemmater.2c03164.

152. T. K. Dinda, A. Manna and P. Mal, En Route to Recyclable Semi-Heterogeneous Photocatalysis with Photoinert CeCl3, *ACS Catal.*, 2024, **14**, 7664-7673. 10.1021/acscatal.4c01130.

153. R. G. J. O. Hicks and b. chemistry, What's new in stable radical chemistry?, *Org. Biomol. Chem.*, 2007, **5**, 1321-1338.

154. M. P. Plesniak, H.-M. Huang and D. J. Procter, Radical cascade reactions triggered by single electron transfer, *Nat. Rev. Chem.*, 2017, **1**, 0077. 10.1038/s41570-017-0077.

155. R. Ardkhean, D. F. J. Caputo, S. M. Morrow, H. Shi, Y. Xiong and E. A. Anderson, Cascade polycyclizations in natural product synthesis, *Chem. Soc. Rev.*, 2016, **45**, 1557-1569. 10.1039/C5CS00105F.

156. B. Pal, A. Mathuri, A. Manna and P. Mal, $CsPbBr_3$ Perovskite Photocatalyst in Chemodivergent Functionalization of *N*-Methylalkanamides Using CBr_4, *Org. Lett.*, 2023, **25**, 4075-4079. 10.1021/acs.orglett.3c01268.

157. S. Sau and P. Mal, 3-Nitro-coumarin synthesis via nitrative cyclization of aryl alkynoates using tert-butyl nitrite, *Chem. Commun.*, 2021, **57**, 9228-9231. 10.1039/D1CC03415D.

158. P. Appukkuttan, V. P. Mehta and E. V. Van der Eycken, Microwave-assisted cycloaddition reactions, *Chem. Soc. Rev.*, 2010, **39**, 1467-1477. 10.1039/B815717K.

159. M. Lautens, W. Klute and W. Tam, Transition Metal-Mediated Cycloaddition Reactions, *Chem. Rev.*, 1996, **96**, 49-92. 10.1021/cr950016l.

160. Y. Lin and Y. Yan, CsPbBr3 Perovskite Nanocrystals for Photocatalytic [3+2] Cycloaddition, *ChemSusChem*, 2024, **17**, e202301060. https://doi.org/10.1002/cssc.202301060.

161. Q. Fan, H. Zhang, D. Liu, C. Yan, H. Zhu, Z. Xie and Z. Le, Visible-Light Photocatalytic Aerobic C═C Bond Cleavage of Alkenes to Carbonyls by CsPbBr3 Nanocrystals, *J. Org. Chem.*, 2023, **88**, 7391-7400. 10.1021/acs.joc.3c00653.

162. J. A. Dantas, J. T. M. Correia, M. W. Paixão and A. G. Corrêa, Photochemistry of Carbonyl Compounds: Application in Metal-Free Reactions, *ChemPhotoChem*, 2019, **3**, 506-520. https://doi.org/10.1002/cptc.201900044.

163. P. Nayek and P. Mal, Mimicking Ozonolysis via Mechanochemistry: Internal Alkynes to 1,2-Diketones using H5IO6, *Chem. Eur. J.*, 2024, e202401027. https://doi.org/10.1002/chem.202401027.

164. Q. Fan, D. Liu, Z. Xie, Z. Le, H. Zhu and X. Song, Visible-Light Photocatalytic Highly Selective Oxidation of Alcohols into Carbonyl Compounds by CsPbBr3 Perovskite, *J. Org. Chem.*, 2023, **88**, 14559-14570. 10.1021/acs.joc.3c01573.

165. R. C. Cioc, E. Ruijter and R. V. A. Orru, Multicomponent reactions: advanced tools for sustainable organic synthesis, *Green Chem.*, 2014, **16**, 2958-2975. 10.1039/C4GC00013G.

166. S. E. John, S. Gulati and N. Shankaraiah, Recent advances in multi-component reactions and their mechanistic insights: a triennium review, *Org. Chem. Front.*, 2021, **8**, 4237-4287. 10.1039/D0QO01480J.

167. R. O. Rocha, M. O. Rodrigues and B. A. D. Neto, Review on the Ugi Multicomponent Reaction Mechanism and the Use of Fluorescent Derivatives as Functional Chromophores, *ACS Omega*, 2020, **5**, 972-979. 10.1021/acsomega.9b03684.

168. S. Nandi, R. Jamatia, R. Sarkar, F. K. Sarkar, S. Alam and A. K. Pal, One-Pot Multicomponent Reaction: A Highly Versatile Strategy for the Construction of Valuable Nitrogen-Containing Heterocycles, *ChemistrySelect*, 2022, **7**, e202201901. https://doi.org/10.1002/slct.202201901.

169. A. Dömling, W. Wang and K. Wang, Chemistry and Biology Of Multicomponent Reactions, *Chem. Rev.*, 2012, **112**, 3083-3135. 10.1021/cr100233r.

170. J. Paul, M. Presset and E. Le Gall, Multicomponent Mannich-Like Reactions of Organometallic Species, *Eur. J. Org. Chem.*, 2017, **2017**, 2386-2406. https://doi.org/10.1002/ejoc.201700038.

171. M. Funicello, I. Cerminara, L. Chiummiento, P. Lupattelli, F. Felluga and F. Berti, Biginelli Reaction and β-Secretase Inhibition: A Multicomponent Reaction as a Friendly Educational Approach to Bioactive Compounds, *J. Chem. Educ.*, 2021, **98**, 1756-1761. 10.1021/acs.jchemed.0c01298.

172. S. Maeda, S. Komagawa, M. Uchiyama and K. Morokuma, Finding Reaction Pathways for Multicomponent Reactions: The Passerini Reaction is a Four-Component Reaction, *Angew. Chem. Int. Ed.*, 2011, **50**, 644-649. https://doi.org/10.1002/anie.201005336.

173. M. A. Fouad, H. Abdel-Hamid and M. S. J. R. a. Ayoup, Two decades of recent advances of Ugi reactions: synthetic and pharmaceutical applications, *RSC advances*, 2020, **10**, 42644-42681.

174. F. Mohamadpour, Recyclable photocatalyst perovskite as a single-electron redox mediator for visible-light-driven photocatalysis gram-scale synthesis of 3,4-dihydropyrimidin-2-(1H)-ones/thiones in air atmosphere, *Scientific Reports*, 2023, **13**, 10262. 10.1038/s41598-023-37526-x.

175. H. Nagarajaiah, A. Mukhopadhyay and J. N. Moorthy, Biginelli reaction: an overview, *Tetrahedron Lett.*, 2016, **57**, 5135-5149. 10.1016/j.tetlet.2016.09.047.

176. A. Mathuri, B. Pal, M. Pramanik, A. Manna and P. Mal, Enhancing the photocatalytic efficiency and stability of $CsPbBr_3$ nanocrystals for visible-light driven aerobic diaryl thio/seleno etherification, *Catal. Sci. Technol.*, 2024, **14**, 183-189. 10.1039/D3CY01478A.

177. Q. Yang, Y.-H. Wang, Y. Qiao, M. Gau, P. J. Carroll, P. J. Walsh and E. J. J. S. Schelter, Photocatalytic C–H activation and the subtle role of chlorine radical complexation in reactivity, *Science*, 2021, **372**, 847-852.

178. H. M. L. Davies, T. Hansen and M. R. Churchill, Catalytic Asymmetric C−H Activation of Alkanes and Tetrahydrofuran, *JACS*, 2000, **122**, 3063-3070. 10.1021/ja994136c.

179. J. Meiners, A. Friedrich, E. Herdtweck and S. Schneider, Facile Double C−H Activation of Tetrahydrofuran by an Iridium PNP Pincer Complex, *Organometallics*, 2009, **28**, 6331-6338. 10.1021/om9006906.

180. Y. Matsuo, Y. Zhang and E. Nakamura, Addition of Tetrahydrofuran to [60]Fullerene through C−H Bond Activation Induced by Arylzinc Reagents, *Org. Lett.*, 2008, **10**, 1251-1254. 10.1021/ol800143b.

181. S. Mondal, S. Banerjee, S. Bera, S. Mondal, S. P. Midya, R. Jana, R. K. Behera, A. Datta, N. Pradhan and P. Ghosh, CsPbBr3 Perovskite Polyhedral Nanocrystal Photocatalysts for Decarboxylative Alkylation via Csp3–H Bond Activation of Unactivated Ethers, *ACS Catal.*, 2024, **14**, 6633-6643. 10.1021/acscatal.4c01643.

182. X.-J. Wei, W. Boon, V. Hessel and T. Noël, Visible-Light Photocatalytic Decarboxylation of α,β-Unsaturated Carboxylic Acids: Facile Access to Stereoselective Difluoromethylated Styrenes in Batch and Flow, *ACS Catal.*, 2017, **7**, 7136-7140. 10.1021/acscatal.7b03019.

183. S. Fukushima, N. Takada, T. Hori and H. J. J. o. C. B. Wanibuchi, Cancer prevention by organosulfur compounds from garlic and onion, *J. Cell. Biochem.*, 1997, **67**, 100-105.

184. C. Zhao, K. P. Rakesh, L. Ravidar, W.-Y. Fang and H.-L. Qin, Pharmaceutical and medicinal significance of sulfur (SVI)-Containing motifs for drug discovery: A critical review, *Eur. J. Med. Chem.*, 2019, **162**, 679-734. https://doi.org/10.1016/j.ejmech.2018.11.017.

185. H. Zhu, V. Dronamraju, W. Xie and S. S. More, Sulfur-containing therapeutics in the treatment of Alzheimer's disease, *Med. Chem. Res.*, 2021, **30**, 305-352. 10.1007/s00044-020-02687-1.

186. S. Pathania, R. K. Narang and R. K. Rawal, Role of sulphur-heterocycles in medicinal chemistry: An update, *Eur. J. Med. Chem.*, 2019, **180**, 486-508. https://doi.org/10.1016/j.ejmech.2019.07.043.

187. T. K. Dinda, A. Manna, P. Nayek, B. Mandal and P. Mal, Ultrasmall CsPbBr3 Nanocrystals as a Recyclable Heterogeneous Photocatalyst in 100% E- and Anti-Markovnikov Sulfinylsulfonation of Terminal Alkynes, *ACS Appl. Mater. Interfaces*, 2024. 10.1021/acsami.4c10579.

188. M. Chen, Y. Zou, L. Wu, Q. Pan, D. Yang, H. Hu, Y. Tan, Q. Zhong, Y. Xu, H. Liu, B. Sun and Q. Zhang, Solvothermal Synthesis of High-Quality All-Inorganic Cesium Lead Halide Perovskite Nanocrystals: From Nanocube to Ultrathin Nanowire, *Adv. Funct. Mater.*, 2017, **27**, 1701121. https://doi.org/10.1002/adfm.201701121.

189. Y. Tong, E. Bladt, M. F. Aygüler, A. Manzi, K. Z. Milowska, V. A. Hintermayr, P. Docampo, S. Bals, A. S. Urban, L. Polavarapu and J. Feldmann, Highly Luminescent Cesium Lead Halide Perovskite Nanocrystals with Tunable Composition and Thickness by Ultrasonication, *Angew. Chem. Int. Ed.*, 2016, **55**, 13887-13892. https://doi.org/10.1002/anie.201605909.

190. L. Protesescu, S. Yakunin, O. Nazarenko, D. N. Dirin and M. V. Kovalenko, Low-Cost Synthesis of Highly Luminescent Colloidal Lead Halide Perovskite Nanocrystals by Wet Ball Milling, *ACS Applied Nano Materials*, 2018, **1**, 1300-1308. 10.1021/acsanm.8b00038.

191. J. Chen, Y. Fu, L. Samad, L. Dang, Y. Zhao, S. Shen, L. Guo and S. Jin, Vapor-Phase Epitaxial Growth of Aligned Nanowire Networks of Cesium Lead Halide Perovskites (CsPbX3, X = Cl, Br, I), *Nano Lett.*, 2017, **17**, 460-466. 10.1021/acs.nanolett.6b04450.

192. X. Li, Y. Wu, S. Zhang, B. Cai, Y. Gu, J. Song and H. Zeng, CsPbX3 Quantum Dots for Lighting and Displays: Room-Temperature Synthesis, Photoluminescence Superiorities, Underlying Origins and White Light-Emitting Diodes, *Adv. Funct. Mater.*, 2016, **26**, 2435-2445. https://doi.org/10.1002/adfm.201600109.

193. Q. Pan, H. Hu, Y. Zou, M. Chen, L. Wu, D. Yang, X. Yuan, J. Fan, B. Sun and Q. Zhang, Microwave-assisted synthesis of high-quality "all-inorganic" CsPbX3 (X = Cl, Br, I) perovskite nanocrystals and their application in light emitting diodes, *J. Mater. Chem. C*, 2017, **5**, 10947-10954. 10.1039/C7TC03774K.

194. P. Mal, B. Breiner, K. Rissanen and J. R. Nitschke, White Phosphorus Is Air-Stable Within a Self-Assembled Tetrahedral Capsule, *Science*, 2009, **324**, 1697-1699. doi:10.1126/science.1175313.

195. M. Schmittel, B. He and P. Mal, Supramolecular Multicomponent Self-Assembly of Shape-Adaptive Nanoprisms: Wrapping up C60 with Three Porphyrin Units, *Org. Lett.*, 2008, **10**, 2513-2516. 10.1021/ol800796h.

196. S. Liang, M. Zhang, G. M. Biesold, W. Choi, Y. He, Z. Li, D. Shen and Z. Lin, Recent Advances in Synthesis, Properties, and Applications of Metal Halide Perovskite

Nanocrystals/Polymer Nanocomposites, *Adv. Mater.*, 2021, **33**, 2005888. https://doi.org/10.1002/adma.202005888.

197. J. Kong, H. Wang, J. A. Röhr, Z. S. Fishman, Y. Zhou, M. Li, M. Cotlet, G. Kim, C. Karpovich, F. Antonio, N. P. Padture and A. D. Taylor, Perovskite Solar Cells with Enhanced Fill Factors Using Polymer-Capped Solvent Annealing, *ACS Applied Energy Materials*, 2020, **3**, 7231-7238. 10.1021/acsaem.0c00854.
198. H. Zhang, X. Wang, Q. Liao, Z. Xu, H. Li, L. Zheng and H. Fu, Embedding Perovskite Nanocrystals into a Polymer Matrix for Tunable Luminescence Probes in Cell Imaging, *Adv. Funct. Mater.*, 2017, **27**, 1604382. https://doi.org/10.1002/adfm.201604382.
199. F. Yi, Q. Guo, D. Zheng, R. Zhuang, J. Zhang, Q. Tang and J. Duan, Multifunctional Polymer Capping Frameworks Enable High-Efficiency and Stable All-Inorganic Perovskite Solar Cells, *ACS Applied Energy Materials*, 2022, **5**, 6432-6441. 10.1021/acsaem.2c00923.
200. S. Hou, Y. Guo, Y. Tang and Q. Quan, Synthesis and Stabilization of Colloidal Perovskite Nanocrystals by Multidentate Polymer Micelles, *ACS Appl. Mater. Interfaces*, 2017, **9**, 18417-18422. 10.1021/acsami.7b03445.
201. Y. J. Yoon, Y. Chang, S. Zhang, M. Zhang, S. Pan, Y. He, C. H. Lin, S. Yu, Y. Chen, Z. Wang, Y. Ding, J. Jung, N. Thadhani, V. V. Tsukruk, Z. Kang and Z. Lin, Enabling Tailorable Optical Properties and Markedly Enhanced Stability of Perovskite Quantum Dots by Permanently Ligating with Polymer Hairs, *Adv. Mater.*, 2019, **31**, 1901602. https://doi.org/10.1002/adma.201901602.
202. S. Liang, S. He, M. Zhang, Y. Yan, T. Jin, T. Lian and Z. Lin, Tailoring Charge Separation at Meticulously Engineered Conjugated Polymer/Perovskite Quantum Dot Interface for Photocatalyzing Atom Transfer Radical Polymerization, *J. Am. Chem. Soc*, 2022, **144**, 12901-12914. 10.1021/jacs.2c04680.
203. J. Shen, Y. Wang, Y. Zhu, Y. Gong and C. J. N. Li, A polymer-coated template-confinement CsPbBr 3 perovskite quantum dot composite, *Nanoscale*, 2021, **13**, 6586-6591.
204. S. N. Raja, Y. Bekenstein, M. A. Koc, S. Fischer, D. Zhang, L. Lin, R. O. Ritchie, P. Yang and A. P. Alivisatos, Encapsulation of Perovskite Nanocrystals into Macroscale Polymer Matrices: Enhanced Stability and Polarization, *ACS Appl. Mater. Interfaces*, 2016, **8**, 35523-35533. 10.1021/acsami.6b09443.